Technische Universität München

Fakultät für Chemie

Professur für Zelluläre Proteinbiochemie

MOLECULAR MECHANISMS OF

MEMBRANE PROTEIN QUALITY CONTROL

JOÃO PEDRO LOURENÇO COELHO

Vollständiger Abdruck der von der Fakultät für Chemie der Technischen Universität München zur Erlangung des akademischen Grades eines

Doktors der Naturwissenschaften (Dr. rer. nat.)

genehmigten Dissertation.

Vorsitzender(r):   Prof. Dr. Bernd Reif

Prüfer der Dissertation:

    1.   Prof. Dr. Matthias Feige

    2.   Prof. Dr. Johannes Buchner

    3.   Prof. Dr. Marius Lemberg (Universität zu Köln)

Die Dissertation wurde am 26.01.2021 bei der Technischen Universität München eingereicht und durch die Fakultät für Chemie am 17.05.2021 angenommen.

Parts of this thesis have been published in peer-reviewed journals:

A network of chaperones prevents and detects failures in membrane protein lipid bilayer integration

João P L Coelho, Matthias Stahl, Nicolas Bloemeke, Kevin Meighen-Berger, Carlos Piedrafita Alvira, Zai-Rong Zhang, Stephan A Sieber, Matthias J Feige. *Nat Commun* 10, 672 (2019). https://doi.org/10.1038/s41467-019-08632-0

Parts of these thesis have been presented at scientific conferences:

EMBO Practical Course: Targeted proteomics: Experimental design and data analysis
November 13th-18th, 2016, Centro de Regulación Genómica, Barcelona, Spain
Poster presentation

14th ER & Redox Club meeting
May 8th-10th, 2019, Haus der bayerischen Landwirtschat Herrsching, Herrsching am Ammersee, Germany
Oral presentation

Other publications

In case of stress, hold tight: phosphorylation switches PDI from an oxidoreductase to a holdase, tuning ER proteostasis

João P L Coelho, Matthias J Feige. *EMBO J* 39, e104880 (2020). https://doi.org/10.15252/embj.2020104880

Quality control of mislocalized and orphan proteins

Ka-Yiu Edwin Kong, João P L Coelho, Matthias J Feige, Anton Khmelinskii *Exp Cell Res* (under review)

Acknowledgments

First and foremost, my biggest thank you goes to Matthias. For all the knowledge and confidence deposited in me, for the good environment he created in the lab, for the motivation and discipline incited, and for all the science discussions we got to share. And the Christmas food and liquor.

To Marius Lemberg for the highly critical spirit that drove me to look at my work with new, "devil-advocating" eyes, and for the stream of knowledge, and the brain-marathons I had to run in order to keep up.

To Prof. Dr. Zai-rong Zhang for allowing me to experience Shanghai and its (mostly lab) culture for one month. And the cheap, eye-watering, nose-running food.

To Prof. Dr. Stephan Sieber, and to Mathias Stahl for contributing with such technical and intellectual expertise to our first story.

To the CPB lab. To Susi and Stephie for being my mentors especially when starting, for unknowingly imparting in me some of the German way of doing things. Thank you, Susi, for the Christmas sweater, I will be wearing it today. To Yonatan for the company for coffee and cigarettes, and for the laughs too. I will not thank you for constantly turning off the lights when I was pipetting. To Nico for the company in the lab and for always putting my DNAs back in the fridge, somewhere in the fridge, also thank you for the translation. To Isabel, Karen, and Anna for keeping me company in the office every time we all arrived before 8:30, fresh out of our weekly jog, but above all, for the creativity you brought to the office. To my interns, Eva and Carlos, for starting me off with the difficult task of trying to teach, vocalize, and explain to someone what we were doing that day. To Dinah and Kevin, for making the explaining easier, and for the work and dedication they keep on showing with not-so-easy projects. To Andrea Zanotti, in Heidelberg, for the help and drive in the SPC project.

Thank you, Flo, you gave me the life that I came to live (if you read this, it's from a song, we have probably been over this), a life I'm happy I got to experience (this part is not from the song anymore).

À Cabrita, pelos fins-de-semana e pelas alegres histórias sem fim e pelas vezes que ficávamos acordados com vinho a discutir anoctaminas e o rim. Ao

Nuninho pelas vezes que ele me obrigava a ficar acordado ou a prestar atenção quando falava do que quer que ele estivesse a falar e todos os problemas associados. À Ana por seres uma inspiração de senhora. Ao Lucasino e ao Custódio por todas as vezes que fui à motherland e pela vez que vieram a esta land. À Magda e à Guida, desde a CFTR até Regensburg até Heidelberg, até onde formos a seguir. Aos "Migos do mundo ᴘᴛɢʙᴅᴇ" por me fazerem rir e me fazerem sentir saudades e vontade de regressar a Portugal.

À Joana Rita, por ser o que eu provavelmente mais precisava numa irmã, por ser compreensiva, interessada e terna. Por me ter dado uma sobrinha, à tua, Gabriela, que continues a pôr-me um sorriso na cara e pela vontade de te ver crescer. Aos meus pais por me deixarem ser eu, por se preocuparem, por me lembrarem de comer, pelos abraços apertados. Obrigado, família.

À Mia e à Micas.

Summary

Membrane proteins on the cell surface are essential for multicellular organism homeostasis, with their synthesis and folding taking place at the endoplasmic reticulum of eukaryotic cells. Membrane protein folding relies on both the correct folding of cytosolic and endoplasmic reticulum domains, but also the precise packing of hydrophobic helices in the lipid bilayer. In case membrane protein folding or assembly fail, the endoplasmic reticulum is equipped with a machinery to recognize these faulty proteins, aid their structure formation or send them to degradation in the cytosol. Connexins are a group of membrane proteins that play a central role in multiple tissues, by enabling small-molecule transport across the plasma membrane via gap junction channels, effectively coupling two cytoplasms together. Connexin 32 (Cx32) is a member of this family, whose expression in the peripheral nervous system is vital for human health. Mutations in Cx32 give rise to X-linked Charcot-Marie-Tooth disease, one of the most prevalent neuropathies in humans. Within this work we have characterized how Cx32 disease-causing mutants give rise to aberrant membrane protein fold, e.g. through TM segment misintegration, and which cellular machineries are responsible for recognizing and handling faulty Cx32.

One group of mutants destabilizes the membrane integration of two -helices, exposing them to the ER lumen. These proteins are retained intracellularly, becoming unable to reach the plasma membrane, and are degraded faster than wild-type protein by the proteasome. In the endoplasmic reticulum, the endoplasmic reticulum membrane protein complex aids in the membrane integration of these transmembrane segments. In case they continue to fail to integrate, the luminal chaperone BiP binds them, preventing their aggregation. Finally, proteins deemed terminally misfolded are sent to degradation through polyubiquitination by the E3 ligase gp78. Through the identification of these misintegrated mutants, we could thus characterize a previously unexplored network within the endoplasmic reticulum quality control machinery.

On the other hand, another group of disease-causing mutants shows proteolytical cleavage at their N-termini. We could identify the signal peptidase complex as the responsible enzyme for this cleavage, acting in a non-canonical fashion. We characterized how connexin misfolding triggers this cleavage event, and found that by correcting folding in the plane of the membrane, we could

partially revert the cleavage phenotype. Since the cleaved protein cannot form physiological relevant ensembles, but can still interact with full-length protein, we speculate the cleavage phenotype could have implications for the etiology of Charcot-Marie-Tooth disease.

Taken together, we have elucidated how different mutations in the same protein can lead to a variety of topogenic phenotypes, and how distinct cellular protein quality control mechanisms have evolved to handle aberrant membrane proteins.

Zusammenfassung

Membranproteine sind für die Homöostase mehrzelliger Organismen unverzichtbar. Ihre Synthese und Faltung finden in eukaryotischen Zellen am endoplasmatischen Retikulum statt. Die Faltung von Membranproteinen beruht dabei sowohl auf der korrekten Faltung von Domänen im Zytosol und innerhalb des endoplasmatischen Retikulums als auch auf der exakten Anordnung hydrophober -Helices in der Lipiddoppelschicht. Für den Fall, dass die Faltung oder Assemblierung von Membranproteinen fehlschlägt, besitzt das endoplasmatische Retikulum Mechanismen, durch welche fehlerhafte Proteine erkannt und nach Überführung ins Zytosol abgebaut werden. Connexine bilden eine Gruppe von Membranproteinen, die eine zentrale Rolle bei dem Transport von Metaboliten durch die Plasmamembran spielen. Der Transport erfolgt dabei über Gap Junction-Kanäle, welche das Zytoplasma zweier benachbarter Zellen effektiv miteinander verbinden. Ein Mitglied dieser Gruppe von Membranproteinen ist Connexin 32 (Cx32), dessen Expression wichtig für die Gesundheit des Menschen ist. Mutationen in Cx32 verursachen die mit dem X-Chromosom zusammenhängende Charcot-Marie-Tooth Erkrankung, eine der am häufigsten auftretenden Neuropathien beim Menschen. In der vorliegenden Arbeit untersuchten wir, wie krankheitsverursachende Mutationen in Cx32 zur Entstehung von fehlerhaften Konformationen im Membranbereich des Proteins führen.

Eine Gruppe von Mutationen destabilisiert die Membranintegration von zwei Helices, was dazu führt, dass diese Segmente frei exponiert im ER-Lumen vorliegen. Solch fehlerhafte Proteine werden intrazellulär zurückgehalten, nicht mehr zur Plasmamembran transportiert und vom Proteasom schneller abgebaut. Innerhalb des endoplasmatischen Retikulums unterstützt der endoplasmatische Retikulum-Membranproteinkomplex die Membranintegration fehlerhafter Transmembransegmente. Lassen sich fehlerhafte Transmembransegmente jedoch auch weiterhin nicht integrieren, werden diese durch das lumenale Chaperon BiP gebunden, wodurch ihre Aggregation verhindert wird. Proteine, die schlussendlich als fehlgefaltet gelten, werden durch die E3-Ligase gp78 poly-ubiquitiniert und dadurch degradiert. Durch die Identifizierung solch fehlerhaft in die Membran integrierten Mutanten konnten wir ein bislang unerforschtes Gebiet

der Qualitätskontrollmaschinerie des endoplasmatischen Retikulums charakterisieren.

Eine andere Gruppe von krankheitsverursachenden Mutationen weist eine proteolytische Spaltung des Proteins am N-Terminus auf. Das für diese Spaltung verantwortliche Enzym konnten wir als den Signalpeptidase-Komplex identifizieren, dessen Funktionsweise nicht-kanonisch ist. Wir charakterisierten, wie eine Fehlfaltung von Connexin das Spaltungsereignis auslöst und konnten zeigen, dass wir durch eine Korrektur der Faltung in der Membranebene den Phänotyp der Spaltung teilweise umkehren können. Da die gespaltene Form von Connexin 32 keine physiologisch relevanten Ensembles bilden, aber dennoch mit Volllängen-Proteinen interagieren kann, nehmen wir an, dass der Spaltungsphänotyp Auswirkungen auf die Ätiologie der Charcot-Marie-Tooth Krankheit haben kann.

Zusammengefasst klären wir auf, wie unterschiedliche Mutationen in demselben Protein zur Entstehung von einer Vielzahl von topogenen Phänotypen führen kann und wie sich zelluläre Proteinqualitätskontrollmechanismen entwickelt haben, um mit fehlerhaften Membranproteinen umzugehen.

Abbreviations

AAA, ATPase associated with diverse cellular activities **ATF6,** Activating transcription factor 6 **ATP,** Adenosine triphosphate **AUP1,** Ancient ubiquitous protein 1 **BAP,** B cell-associated protein **BCL2,** B cell lymphoma 2 **BiP,** Immunoglobulin heavy-chain binding protein **BSA,** Bovine serum albumine **CAML,** Calcium-modulating cyclophilin ligand **CANX,** Calnexin **CANX,** Calnexin **CCDC47,** Coiled-coil domain-containing protein 47 **CD3,** Cluster of differentiation 3 **cDNA,** Complementary DNA **CFTR,** Cystic fibrosis transmembrane conductance regulator **CHIP,** Carboxy-terminus of the Hsc70 interacting protein **CHOP,** CCAAT enhancer binding protein homologous protein **CHX,** Cycloheximide **CL,** Constant domain of the light-chain **CMT,** X-linked Charcot-Marie-Tooth disease **CMT1X,** Charcot-Marie-Tooth disease **CMV,** Cytomegalovirus **COS,** CV-1 in origin, and carrying the SV40 genetic material **CRT,** Calreticulin **CRT,** Calreticulin **CTD,** C-terminal domain **Cue1,** Coupling of ubiquitin conjugation to ER degradation protein 1 **Cx,** Connexin **DMEM,** Dulbecco's Modified Eagle Medium **DNA,** Deoxyribonucleic acid **DTT,** Dithiothreitol **DUB,** Deubiquitinating **EC,** Extracellular **EDEM,** ER degradation-enhancing mannosidase-like proteins **eIF2α,** Eukaryotic translation initiation factor 2 α **EM,** Electron mycroscopy **EMC,** ER membrane protein complex **ER,** Endoplasmic reticulum **ER Man I,** ER alpha1,2 mannosidase I **ERAD,** Endoplasmic reticulum associated degradation **Erdj,** ER-localized DnaJ **ERES,** ER exit sites **ERGIC,** ER-Golgi Intermediate compartment **Ero1,** ER oxidoreductin 1 **ERSE,** ER stress response elements **FBS,** Fetal bovine serum **GAPDH,** Glyceraldehyde 3-phosphate dehydrogenase **GJ,** Gap junction **GJIC,** Gap junction intercellular communication **Glc,** Glucose **GlcNac,** N-Acetylglucosamine **gp78,** Cell surface glycoprotein of 78 kDa **GPCR,** G-protein-coupled receptor **Grp170,** Glucose regulated protein of 170 kDa **Grp94,** Glucose regulated protein of 94 kDa **GTP,** Guanosine triphosphate **HA,** Hemagglutinin **HC,** Hemichannel **HCD,** Higher energy collision dissociation **HERP,** HomoCys-responsive ER resident protein **Hrd1,** HMG-CoA reductase degradation **HSP,** Heat shock protein **IB,** Immunoblot **ICL,** Intracellular loop **IF,** Immunofluorescence **IgGSF1,** Immunoglobulin superfamily member 1 **IRE1,** Inositol-requiring protein 1 **KDELR,** KDEL receptor **MagT1,** Magnesium transporter protein 1 **Man,** Mannose **MANF,** Mesencephalic astrocyte-derived neurotrophic factor **MAPK,** Mitogen-activated protein kinase **MARCH6,** Membrane-associated RING-CH-type 6 **NAC,** Nascent polypeptide-associated complex **NaDOC,** Sodium deoxycholate **NBD,** Nucleotide binding domain **NEF,** Nucleotide exchange factor **NEM,** N-ethylmaleimide **NGly1,** N-glycanase 1 **NPL4,** Nuclear protein localization protein 4 **NTH,** N-terminal helix **O/N,** Overnight **OS-9,** Amplified in osteosarcoma 9 **OST,** Oligosaccharyltransferase **PAGE,** Polyacrilamide gel electrophoresis **PAT10,** Protein associated with the ER translocon of 10 kDa **PBS,** Phosphate-buffer saline **PCR,** Polymerase chain reaction **PDI,** Protein disulfide isomerase **PERK,** Protein kinase RNA-like ER kinase **PKC,** Protein kinase C **PMP22,** Peripheral myelin protein 22 kDa **PNGase,** Peptide:N-glycosydase **PTM,** Post-translational modification **PVDF,** Polyvinylidene fluoride **RER1,** Retention in the ER 1 **RHBDL4,** Rhomboid-like 4 **RING,** Really interesting new gene **RNA,** Ribonucleic acid **RNC,** Ribosome-nascent chain complex **RT,** Room temperature **S1P,** Site 1 protease **S2P,** Site 2 protease **SBD,** Substrate binding domain **SCAM,** Substituted cysteine accessibility method **SDS,** Sodium dodecyl sulfate **SEL1L,** suppressor/enhancer of Lin-12-like **SGTA,** Small glutamine-rich tetratricopeptide repeat-containing protein alpha **siRNA,** Small interfering RNA **SND,** SRP-independent **SPC,** Signal peptidase complex **SPP,** Signal peptide peptidase **SRP,** Signal recognition particle **SV40,** Simian vacuolating virus 40 **TA,** Tail-anchored **TBS,** Tris-buffered saline **TCR,** T-cell receptor **TM,** Transmembrane **TRAM,** Translocating chain-associated membrane protein **TRAP,** Translocon-associated protein **TRC40,** TMD recognition complex of 40 kDa **Ub,** Ubiquitin **Ubc,** Ubiquitin conjugating **UBQLN,** Ubiquilin **UBX,** Ub regulatory X **UFD1,** Ubiquitin fusion degradation protein 1 **UGGT,** UDP-glucose:glycoprotein glucosyltransferase **UPR,** Unfolded protein response **US11,** Unique short region protein 11 **VCP,** Valosin-containing protein **WRB,** Tryptophan-rich basic protein **wt,** Wild type **XBP1,** X-box binding protein 1 **ZO-1,** Zonula occludens 1 **β-ME,** β-mercaptoethanol

Table of contents

Introduction

1. Membrane protein biogenesis

Cellular communication is essential for homeostasis in multicellular organisms. Some of the major players involved in this are membrane proteins, which enable molecule transport across membranes, allow for intracellular trafficking and organelle biogenesis to occur, and also play a vital role in signaling pathways, by modulating and transducing information through membranes. The hallmark feature of membrane proteins is the presence of at least one <u>t</u>rans<u>m</u>embrane (TM) segment, made up of mostly hydrophobic amino acid residues that will span a membrane in eukaryotic cells. Ca. 30% of all human protein-coding genes will give rise to a membrane protein (1) and most of these proteins are destined to the secretory pathway, where the <u>e</u>ndoplasmic <u>r</u>eticulum (ER) serves as a hub for their synthesis, folding, assembly, and often, degradation.

a. ER targeting and insertion

Membrane protein synthesis starts at the ribosome and is dependent on targeting of the newly synthesized polypeptide chain to the ER, either co- or post-translationally. ER signal sequences (targeting sequence) can be widely different in both amino acid sequence and length, but their characteristic hydrophobic nature makes early recognition and shielding by cytosolic factors essential. A recent report showed one of the earliest interactors with a <u>r</u>ibosome-<u>n</u>ascent chain <u>c</u>omplex (RNC) to be the <u>n</u>ascent polypeptide-<u>a</u>ssociated <u>c</u>omplex (NAC), which, without necessarily entailing ER targeting, can insert itself into the ribosome exit tunnel, presumably aiding organelle targeting reactions (2,3).

When it comes to co-translational ER targeting, the most studied and used factor is the <u>s</u>ignal <u>r</u>ecognition <u>p</u>article (SRP). SRP is a ribonucleoprotein that binds RNC early in translation so that once a signal sequence emerges from the ribosome exit tunnel, the SRP can recognize it and shield it from the aqueous cytosol (4). The SRP is composed of one RNA molecule and six protein subunits, where the signal sequence recognition is mediated by the GTPase SRP54 (5-7). SRP54 recognition and accommodation of hydrophobic signal sequences is mediated by a Met-rich groove on the SRP54 M-domain. The cryo EM structure

of SRP-RNC complex showed that an SRP54 C-terminal α-helix can occupy this groove when the complex is in a scanning, unoccupied mode. This led to a model where sufficiently hydrophobic emerging signal sequences can displace this SRP54 α-helix, which will in turn shield the signal sequence from the cytosol (8). Delivery to the ER is mediated through docking of SRP to its receptor, in a GTP-dependent manner (9). The SRP receptor is a heterodimer of a cytoplasmic α subunit (highly homologous to the GTPase domain of SRP54), and a single-span ER membrane β subunit. Upon binding to its receptor and GTP hydrolysis, SRP is released from the RNC, while the polypeptide chain is handed to the Sec61 translocon through interaction between the RNC and Sec61 (10,11). The Sec61 is a heterotrimeric complex made up of the essential α and γ subunits, as well as the non-essential β subunit. Early crosslinking and electrophysiological studies have revealed Sec61α as the aqueous pore-forming subunit of the translocon (12-14), where the lateral gate of the translocon can be found, for ER membrane insertion of the signal sequence (15). On its inactive, quiescent state, the Sec61 translocon is kept closed axially by a short helix, corresponding to a central plug, and laterally by closure of its lateral gate, facing the lipid bilayer (16,17). Furthermore, the immunoglobulin heavy-chain <u>b</u>inding <u>p</u>rotein (BiP), also acts as a seal in the ER luminal side of the membrane, ensuring the impermeability of the channel (18). Cryo EM structures of Sec61 associated with the RNC and a signal sequence showed that the displacement of a Sec61α α-helix by a signal sequence leads to a conformational shift in the translocon which results in the opening of both its pore into the ER lumen (through displacement of its luminal plug), and its lateral gate into the lipid bilayer (via displacement of the aforementioned α-helix by the signal sequence) (19-21). This also led to the hypothesis that the hydrophobicity of the signal sequence is a requirement for lateral gate opening, since interaction between two Sec61 α-helices needs to be disrupted.

Sec61 further associates with other protein complexes that aid on translocation, such as the <u>t</u>ranslocating <u>c</u>hain-<u>a</u>ssociating <u>m</u>embrane protein (TRAM), and the <u>tr</u>anslocon-<u>a</u>ssociated <u>p</u>rotein (TRAP) complex, observed from pulling down Sec61 from canine microsomes (22). TRAM is a multipass TM protein, and is described to mostly play a role in the biogenesis and insertion of

particularly hydrophilic TM segments, particularly in the early stages of synthesis (23-25). Furthermore, an homolog of TRAM, TRAM2, was found to play a role in the topology of a multipass ER protein, by promoting a type I orientation on the signal sequence of its client protein (26). TRAP on the other hand, is a protein complex composed of four different proteins, constitutively associated with Sec61 (27,28). It was originally identified by cross-linking signal sequences in the ER (29), and recently shown to have a binding preference to Gly and Pro-rich signal sequences (30). TRAP plays an important role in the translocation of relatively weak signal sequences, as shown for different model proteins (31,32). A recent study made use of ribosome stalling and crosslinking to show one of the subunits of TRAP, TRAPß, is able recognize substrate signal sequences in the cytosolic side of the ER membrane, enabling their subsequent interaction with Sec61 (33).

Early hints towards SRP-independent targeting came to light with the viability of yeast cells lacking both the SRP complex and its ER membrane receptor (34), and from the fact small proteins could be handed to the ER post-translationally, in an SRP-independent manner (35,36). Additionally, proteins with a signal sequence at their C-terminal, commonly known as tail-anchored (TA) proteins, also do not rely on SRP for ER targeting. For TA and small secretory proteins, translation has been terminated before the signal sequence emerges from the ribosome. Lastly, the third major group of SRP-independent targeting is made up of proteins with a low-hydrophobicity signal sequence where recognition by the SRP is not efficient (36).

Mildly hydrophilic signal sequences can be chaperoned in the cytosol by the heat shock proteins of 40 and 70 kDa (Hsp70/Hsp40) systems (37,38), while small secretory proteins are chaperoned by calmodulin (39), and TA proteins by a relay between small glutamine-rich tetratricopeptide repeat-containing protein alpha (SGTA) and TMD recognition complex of 40 kDa (TRC40) (40,41). Insertion into the ER lumen of SRP-independent small or mildly hydrophilic signal sequences is still taken care of by Sec61, this time in association with the mammalian Sec62 and Sec63 (42,43). Polypeptide translocation is aided by the Sec63 ER luminal J-domain which recruits BiP to this complex, supporting the unidirectional pulling of the polypeptide into the ER lumen (44). On the other hand, TA proteins loaded on TRC40 (Get3 in yeast) are handed to its heterodimeric receptor expressed in the ER membrane: the tryptophan-rich basic

protein (WRB) and the c̲alcium-m̲odulating cyclophilin l̲igand (CAML) (Get1 and Get2 in yeast, respectively) which constitute the minimal machinery for insertion, even though the integration mechanism itself is yet to be characterized (45-48).

In yeast, another S̲RP-in̲dependent (SND) pathway was recently uncovered while searching for the ER targeting pathway of a protein with no SRP dependency (49). Clients of the SND pathway usually have a TM segment in the central region of their polypeptide chain. The working model revolves around the co-translational capture of cytosolic signal sequences by Snd1, which can associate with the ribosome, with later delivery to the Snd2/3 complex at the ER membrane, and translocation via the Sec61/62/63 translocon. This system also reinforced the idea that ER targeting and insertion of many substrates can occur through different pathways, which are able to compensate for each other in loss of function or overloading scenarios (50). Similar aspects have been described mainly in yeast, which has been previously shown to contain an alternative translocon that compensates in cases where the canonical Sec61 translocon is overloaded. This is composed by Ssh1 (SEC61A2 in humans) which is the main pore-forming subunit, Sss1 (Sec61γ homolog) and Sbh2, a paralogue from the yeast Sbh1 subunit (Sec61β in humans) (51).

b. Membrane protein topology

Membrane protein topology is usually defined as the number of TM segments a membrane protein has, and their relative orientation in relation to the membrane (Fig. 1) (52). TM segment orientation is controlled greatly by the degree of interaction of the RNC with the Sec61 translocon: tighter association leads the polypeptide chain into the Sec61 pore and through its luminal gate, while looser interaction will lead the polypeptide chain slip into the cytosol. The strength of this
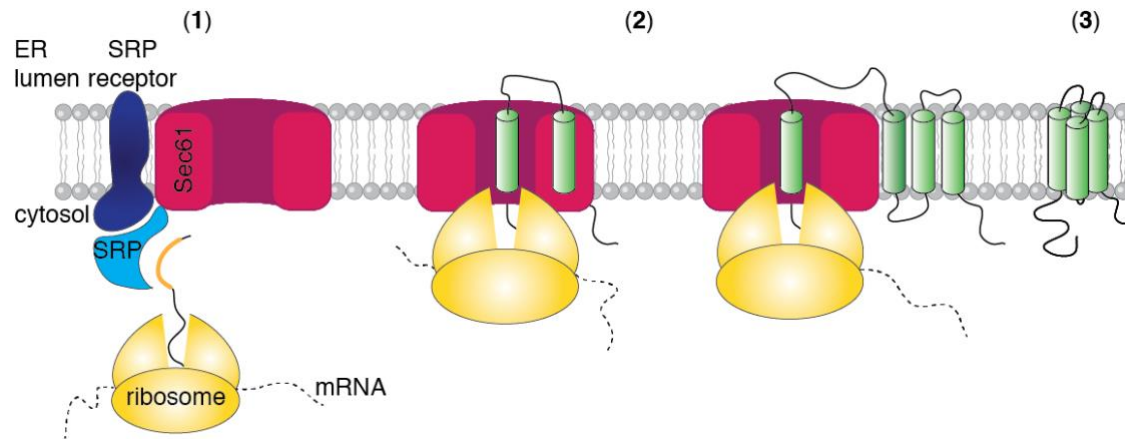
4

Figure 1: Targeting, insertion, and folding of a multipass membrane protein. (**1**) A translating ribosome is shown after synthesis of a signal sequence, in orange. Through the SRP and its receptor, the RNC is targeted to the ER membrane. (**2**) After synthesis of hydrophobic TM segments, membrane will spontaneously partition into the lipid bilayer, culminating in a (**3**) fully folded TM protein, with packed TM segments.

interaction can thus determine the orientation of first TM segment of a protein, and therefore its overall topology (Fig .2) (53,54).

Similar to the ability of a protein sequence to dictate membrane insertion, the same primary structure, and sometimes secondary structure elements, usually have most of the information needed for membrane topology. TM segment orientation is thus dependent on a myriad of factors from the presence of charges to the hydrophobicity of a given TM segment. Long, highly hydrophobic segments will be usually found in a type-I (N_{out}/C_{in}) topology, since inversion of the signal sequence (which depends on further polypeptide chain accumulation between the RNC and the translocon) is probably not favored before the TM segment partitions into the membrane (54,55). Additionally, the upstream presence of a cytoplasmic fast folding domain will restrict a following TM segment from ever taking a type I topology, since that would require translocation of the mentioned domain through Sec61 (56).

The first identified and probably most relevant factor determining TM segment orientation is the "positive-inside rule". Early work on the orientation of TM segments observed an enrichment for positively charged amino acid residues on the "inside" of a cell, i.e. the cytosolic side (57,58), which has been postulated in E. coli to be dependent on the asymmetric enrichment of anionic phospholipids in the cytoplasmic leaflet of the lipid bilayer (59). Interestingly, this is easily
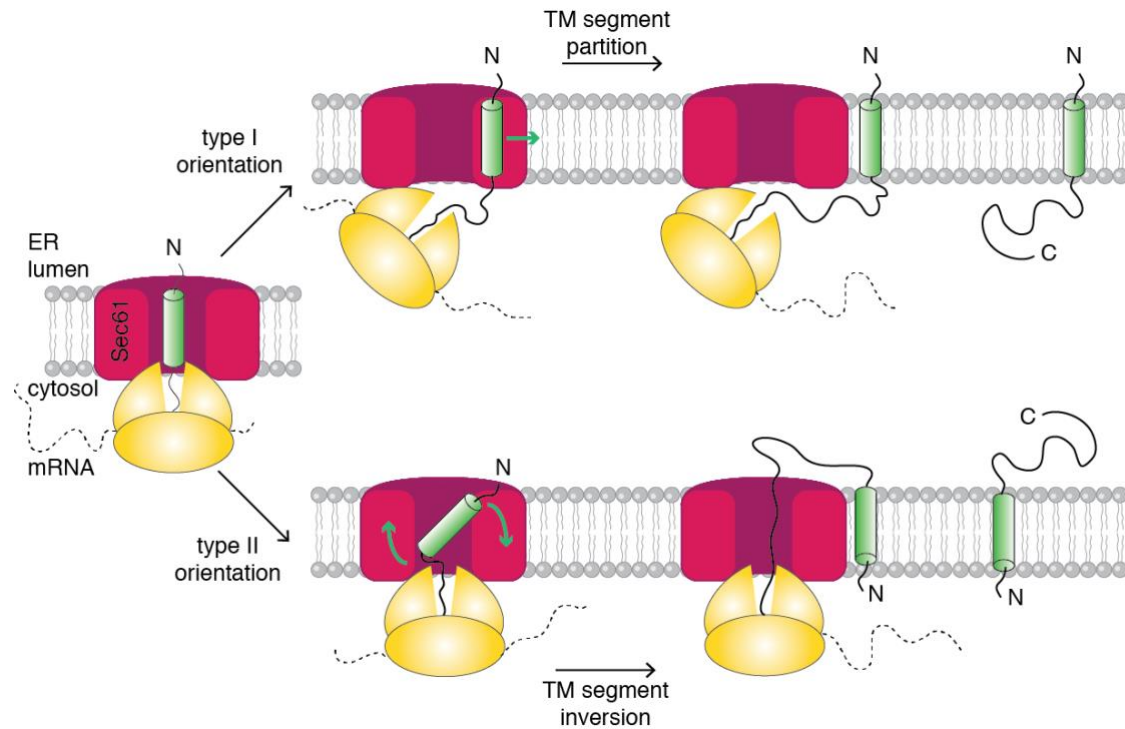
Figure 2: Establishment of the membrane orientation of a signal sequence. A translating ribosome is associated with the Sec61 translocon, where a signal sequence is placed, head-first. If the signal sequence adopts a type I orientation (upper row), it can partition into the lipid bilayer without reorientation. If the signal sequence has a type II signature (lower row), it will invert, looping in the translocon as seen by the green arrows, and exposing its N-terminal to the cytosol.

observed in signal peptides, in which a positively charged n-region is located in the cytoplasmic side of the membrane, warrantying polypeptide entry into the ER lumen (discussed below). However, both the presence of positive charges in the cytoplasmic side, as well as phospholipid charge asymmetry is less strong in eukaryotes. Instead of positive charges in the cytoplasmic side, it has been shown that the eukaryote positive-inside rule is mostly governed by the difference in charge between the two flanking regions of a TM segment, e.g. the cytoplasmic side can be negatively charged, but it will generally by less negatively charged than the luminal side (60). Furthermore, instead of lipid asymmetry, it has been shown that charges in the Sec61 translocon of C. elegans can favor a "positive-inside" orientation (61).

As it is to be expected, exceptions exist to a strict and immovable protein topology. An interesting observation came from in vitro translation systems analyzing the apparent free energy (ΔG_{app}) for TM segment integration into the lipid bilayer. These calculations were later applied to multipass TM proteins with a deciphered three-dimensional structure (62,63), and strikingly ca. 25% of these TM segments were predicted to be unstable in the membrane ($\Delta G_{app} > 0$ kcal/mol). When this is information is applied to protein topology, it hints towards
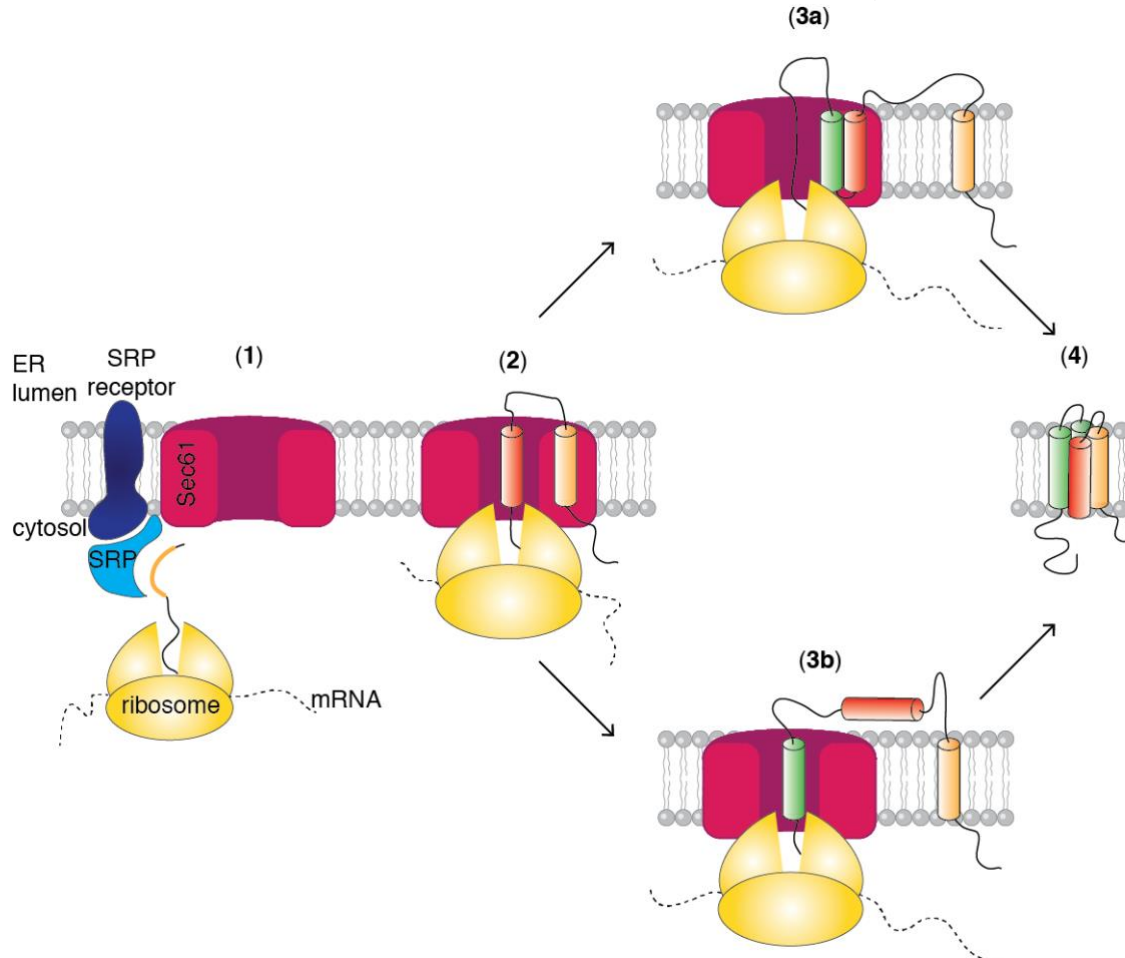
Figure 3: Targeting, insertion, and folding of a multipass protein with hydrophilic TM segments. (**1**) A translating ribosome is shown after synthesis of a signal sequence, in orange. Through the SRP and its receptor, the RNC is targeted to the ER membrane. (**2**) A mildly hydrophobic TM segment, in red, is translated into the Sec61 translocon. Insertion of such a segment into the ER membrane can take several routes. One of the possibilities is (**3a**) lingering of the TM helix at the translocon, until synthesis of an interacting TM helix, seen in green. Alternatively, (**3b**) the less hydrophobic TM segment can be temporarily exposed to the ER lumen, until synthesis of a downstream segment (in green) promotes its membrane insertion. (**4**) Both scenarios should culminate with a fully membrane-integrated TM protein, where TM-TM interactions can stabilize helices in the membrane. Adapted from (53).

topogenesis being a well-controlled process, often dependent on interactions between TM segments within the same protein (Fig. 3).

Accordingly, there are several examples of TM-TM interaction driving protein topogenesis in multipass membrane proteins. Mechanistically, this is observed by the temporary exposure of TM segments to either the cytosol or the ER lumen, until downstream TM segments are synthesized (Fig. 2). The six TM segment protein aquaporin-1 is a classic example of this phenomenon. Its TM2 and TM4 are exposed to the ER lumen and cytosol, respectively, upon synthesis, and its TM3 has a type I orientation; preferentially after synthesis of TM6, TM3 inverts in the membrane due to retrotranslocation of its N-terminal portion from the ER lumen to the cytosol, with consequent integration of both TM2 and TM4 in the membrane (64,65). Other examples include exposure of both the TM10 of band 3 (66), as well as the TM6 of cystic fibrosis transmembrane conductance regulator (CFTR) to the ER lumen during biogenesis (67).

Despite these examples depending on interactions contained in the same polypeptide chain, different instances exist in which TM-TM interactions stemming from different proteins are required for topogenesis. If the single-pass T-cell receptor α (TCR α) fails to assemble through TM-TM interactions with the heterodimer formed by the cluster of differentiation 3 chains δ and ε (CD3δε), the polar TM segment of TCR α will slip into the ER lumen, and the protein sent to ER associated degradation (ERAD) (68,69). Another example comes from the multipass CAML, which fails to insert all of its TM segments without its TM partner WRB (70,71).

i. The ER membrane protein complex

The ER membrane protein complex (EMC) is a protein complex with a role on membrane protein topogenesis. Initially discovered through a yeast screen used to identify genes required for protein folding, where it was observed that deletion of the EMC resulted in the accumulation of misfolded membrane proteins (72). The mammalian EMC is composed of 10 subunits (EMC1-10) (73), seven of which are ER membrane-embedded, and three (EMC2, 8, and 9) are expressed in the cytosol (Fig. 4).

According to a stream of recent data, the EMC acts as a membrane protein chaperone and insertase, i.e. a protein that is able to insert TM segments into a lipid bilayer. This seems to be true for both co-translational assistance with signal anchors (75-77), but also a post-translational role with TA proteins (76,78,79). Additionally, ribosome profiling experiments performed in yeast have found that pulling down ribosomes in close proximity to EMC5, led to an enrichment for transcripts where the translation of a TM cluster had already happened. This enrichment was particularly pronounced for multipass proteins with charged amino acid residues in their TM sequence, usually transporter proteins (77). With this unbiased approach it became clear that the EMC has an affinity for polar, low hydrophobicity TM segments. Additionally, the EMC was also implicated in the insertion of the first TM segment of G protein-coupled receptors (GPCR) in the right orientation. Depletion of the complex led to a marked decrease in the correct topology of GPCRs, whose TM1 was now being inserted by the Sec61 translocon
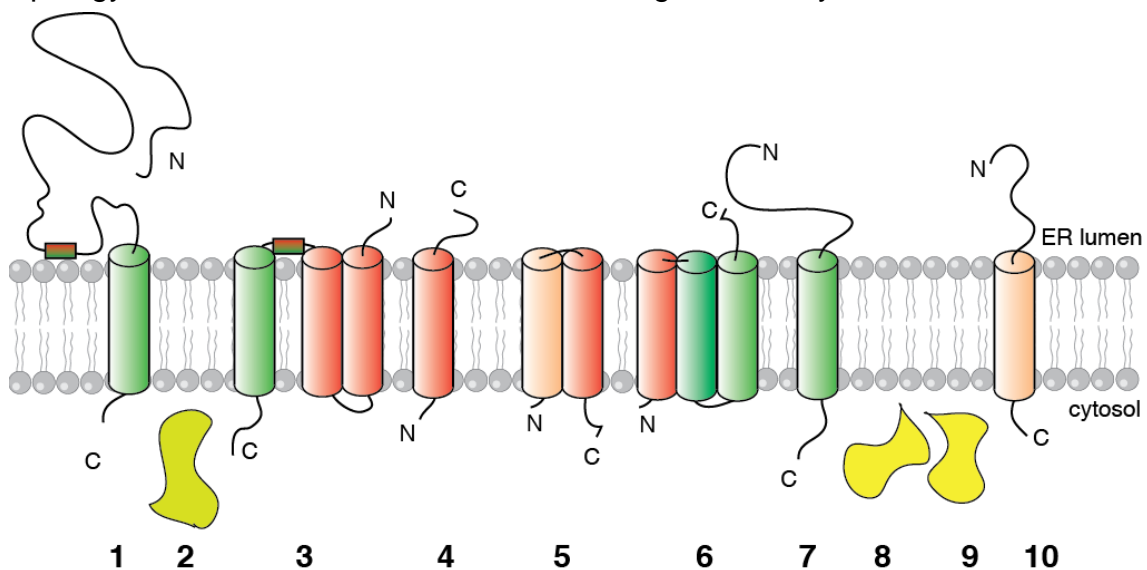
Figure 4: Schematic of the EMC. The different EMC subunits are presented as cartoons showing their cellular expression and membrane topology. Numbers represent the respective EMC subunit, and "N" and "C" of the N- and C-terminal, respectively. ER luminal loops for EMC1, EMC7, and EMC10 are meant to represent the presence of long domains. TM helices are colored according to their propensity for membrane integration, according to dgpred.cbr.su.se and topcons.cbr.su.se. Both EMC1 and EMC3 have an amphipathic helix which can associate with the ER lumen membrane leaflet (74).

(75). Furthermore, viral multipass protein biogenesis has also been extensively accredited to the EMC (80,81).

Three recent cryo EM structures of the human and yeast EMC (74,82,83) as well as characterization of the cytosolic components of the complex (84) have brought to light the possible mechanism of action of this complex. One of the findings was that the cytosolic architecture of the EMC is only composed by two subunits and not three. The cryo EM structures identified only EMC8, and not EMC9, and purification of EMC2 showed this subunit in a complex with either EMC8 or EMC9, never both. Interestingly these two subunits share high sequence identity, and the presence of both genes is not conserved across species (85).

When it comes to targeting, it was found that on the cytosolic side of the membrane, EMC3 (also found to be the main interactor with a TA substrate) contained an unstructured stretch of Met residues. This is highly similar to what has been observed for the SRP54, but also for Get3 (yeast homolog of TRC40) (8,86). This way, a TM segment can be initially accommodated in the cytosolic face of the complex. Not only this, it was also confirmed that, structurally, EMC3 shows similarities with the mitochondrial Oxa1 superfamily of membrane insertases. This had been postulated before to both the EMC3 and WRB through topology and co-evolution bioinformatical approaches (87). Furthermore, two amphipathic helices from the EMC1 and EMC3 are placed on the cytosolic side of the membrane (74,83). Amphipathic helices are known to be able to remodel the lipid bilayer (88), and are often implicated in lipid stress sensing (89), aspects that can be associated with the EMC.

Right at the membrane side of the Met groove in EMC3 is a vestibule, partially open to the cytosol, and highly enriched in conserved hydrophilic residues. Some differences arose from the structures of human and yeast EMC, where in the first one this vestibule is postulated to be formed mostly by EMC3 and EMC6, and in the second largely by EMC3 and EMC4. The first TM segment from the EMC6, previously thought to be expressed in the ER lumen (90), contributes to the formation of this hydrophilic vestibule. Based on the preference of the EMC for polar (low hydrophobicity) TM segments, the presence of such a hydrophilic vestibule in both the yeast and mammalian complexes makes sense mechanistically. Not only this, consistent with other translocases, it was also observed that the EMC can locally thin the lipid bilayer, which could potentially enable both TM integration and substrate treading into the ER lumen (74).

10

On the luminal side of the membrane mostly lie domains from EMC1, EMC4, EMC7, and EMC10. EMC1 forms two beta-propeller domains, which could in principle interact with a polypeptide chain coming into the ER lumen, or serve as a scaffold for quality control factors (83,90,91). Furthermore, the deciphered structures also revealed that a EMC4 segment previously thought to be membrane embedded, is actually expressed in the ER lumen.

The recent data into the EMC functions and its structure has definitely clarified a lot of aspects regarding the complex, ca. ten years after its first discovery (72). From its insertase activity to its chaperoning functions (83), the complex has quickly provided new insights into membrane protein biogenesis.

c. Signal peptidase

The signal peptidase complex (SPC) is an ER membrane protein complex responsible for the cleavage of signal peptides from ER-targeted soluble and transmembrane proteins. The discovery of signal peptides came from the observation that an antibody light chain was synthesized as a higher molecular weight precursor, which would be converted to the "authentic product" if the synthesis was performed in the presence of microsomes (92). The SPC would later be purified from canine microsomes and described as a six-subunit, later to be rectified to a five-subunit complex by work from the same group (93,94). The subunits were named based on their molecular weight – SPC12 (gene name *SPCS1*), SPC18 (*SEC11A*), SPC21 (*SEC11C*), SPC22/23 (*SPCS3*), and SPCS25 (*SPCS2*) – and shortly after their discovery both topology, glycosylation, and primary structure had been characterized for all (94-99). All proteins are membrane embedded, and share a type II topology on their first TM segment. SPC12 and SPC25 span the ER membrane twice, while the three other subunits are single-pass. Only SPC22/23 is glycosylated, and different glycosylation patterns generated the initial believe this subunit was in fact two. Interestingly all eukaryotes seem to conserve one and only one glycosylated subunit in the SPC (Fig. 5) (100).

The mammalian SPC is a Ser protease that uses a SHD catalytic triad (101). Briefly, the basic His residue in this active site can form hydrogen bonds with the Ser, and the acidic Asp. This turns the Ser hydroxyl oxygen into a good
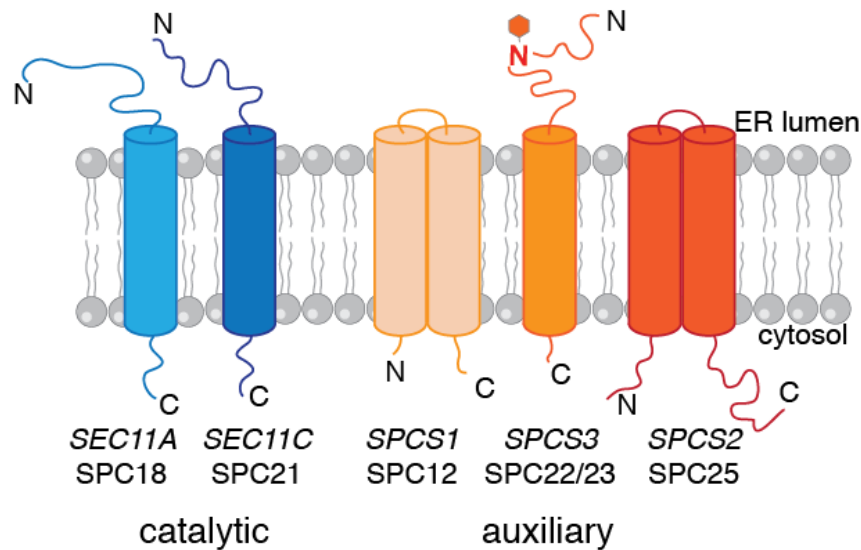
Figure 5: Schematic of the SPC. Membrane topology of the catalytic (in shades of blue) and the auxiliary subunits (in shades of orange) of the SPC. Gene (in italic) and protein names are given below each subunit. Termini are indicated with a "N" and "C". A red "N" and hexagon in *SPC3* represents glycosylation.

nucleophile, which will attack the carbonyl oxygen on the scissile bond of the substrate. This then results in the release of the C-terminal portion of the substrate. A similar reaction occurs after, this time with an activated water molecule taking the role of the nucleophile due to activation by the His residue, with consequent release of the substrate (102,103). Work in yeast has first attributed the catalytic activity of the SPC to its Sec11 subunit (104), which was later found to be a homolog of both SPC18 and SPC21. These two subunits contain the conserved SHD catalytic triad, similarly to Sec11, leading to the speculation that SPC18 and SPC21 would act as the catalytic center for the SPC, perhaps in two different sets of complexes (95,96,105). Further studies in yeast have also reported the SPC22/23 homolog subunit to be essential for SPC activity (106), and that the yeast homolog SPC25 interacts with the translocon (107,108). Interestingly enough, the different published structures for the Sec61 translocon have not identified any densities corresponding to any SPC subunit (19,109).

Signal peptides are found in the N-terminal of ER targeted proteins and act as its signal sequence, when present. Mechanistically, once a signal peptide interacts with Sec61, it will invert its orientation in the membrane, adopting a looped conformation, in which its N-terminal faces the cytoplasmic side of the ER membrane, allowing for the downstream polypeptide to be exposed to the ER lumen (110). Signal peptides are ca. 20-30 amino acid residues in length, extremely heterogeneous in sequence, but share three main regions deciphered early by sequence analysis: a positively charged N-terminal region (termed n), an hydrophobic (h) central section, and a slightly polar C-terminal (c) region where the SPC cleavage site is located (111,112). The same type of sequence analysis showed sequence features that seemed conserved, namely helix-disrupting Gly or Pro being found at position -5 and -4 (with the cleavage site being placed between amino acids -1 and 1), and positions -3 and -1 being occupied by small neutral residues, which seem to be excluded of position -2, where aromatic residues seem to be preferred (112,113). Cleaved signal peptides can be further processed at their h-region by the intramembrane protease signal peptide peptidase (SPP) (114). Cleavage by SPP was found to be required for detection of the N-terminal portion of a signal peptide in the cytosol, after extraction from the membrane, where this peptide fragment can bind calmodulin (115).

Non-canonical signal peptides can be defined as SPC-catalyzed proteolytical events that take place outside the first TM segment of a protein, or when a cleavage site is present after the N-terminal portion of a polypeptide chain. Such events seem to be rare on the mammalian proteome, but instances have been described in the literature. Namely, the human immunoglobulin superfamily member 1 (IgSF1) is as a large protein containing five N-terminal immunoglobulin domains, followed by two TM segments, another six immunoglobulin domains, and a C-terminal TM segment. Studies in HEK293 have shown that IgSF1 undergoes SPC-mediated cleavage in its second TM segment, effectively producing two species, one with five, and another with six immunoglobulin domains, both tethered to the membrane by a single TM segment (116). Additionally, in vitro translated murine Astrotactin 1 and 2 have been found to be processed by the SPC on their second TM segment (117), and one example of SPC cleavage of TA protein has also been found (118).

Regardless. the most common substrates for non-canonical SPC cleavage are viral proteins. Early work has observed that multiple viruses can make use of the SPC for multiple processing events of a single polyprotein into individual polypeptide chains, with special relevance for their infectivity (119,120). *SPCS1* has been proposed to have a role in the recognition of this cleavage sites in flaviviruses. Depletion of this SPC subunit has precluded viral polyprotein processing, and infectivity of this class of viruses, in a manner directly dependent on the viruses internal signal peptides (121). As such, even though viruses make extensive use of the SPC in a non-canonical manner, events where the same happens for mammalian proteins are rare and seem to have been selected out through evolution.

d. Trafficking through the secretory pathway

Once membrane proteins are properly folded and/or assembled, a protein destined to another organelle than the ER can proceed trafficking through the secretory pathway. Trafficking is mostly sustained by cytoskeleton proteins, which form the filaments on which vesicular trafficking can occur. In general terms, protein coated vesicles must be packed with the proteins to be carried, targeted to the intended organelle, and fuse with its membrane (122).

Trafficking out of the ER occurs at ribosome-free specialized <u>ER</u> <u>e</u>xit <u>s</u>ites (ERES). ER-to-Golgi trafficking is mediated by COPII-coated vesicles, made up of a multi-protein complex capable of budding the ER membrane (123). Some models indicate membrane proteins to be exported from the ER can directly interact with components of the COPII coating (124). After loaded vesicle budding as occurred at the ERES, the COPII coating is typically shed, and the vesicles fuse to form the <u>ER</u>-<u>G</u>olgi <u>I</u>ntermediate <u>c</u>ompartment (ERGIC). Arrival of vesicles to the Golgi relies on microtubule dependent trafficking of ERGIC vesicles, as well as their fusion with the first cisterna in the *cis*-Golgi (122). Intra-Golgi trafficking is still a heavily debated topic, yet missing any obvious resolution. At least five different models have been proposed. The probably most accepted ones are the vesicular transport model and the cisternal maturation model. In the first, cisternae from the *cis*- to the *trans*-Golgi are viewed as mostly static, and cargo moves from one cisterna to the next via COPI vesicles. On the other hand, the cisternal maturation model proposes cisternae gradually moving from the *cis*-

to the *trans*-Golgi, COPI vesicles trafficking cargo from older cisternae to newer, and, ultimately, disintegration of older *trans*-Golgi cisternae into secretory vesicles (125,126).

In spite of this debate, it is well established that proteins originally glycosylated in the ER can have their sugar moieties further modified in the Golgi apparatus, generally resulting in further branching or oligomerization of their sugar modifications (127). It is also in the Golgi apparatus that most trafficking and secretion decisions are made, in which proteins can usually take up one out of four paths: either back to the ER, being retained in the Golgi, delivered to the plasma membrane, or, lastly, being delivered to the endolysosomal system.

In terms of trafficking pathways, proteins destined back to the ER (e.g. ER resident proteins) will be engulfed in COPI vesicles at the *cis*-Golgi and transporter back (128). This retrieval process is usually mediated by the presence of ER retrieval sequences, such as cytosolic dilysine (e.g. KKXX) motifs, which can interact with COPI (129), or a luminal KDEL motif, which can interact with a KDEL receptor (KDELR) on the Golgi. The structure of the KDELR was recently resolved, informing towards the basis of KDEL binding and KDELR ER-to-Golgi trafficking, and vice-versa (130). In its apo, unbound state, KDELR has an extensive cytosolic negatively charged patch, which is thought to mediate its interaction with COPII and traffic to the Golgi. Previous work had already characterized how the relatively more acidic pH of the Golgi, when compared to the ER, promoted KDEL-KDELR binding (131,132). As such, in the Golgi apparatus, the receptor and its substrate can interact, in a manner that is stabilized by salt bridges and hydrogen bonds between the two proteins. Protonation of a His residues is thought to be at the basis of KDELR pH sensing, since at the lower pH levels of the Golgi, this protonation reaction enables the TM6 of KDELR to be positioned in a way that is prone to substrate binding. Finally, ER retrieval is promoted in the KDEL bound state of KDELR, which was found to expose Lys residues (buried in the apo state), that are able to interact with COPI and traffic back to the ER (130).

Other interesting models for sorting exist, in which the length of a TM segment can determine the steady-state expression of a given membrane protein: proteins retained in the ER without any COPII interacting motifs, can be made to progress in the secretory pathway by extending their TM lengths

(133,134). Furthermore, Golgi resident proteins are retained through a myriad of mechanism which can also involve the presence of retention motifs, such as KXD/E (135). Trafficking from the Golgi to the endolysosomal system is mostly mediated by clathrin-coated vesicles, while transport to the plasma membrane does not necessarily rely on clathrin and seems to be relatively more heterogeneous (136,137).

Once at the plasma membrane, proteins can be endocytosed both in clathrin-dependent and independent ways. Both types of endocytosis result in trafficking to early endosomes, from where proteins can be recycled back to the membrane in a fast, clathrin-independent way, or traverse first to an endocytic recycling compartment or even the Golgi complex, in ways largely dependent on Rab proteins (138). Protein recycling is especially relevant since it has been reported cells can internalize their membrane proteome from one to five times in an hour (139). Proteins that fail to be recycled back are terminally sent to the late endosome, which once fused to a lysosome will form an endolysosome where degradation takes place (140).

2. Membrane protein quality control and ERAD

From the moment a protein enters the mammalian ER, an extensive network of chaperones and folding enzymes collaborate to ensure correct protein folding. The physical separation of its lumen from the cytosol and the presence of specific enzymes allows for an environment that is unique when it comes to folding and post-translation modifications (PTMs). The oxidative environment allows for the formation of disulfide bonds, and the presence of an oligosaccharyltransferase (OST) enzyme complex for Asn-linked glycosylation to occur. These modifications can aid in protein folding but also be used to detect the folding status of a protein. As such, the ER has also evolved machineries to detect and handle terminally misfolded proteins, and send them to degradation in the cytosol.

One of the aspects that makes quality control of membrane proteins so complex is the fact that, when compared to their soluble counterparts, membranes proteins are exposed to at least two different environments: a lipid bilayer as a way of membrane integration; and an aqueous environment in the form of the lumen of a secretory organelle, the cytosol, or the extracellular space.

Different machineries and mechanisms for quality control can be found in any of these environments.

a. Lectin based ER protein quality control

As a polypeptide chain is emerging into the ER lumen, the OST can catalyze the transfer of a sugar moiety to the Asn residue of an NXS/T sequence. Glycosylation was shown to occur 65-75 residues away from the peptidyltransferase site in the ribosome, which puts the distance for glycosylation ca. 12-14 amino acid residues away from the membrane (141). Importantly these considerations assume an extended conformation for the polypeptide chain (142), since structure formation has been observed to thwart glycosylation (143).

Glycosylation can help shielding hydrophobic patches in the surface of a protein, improve solubility and reduce aggregation, and perhaps most importantly, serve as a binding moiety for <u>ca</u>l<u>n</u>e<u>x</u>in (CANX) and <u>ca</u>l<u>re</u>t<u>i</u>culin (CRT), and hence be used as a folding sensor in the ER (144).

The human OST is hetero-heptameric protein complex where the paralog STT3A and STT3B subunits have the active site of the complex. STT3A is located close to the translocon thus being able to add the sugar moiety to sequons co-translationally (145), while STT3B is able to do so post-translationally and to compensate for failed transfer reactions from STT3A (143). Additionally, one auxiliary subunit of the complex, N33, was discovered to have a CXXC motif, later characterized to form transient disulfide bonds with OST substrates, delaying

their folding, and presumably improving glycosylation rates (146). In alternative OST complexes, the N33 subunit is replaced by magnesium transporter protein 1 (MagT1), which interestingly keeps the ability of the complex to form mixed disulfides with glycosylated substrates (147).

Glycosylation starts with the attachment a sugar molecule composed of $GlcNAc_2Man_9Glc_3$. The two terminal Glc can be trimmed by action of the glucosidases 1 and 2, generating $GlcNAc_2Man_9Glc_1$ (148), which is the core glycosylated form that can enter the CANX/CRT cycle by interacting with both proteins (149,150). These two lectins both contain a Pro rich P-domain which can recruit different chaperones (such as ERp29, ERp57, and cyclophilin B) to their glycosylated substrate thus helping in folding (151). Removal of the last Glc by glucosidase 2 renders the substrate unable to bind to CANX/CRT, ending a first cycle of folding. Proteins decorated with $GlcNAc_2Man_9$, and deemed correctly folded can progress in the secretory pathway. However, if at this point the protein is still not folded into

Figure 6: Simplified overview of the processing and fate of glycans in the ER. Protein glycosylation starts with the attachment of $GlcNAc_2Man_9Glc_3$ to an Asn residue. Glucosidases 1 and 2 remove two terminal Glc residues, in red, resulting in the glycan that can enter the CANX/CRT cycle. The removal of the last Glc residue allows the glycosylated protein to proceed in the secretory pathway. If the native state has not been reached yet, UGGT can add a terminal Glc back to the glycan, warrantying its reentry in the CANX/CRT cycle. Proteins deemed terminally misfolded have some of their Man residues, in orange, removed to different extents, as seen by the shading of the Man residues. This reaction is catalyzed by ER Man I and EDEMs, which results in ERAD targeting. GlcNAc are colored yellow.
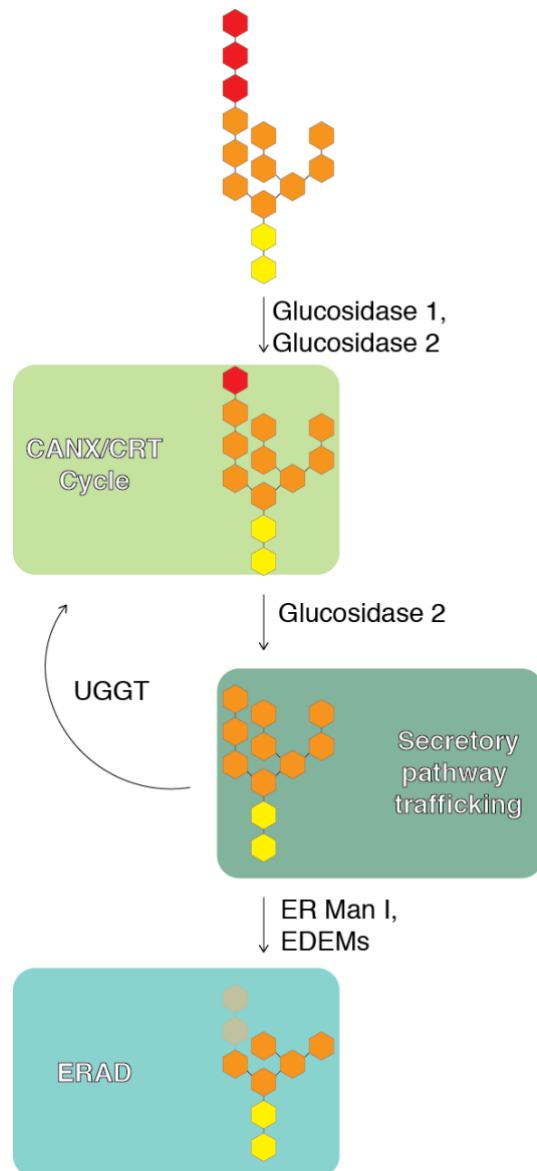
its native structure, the glycoprotein has a new Glc added back by the UDP-glucose:glycoprotein glucosyltransferase (UGGT). The activity of this enzyme is restricted to glycosylate non-native proteins only, meaning the substrate can reenter the CANX/CRT cycle (Fig. 6) (152,153).

Finally, proteins which are deemed terminally misfolded have some of their Man moieties removed by the ER alpha1,2 mannosidase I (ER Man I) and the ER degradation-enhancing mannosidase-like proteins (EDEMs), usually resulting in $GlcNAc_2Man_{5-7}$ (Fig. 6) (154). A mannose trimming timer model has been proposed, where the slow rates of these enzymes give time for slow folding proteins to achieve their native conformation without being preemptively sent to ERAD (155). The progressive increase in affinity of sequentially mannose trimmed glycoproteins to both XTP3-B and OS-9 (156,157), shuttles the deemed terminally misfolded protein to the HMG-CoA reductase degradation 1 (Hrd1) ERAD pathway outlined below (158).

Finally, an interesting mechanism for QC was described for transthyretin which is usually non-glycosylated: protein misfolding induces post-translational glycosylation of a cryptic site, allowing the protein to be handled via a lectin-based quality control (159).

b. Chaperoning in the ER

As mentioned, membrane proteins of the ER are exposed to different folding environments, all of which need to be chaperoned to ensure proper folding, and avoid premature protein degradation. Their mechanism of action for chaperones is discussed below, but in general terms, cytosolic chaperones must shield hydrophobic regions on a polypeptide chain, the same regions that will be buried in the core of a native state protein, away from the aqueous cytosol. When it comes to chaperoning in the cytosol, CFTR is one of the membrane proteins with the most well characterized folding pathways. Since ca. 70% of the twelve TM segment protein is expressed outside the ER, cytosolic quality control factors play an important role in CFTR maturation and folding. The constitutively expressed Hsc70 and its inducible homolog, Hsp70, have been shown to help CFTR maturation (160). Hsc70 and Hdj-2, one of its J-domain co-chaperones, were shown to interact with CFTR[wt] in the early stages of synthesis, but also to preferentially interact with a CFTR folding-deficient mutant (161). A recent study

aiming to streamline the binding of Hsc70 and its co-chaperones to CFTR peptides, has also revealed that (co-)chaperone interaction to native-state buried portions of CFTR can readily be detected (162). Additionally, overexpression of Hsp70 and its Hdj-1 co-chaperone, enhance plasma membrane expression of CFTR (163). Hsp90 is another cytosolic chaperone, whose inhibition accelerates CFTR degradation, arguing for Hsp90-assisted CFTR folding (164).

On the ER lumen, chaperoning mechanisms are often based on the emergence of an unstructured polypeptide chain into the ER lumen. As such, interaction of particularly hydrophobic patches that would normally be buried in the hydrophobic core of a protein can occur in the aqueous environment of the ER, possibly leading to protein aggregation. One of the major proteins chaperoning these regions is the Hsp70 of the ER, BiP. First discovered for binding to free (unpaired from their light chains) antibody heavy chains (165), it was soon thereafter discovered this chaperone can recognize relatively short sequences (seven amino acids long) of preferably aliphatic, apolar amino acids (166).

BiP has two domains, an N-terminal n̲ucleotide b̲inding d̲omain (NBD), followed by a linker region, and a C-terminal s̲ubstrate b̲inding d̲omain (SBD). Binding to substrates is regulated through nucleotide binding as is true for other members of the Hsp70 family. A cleft on the NBD can bind ATP which results in association between the NBD and SBD, where a lid in the latter is opened, resulting in a high on/off rate of substrate binding, meaning substrates released from this state are given a chance to fold. Once ATP hydrolysis occurs, the two domains undock from each other, the lid in the SBD is closed, and binding of unfolded substrates to this domain is stabilized (167).

Two groups of proteins are involved in the BiP chaperone cycle – n̲ucleotide e̲xchange f̲actors (NEFs) and E̲R̲-localized D̲na̲J (ERdj) proteins. In the ER both SIL1 (168) and g̲lucose r̲egulated p̲rotein of 1̲7̲0̲ kDa (Grp170) serve as NEFs for BiP (169). These proteins promote the ADP release from the BiP-substrate complex, allowing then for a new ATP molecule to bind to BiP and consequently for the client substrate to be released from the chaperone (170). Their importance for cell physiology comes from data showing mutations in SIL1 can lead to Marinesco-Sjörden syndrome in humans (171), and that knockouts of Grp170

lead to embryonic lethality in mice (172). Interestingly, Grp170 seems to also have chaperone activity, sharing the binding preference of BiP to unfolded proteins (173). Grp170 has also been shown to have an holdase-dependent role in the ERAD of a sodium channel, in a way independent of its own ATPase activity, or interaction with BiP (174,175). Further support of the function of this chaperone in ERAD came from the observation that Grp170 interacts with SEL1L, an adaptor of Hrd1, to assist in substrate ERAD (176).

ERdj proteins can act on the other side of the BiP cycle, by interacting with the ATP-bound form of BiP, stimulating its hydrolysis and favoring the interaction of BiP with its substrate (Fig. 7) (177). The J domain present in these proteins is a stretch of ca. 70 amino acids with a conserved HPD motif important for ATPase activity stimulation (178). In the ER there are at least seven proteins containing a J- domain in their structure, and four of these have been reported to interact directly with unfolded substrates, where release from these is dependent on the ATPase activity of BiP (179,180). Different ERdj proteins will have different effects on protein folding and degradation, while differences in binding site preferences have also been observed (181). ERdj1 and ERdj2 (Sec63, discussed above) are often associated with the Sec61 translocon and seem to both recruit BiP and guarantee BiP is present in the luminal side of the ER membrane upon translocation; ERdj3 has been also associated with polypeptide entry into the ER lumen, while ERdj4 has been heavily implied in ERAD for having a preference to bind aggregation-prone peptides; ERdj5 is a protein disulfide isomerase (PDI) with high reductase activity, and has been implied in the ERAD of disulfide linked oligomers, and in the reduction of mixed-disulfides. ERdj6 and ERdj7 remain the least studied ERdj proteins, notwithstanding ERdj6 seems to be involved in pro-folding pathways, while ERdj7 may be involved in ERAD of misfolded proteins (180-183).
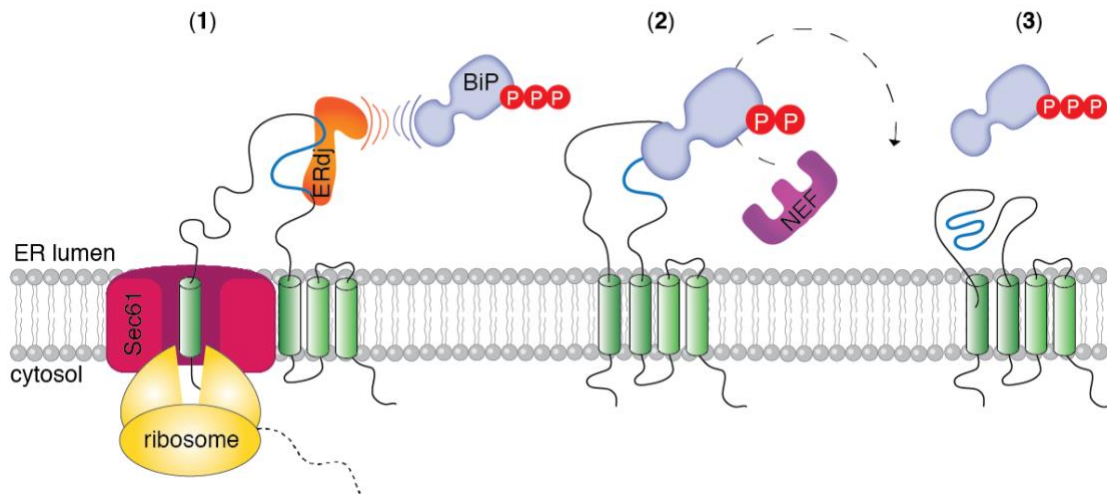
Figure 7: The BiP chaperoning cycle. (**1**) A translocation polypeptide is shown with a hydrophobic patch, in blue, being recognized by an ERdj protein, in orange. Through the action of the ERdj, BiP is recruited to the hydrophobic peptide, will have its ATP hydrolyzed (shown as three circles with a "P"), and bind to its now substrate peptide. (**2**) BiP binding prevents premature aggregation of the peptide, while through the activity of a NEF (in purple), an ATP molecule is added to BiP, replacing the ADP, and the peptide is released from the chaperone, (**3**) folding into the hydrophobic core of the membrane protein.

Lastly, the activity of BiP can also be controlled through PTMs (discussed below), or via stabilization of a specific nucleotide-bound state. The mesencephalic astrocyte-derived neurotrophic factor (MANF) has been shown to interact with BiP (184), and a recent report demonstrated that such interaction is promoted on the ADP-bound state of BiP. Since MANF is able to inhibit nucleotide exchange in the chaperone, this protein is known to stabilize BiP-substrate complexes (185).

The glucose-regulated protein of 94 kDa (Grp94), the Hsp90 of the ER lumen, is the most abundant glycoprotein in the ER and another important chaperone involved in protein folding with (long debated) ATPase activity (186,187). This chaperone has three main domains (N-terminal, N; middle, M; C-terminal, C), and is expressed as a homodimer (though interaction of Grp94 C-domains), similarly to other members of the Hsp90 family (188). Also, similarly to BiP, conformational changes brought by ATP binding (in the N domain) and hydrolysis (by way of the M domain), drive its chaperoning activity (189,190). Most models on Hsp90 interaction with substrate proteins put this interaction at a later stage of client folding, after Hsp70 interaction with the same substrate. It has been shown recently that murine BiP and Grp94 can interact with each other, preferably if BiP is bound to ADP. This gives rise to an attractive model where

BiP can hand substrates to Grp94, where BiP can also promote the Grp94 ATPase activity (191), although several aspects of Grp94 remain to be elucidated.

Chaperoning of TM segments in the plane of the membrane is a less described process. A protein previously shown to associate co-translationally with the first TM segment of an opsin protein, protein associated with the ER translocon of 10 kDa (PAT10) (192), was recently discovered to have chaperoning activity on TM segments (193). PAT10 was identified as a heterodimer, built from Asterix and coiled-coil domain-containing protein 47 (CCDC47). Asterix was shown to be able to bind TM1 segments of GPCRs in a reporter construct, and CCDC47 was considered essential for the stability of Asterix. Mechanistically, Asterix can bind TM segments with hydrophilic amino acid residues, once substrate TM segments have been released from Sec61. Its chaperoning activity comes to light since depletion of the PAT10 complex reduces the expression of different multipass membrane proteins, and its interaction with substrates is mostly lost when such substrate are fully folded (193).

Another major intervenient in protein folding in the ER is the PDI family of folding enzymes. This family is able to catalyze disulfide bond oxidation, reduction or isomerization through the presence of a conserved CXXC motif in their active sites, which can itself be found either reduced or oxidized in the catalytic cycle of these enzymes (194). Since approximately one third of all proteins in the secretory pathway form disulfide bonds (195), chaperoning of this process is most important. The ER lumen is considerably more oxidizing than the cytosol and disulfide formation can be seen during the co-translational translocation of a polypeptide into the ER lumen (196). Accordingly, fidelity of this process must be chaperoned as to avoid the presence of mixed, non-native disulfides in the fully translated protein product. This activity was first attributed to (the canonical) PDI, due to its ability to re-oxidize ribonuclease with reduced disulfides (197). Later research has also characterized different proteins that allow for PDI to remain in an oxidizing active form, namely the ER oxidoreductin 1 (Ero1) (198,199) found to be, among others, one of the donors of disulfides to PDI (200). Further research has identified at least 21 proteins belonging to the PDI family, alongside their unifying feature of containing at least one thioredoxin domain homolog (201). This

diversity also applies to the function of each different PDI, since different PDIs can catalyze different oxidoreduction reactions, from formation, to reduction, to shuffling of disulfides, in different substrates, depending on the PDIs redox potential. Mixed, non-native disulfides have also been observed to play an important role in protein folding, by e.g. bring two regions of a nascent polypeptide in close proximity, albeit in the native state this disulfide bond may be found reduced, effectively driving the equilibrium of sequential folding steps forward (202).

PDIs are also heavily implicated in ERAD mostly through their reductase activity. Translocation from one ERAD substrate from the ER lumen to the cytosol is depend on retrotranslocation machinery, usually envisioned as a pore. The presence of oligomeric complexes with mixed disulfides, or proteins whose structure becomes overly compact to pass through such a pore requires polypeptide extension by way of disulfide reduction. In fact, several examples of this have been observed, putting the reducing activity of PDI or ERdj5 as a prelude to retrotranslocation (203-206).

c. ERAD

Despite evolution of multiple chaperoning mechanisms, mammalian cells will always need to degrade membrane proteins. This can be done simply as a means to control protein levels in a cell, or due to the expression of misfolded proteins. Membrane proteins misfolding takes several forms, from point mutations causing domain destabilization, or membrane misintegration, to the misfolding seen in orphan subunits of a protein complex, where proteins without a binding partner cannot fold correctly, as discussed previously.

ER-phagy is one of the means cell use to dispose of ER proteins, where parts of the ER, including its lipids and proteins, are delivered to a lysosome. Mechanistically speaking, small portions of the ER, or even ER-derived vesicles can fuse with lysosomes. Alternatively, autophagosomes can engulf large portions of the ER, and then fuse with a lysosome. ER-phagy not only controls the size of the ER, but is also important for the disposal of protein aggregates, and proteins that cannot undergo ERAD (discussed below) (207). Such proteins include procollagen, which is recognized by calnexin when misfolded. The lectin

can then interact with FAM13B, an ER-phagy triggering protein, driving ER-phagy and procollagen degradation (208).

Alternatively to ER-phagy, the most common way of protein disposal is ERAD. The ERAD of transmembrane proteins can follow different routes based on the environment and nature the degron in question. A classification system has been proposed for ERAD, to try and unify machineries and mechanisms of action, based on the location of the degron in cause: ERAD-C refers to the presence of degrons in a cytosolic domain of a protein, ERAD-M refers to degradation of membrane proteins with a membrane embedded lesion, and ERAD-L refers to disposal of ER proteins with a degron in the ER lumen (209).

Despite these differences, ERAD always starts with the recognition of a misfolded protein, followed by the ubiquitination of such protein during or after retrotranslocation from the ER to the cytosol, and finally, proteolysis of the faulty protein by the cytosolic 26S proteasome.

i. Recognition

The first step in ERAD of a membrane protein must be recognition of misfolding. It has become clear that there is no signature for recognition and consequent degradation of a membrane protein, a process which becomes even less uniform when comparing e.g. substrates of ERAD-M or ERAD-L. A misfolded luminal domain (ERAD-L) may be so due to abnormal absence of sugar moieties, or disulfide bonds. Alternatively, fold-disrupting mutations could potentially expose hydrophobic patches that would normally be buried within a domain fold. For transmembrane proteins, the ERAD-M machinery will expectedly not recognize the same features, as hydrophobicity is to be anticipated. Instead, TM mutations may destabilize the α-helical fold of a TM segment, or alternatively, the absence of a binding partner may expose polar, otherwise hidden, residues to the lipid bilayer.

Recognition of degrons for ERAD-C is usually done through the exposure of hydrophobic patches in the surface of a protein, mostly recognized by the cytosolic Hsp70/Hsp40 systems (210,211). The most well-studied E3 ligase associated with ERAD-C is the yeast Doa10, with a less well characterized human homolog membrane-associated really interesting new gene (RING)-CH-type 6 (MARCH6), also known as TEB4 (212). After recognition of a degron by

the cytosolic chaperones it is unclear how handing to MARCH6 occurs, though it was been speculated hand-over is facilitated by prolonged interaction of Hsp70/Hsp40 chaperones with such substrates (213).

As mentioned before, recognition of glycosylated proteins destined to ERAD relies on their glycosylation status by means of Man trimming, and redundant recognition by the luminal lectins OS-9 and XTP3-B (214). Interestingly, it has been reported that targeting does not depend on the sugar moiety recognition alone, but also in the presence of unfolding in the same polypeptide segment, safeguarding premature degradation by enhancing stringency (215). The lectin-bound substrate can then associate with <u>s</u>uppressor/<u>e</u>nhancer of <u>L</u>in-<u>12</u>-<u>l</u>ike (SEL1L), the cofactor of the E3 Hrd1 (216).

Recognition of non-glycosylated substrates is less well characterized and was mostly done, similarly to other ERAD studies, in yeast. However, substrates are mostly thought to be recognized due to the exposure of hydrophobic patches to BiP or XT3P-B, which can in turn deliver them to SEL1L or the <u>homoCys</u>-responsive <u>ER</u> resident <u>p</u>rotein (HERP) and its interaction partner Derlin-1 (73,204,216). The trigger which commits a BiP non-glycosylated substrate to degradation remains mostly elusive, but will most likely rely on substrate interaction with BiP and ERdj proteins associated with ERAD machinery (181,217,218).

When it comes to recognition of ERAD-M substrates this seems to mostly depend on Hrd1, but also its homolog, cell surface <u>g</u>lyco<u>p</u>rotein of <u>78</u> kDa (gp78), as well as Derlin proteins. Recognition is done directly in the plane of the membrane through mechanisms mostly still to be characterized (219). All three of these proteins are embedded in the ER membrane, and at least for Hrd1, its role in recognition has been attributed to the presence of hydrophilic amino acids in its TM domain, which are mostly conserved in gp78 (220). Gp78 has also been implicated in the degradation of ERAD-M substrates, such as orphaned CD3δ (221) or membrane tethered ERAD-L substrates, although a module for recognition has not been elucidated fully (222).

The Derlin family of proteins has three members in mammals all of which are inactive forms of rhomboid intramembrane proteases, and contain TM segments with little hydrophobicity (223). Derlin-1 has been implied in the degradation of transmembrane proteins, possibly through recognizing ERAD-M

degrons (224), and has been shown to form complexes with either Hrd1 or gp78 (225). It has thus been speculated that Derlin proteins may serve as adaptors for E3 ligases and its substrates, by broadening the lineup of substrates recognized and ubiquitinated by the E3 ligase (226).

Another mechanism for protein degradation relies on recognition and intramembrane proteolysis of ERAD substrates. The intramembrane rhomboid-like 4 (RHBDL4) has been shown to recognize orphaned pre-TCRα, and the STT3A subunit of the OST, cleaving both and targeting them to degradation (227,228), while SPP has been implicated in targeting unspliced X-box binding protein 1 (XBP1u) to degradation, by complexing with Derlin-1 and the E3 ligase TRC8 (229,230).

Lastly, sorting receptors are another class of quality control proteins, involved in the recognition of substrates. B cell-associated proteins of 29 and 31 kDa (BAP29/BAP31) are two homologous proteins involved in the recognition and ER retention of several clients (231,232). Membrane-bound IgDs have particularly hydrophilic TM segments, and if association with their membrane binding partners fails, they are recognized by BAP29/BAP31, leading to ER retention, and precluding plasma membrane expression (233). Another well characterized sorting receptor is the retention in the ER 1 (RER1) protein, a membrane protein able to cycle between the ER and the Golgi apparatus. RER1 has four with low hydrophobicity TM segments, and its canonical role is that of an ER-retrieval factor, based on the recognition of polar residue-based signals lying in the TM segments of a substrate (234,235). The bulk of RER1 substrates are unassembled subunits of protein complexes, retrieved from the *cis*-Golgi to the ER (236,237). However, RER1 has also been associated with the ER retention of mutant peripheral myelin protein of 22 kDa (PMP22), with apolar-to-polar missense mutations in its TM segments (238).

ii. Retrotranslocation

Substrate retrotranslocation refers to the movement of a polypeptide chain from the ER lumen or membrane to the cytosol through a presumably proteinaceous channel. Retrotranslocation must occur before substrate ubiquitination for luminal substrates, but is mostly coupled and dependent on ubiquitination for TM substrates (239). The identity of this channel remains

relatively elusive, with several different potential retrotranslocons having been hinted at, such as Sec61, Hrd1, and Derlin proteins.

The Sec61 translocon was first accredited to perform too the reverse of its canonical role when non-glycosylated (i.e. at least partially exposed to the cytosol) MHC molecules were found to interact with different subunits of the Sec61 complex (240). Additional hints are based on direct interaction of Sec61 with components of the proteasome, and the development of Sec61 mutants which curtail retrotranslocation specifically, without much effect on protein import into the ER (241,242).

The case for Derlin-1 came two light with two studies published at the same time. One of these studies identified Derlin-1 by probing for a p97 (described below) receptor in the ER membrane (243), whilst the other study identified it by looking for interactors of the viral protein <u>u</u>nique <u>s</u>hort region protein <u>11</u> (US11), which promotes the retrotranslocation and consequent degradation of MHC molecules (244). Later quantitative work with purified microsomes showed that retrotranslocation of a luminal substrate was inhibited when the cytosolic C-terminal of Derlin-1 was blocked with an antibody, while blocking either end of Sec61 had no effect on retrotranslocation (245). Recently the yeast Derlin Dfm1 was also shown to be important in the retrotranslocation a self-ubiquitinating ERAD-M substrate, where in its absence, Hrd1 can take over this activity (246).

Hrd1 has up until now been the most relevant candidate for a retrotranslocon. The first hints for this came from crosslinking of yeast Hrd1 TM segments to an ERAD-L substrate, and the fact that Hrd1-mediated ERAD could still occur even in the absence of its complex partners (e.g. the yeast homolog of SEL1L) arguing for a central role of Hrd1 in ERAD and retrotranslocation (247). More recently, experiments performed in liposomes have shown Hrd1 being sufficient to retrotranslocate a membrane-tethered ERAD-L substrate via autoubiquitination of Hrd1 itself (248), while deubiquitination of the E3 by another ER associated <u>deub</u>iquitinating enzyme (DUB) prevents Hrd1 degradation in the face of its autoubiquitination (249). These results were mostly confirmed through electrophysiological experiments where Hrd1 purified into liposomes was able to retrotranslocate another ERAD-L substrate through autoubiquitination (250). Finally, a recent cryo EM structure of the yeast Hrd1 complex showed the E3 forming a lateral vestibule to the membrane, also facing another gate formed by

yeast Derlin-1, which resulted in local membrane thinning, similar to what was previously discussed for the EMC. A proposed retrotranslocation mechanism for glycosylated ERAD-L substrates involves recognition of the glycan moiety and the previously mentioned unstructured segment around the glycosylation site by Yos-9 (the yeast homolog of OS-9 and XTP3-B), and Hrd3 (homolog of SEL1L). This can in turn position the substrate between Derlin-1 and Hrd1, accommodating it between the gates of the two proteins, where the membrane is thinned out (251).

It remains to be described if the same complex participant and rules apply to mammalian systems and ERAD-M substrates, but some studies in mammalian systems are starting to emerge (252).

A recently characterized P5A ATPase, Spf1, was also shown to have dislocation activity (253,254). Based on the cryo EM structure of the protein, its activity relies on TM segment flipping, which does not seem to be the accepted model of extraction for the previously described retrotranslocons (253). Lack of the ATPase had previously been shown to lead to an accumulation of mitochondrial proteins in the ER membrane, through a mostly uncharacterized mechanism (255,256). Through different approaches, Spf1 was shown to remove TM helices from the ER membrane, in an ATPase activity-dependent fashion. Furthermore, the protein was also shown to regulate the abundance of several ER-resident proteins with a type II signal sequence, which may hint towards a role in the retrotranslocation of possible ER substrates.

iii. Ubiquitination and proteasomal degradation

Client ubiquitination takes place on the cytosolic face of the ER. As mentioned the mammalian ER has several E3 ubiquitin (Ub) ligases for this task, but their activity is first reliant on the assembly of a ubiquitination reaction cascade. First, a Cys residue in a E1 Ub activating enzyme binds to the C-terminal Gly residue of the 76 amino acid long Ub, via a high energy thioester bond, followed by transfer of the Ub moiety to another Cys residue, this time in a E2 ubiquitin conjugating (Ubc) enzyme. Finally, the E2 associates with an E3 ligase RING domain to catalyze the transfer of the Ub moiety to a substrate protein via the C-terminal G76 of ubiquitin (257). In most cases this ligation occurs

to the ε-amino group in a Lys residue of the substrate in cause. Ub itself has seven different Lys residues amenable to ubiquitination, and the decision on which of these gets ubiquitinated usually depends on the specificity of E2 enzymes (258). This way, a polyUb chain can contain always the same type of linkage (e.g. all linked through K48, i.e. homotypic), or show heterotypic linkages (e.g. a mix between K11 and K48 Ub linkages). Since substrate ubiquitination can also happen at different Lys (and to a lesser extent Ser, Thr, and Met) residues (259), there is the possibility for a great variety and complexity in the Ub decoration of a protein substrate.

Mono-ubiquitination is usually not a strong enough signal when it comes to proteasomal degradation, and proteasomal targeting will often rely on polyubiquitination, usually through K48 linkages (260). The yeast ER only has two E3 ligases known to date, Hrd1 and Doa10, which mostly depend on the E2 activity of two ER membrane-embedded E2 conjugating enzymes, Ubc1 and Ubc6, and the cytosolic Ubc7 (261).

In the ERAD-C associated Doa10 pathway, both Ubc6 and Ubc7 are used in Ub conjugation. Some studies point towards Ubc6 having a priming role on the activity of Ubc7. A study has found that in the absence of Ubc6, Ubc7 fails to attach polyUb chains to Doa10 substrates (262), while others described how depletion of Ubc6 reduced the amount of K11 linkages in the proteome (263). The Hrd1 pathway depends mostly on Ubc7 and, to a lesser extent Ubc1, activity. Ubc7 activity in both the Hrd1 and Doa10 pathways is also largely dependent on another protein present in these E3 complexes, coupling of ubiquitin conjugation to ER degradation protein 1 (Cue1). This ER membrane protein not only recruits Ubc7 to the ER membrane, but also promotes ubiquitin loading into the E2 and ubiquitin transfer to an ERAD substrate (264,265).

The mammalian ER on the other hand has been shown to have at least 25 different ER associated E3 ligases (266), and even though their activity has yet to be fully characterized, three E2 enzymes seem to be able to handle ERAD for most mammalian substrates (261,267). As such, even though characterization of the ERAD ubiquitination machinery has been extensively studied in yeast, the added complexity in mammalian cells makes some of the possible equivalencies invalid.

30

 Some of the known, but not fully characterized E3 ligases include MARCH6 (268) (the mammalian homolog of Doa10), TRC8 (269), RMA1 (270), or RNF170 (271). Despite this, at least two studies have tried to comprehensively dissect different pathways in ERAD of mammalian cells through genomic and proteomic based approaches (73,267), mostly around on the Hrd1 and the gp78 E3.

 Both Ubc6 and Ubc7 contain two homologs in the mammalian ER: UBE2J1 and UBE2J2 for Ubc6, and UBE2G1 and UBE2G2 for Ubc7 (272). Small differences between yeast and mammalian systems become apparent when comparing the E2 dependency in each E3 branch. While Ubc6 does not participate on yeast Hrd1 ERAD, UBE2J1 does have a role in mammalian Hrd1 ERAD-L, with no apparent role in gp78 mediated ERAD-M (267). On the other hand, comparably to yeast Hrd1 dependency on Ubc7, both Hrd1 and gp78 (the second homolog to yeast Hrd1) use UBE2G2 for efficient substrate ubiquitination, often reliant on the direct transfer of homotypic K48 polyUb chains from UBE2G2 (273). Additionally, even though there is no direct homolog of Cue1 in mammalian cells, another protein, ancient ubiquitous protein 1 (AUP1), seems to serve the same role in recruiting UBE2G2 to the Hrd1/SEL1L complex (274). Interestingly, this AUP1 is dispensable in the gp78 complex, since the E3 is equipped with a domain capable of recruiting UBE2G2 to the ER membrane (73,275).

 It has become clear that regardless of the ERAD targeting pathway, mammalian cells can also use heterotypic polyUb branching in their substrates (such as K11/K48), catalyzed by E3 Ub-chain-diversifying enzymes. These have been proposed to increase degradation, as shown by the increase of affinity of heterotypic chains to the proteasome when compared to their homotypic counterparts (276).

 It is also worth mentioning mammalian ERAD systems often compensate for each other in case of loss of function or overloading. Different substrates can also use multiple E3 ligase pathways for ubiquitination, either be it through Ub priming followed by more extensive polyubiquitination, or substrate ubiquitination at different sites by distinct E3 ligases, among others (277).

 Substrate ubiquitination is also largely significant for the process of retrotranslocation. Most of the topics on retrotranslocation covered until now described the mechanisms and models present in the ER membrane. On the

cytosolic side of retrotranslocation however, the systems that have been described rely on the presence of Ub.

The <u>v</u>alosin-<u>c</u>ontaining <u>p</u>rotein (VCP)/p97 forms cytosolic homohexamers with AAA ATPase activity, and it associates with its heterodimeric cofactor composed of <u>u</u>biquitin <u>f</u>usion <u>d</u>egradation protein <u>1</u> (Ufd1, UFD1L in mammals) and <u>n</u>uclear <u>p</u>rotein <u>l</u>ocalization protein <u>4</u> (Npl4, NPLOC4 in mammals). This complex acts on the cytosol to finish extraction of proteins from the ER membrane, and target them to the proteasome (Fig. 8) (278).

VCP/p97 complexed with Ufd1 and Npl4 can get first recruited to the ER membrane via its cofactors, since both Ufd1 and Npl4 have ubiquitin interacting domains (279). Furthermore, distinct domains in several proteins can recruit VCP/p97 directly to the ER membrane: both gp78 (280) and Hrd1 (281) contain themselves VCP/p97 interacting domains, and different ER protein contain the <u>Ub</u> regulatory <u>X</u> (UBX) domain that can also recruit VCP/p97, such as UBXD8 known to interact with gp78 (73).

The role of VCP/p97 in pulling proteins from the ER membrane relies on initial binding of the Ufd1/Npl4 dimer to greater than five Ub-polyubiquitin chains, which can stimulate the ATPase activity on one of VCP/p97 domains (D2) (282). Sequential cycles of ATP hydrolysis promote sequential, step-wise polypeptide passage and unfolding through a central pore in the hexameric structure of the complex (283,284).

Different protein complexes can associate with VCP/p97 and its dimeric cofactor in the cytosol. The deglycosylating enzyme <u>p</u>eptide:<u>N</u>-<u>g</u>lycosydase (PNGase, also known as <u>N</u>-<u>gly</u>canase <u>1</u>, NGly1) can directly

Figure 8: The ubiquitination cycle of gp78. A faulty membrane protein, with an unstable TM segment (in yellow) is shown associating with gp78. Through the action of the E3 ligase and its cognate E2, UBE2G2, in red, the substrate protein has its cytosolic domain polyubiquitinated. VCP/p97, in brown, is recruited to the complex, where it can pass the polypeptide chain through its central pore. Binding partners of VCP/97 not represented for simplicity.
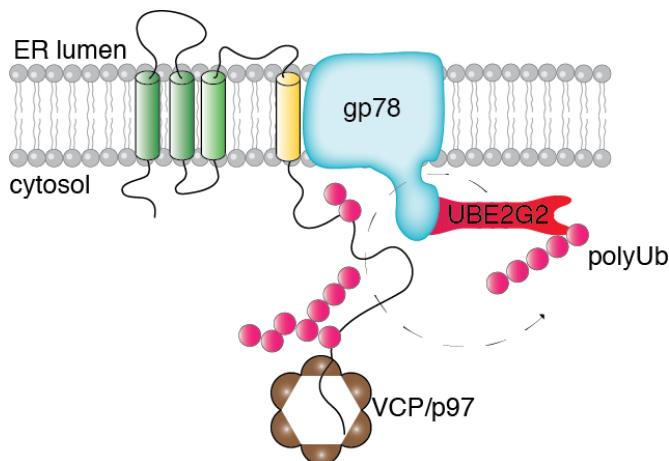
associate with VCP/p97, removing sugar moieties from substrates to facilitate proteasomal clearance (285). Additionally, DUB activity seems to be necessary for release of polypeptides from the VCP/p97 complex, by trimming the polyUb chain (286) which could sterically hinder substrate passing through the aforementioned pore, and enabling Ub recycling. After DUB activity, further polyubiquitination becomes then a requirement for proteasomal degradation of some substrates in which the trimmed polyUb chains are not a strong enough signal. This task is usually performed by E4 ligases, whose name comes from their role in extending preexisting polyUb chains, and include the yeast Ube2 (287), or the mammalian UBE3C and UBR4 (267). A recent report has also shown how a substrate with fewer Ub can still be sent to the proteasome: substrates released from VCP/p97 can be captured in a complex containing BAG6 (288), and the cytosolic E3 ligase RNF126 can reubiquitinate the substrate, warranting a strong proteasomal degradation signal (289).

Delivery of substrates to the yeast 26S proteasome is traditionally mediated by Rad23 (with two mammalian homologs) and Dsk2 (four homologs in mammalian cells, the ubiquilin family, UBQLN1-4 (219)), where both proteins contain ubiquitin binding domains, and are able to interact with the proteasome (290,291). The 26S proteasome itself is composed of two major subunits, the barrel shaped 20S core particle, where the proteolytic active sites around found, and the 19S regulatory particle, which can cover one or both ends of the core particle. Different protomers in 19S can recognize polyUb chains in substrates and by doing so, allow an unstructured peptide to diffuse through 19S and engage with its AAA ATPase machinery, to guide substrate delivery to 20S. Once engagement is set, *en-bloc* deubiquitination can take place, the substrate gets unfolded and ultimately degraded at the core particle by trypsin-, chymotrypsin-, and caspase-like proteases (292,293).

d. ER stress and the UPR

The high influx of proteins to the ER, the action of chaperones and folding enzymes, as well as the degradation machinery associated with this organelle have to be highly controlled for. Spikes in protein production, or the accumulation of misfolded protein can lead to failures in protein folding homeostasis, effectively producing an imbalance between the ER folding load and capacity (294). As

such, cells have evolved safeguard mechanisms in the ER in order to respond to this imbalance, and ultimately restore ER proteostasis, namely the <u>u</u>nfolded <u>p</u>rotein <u>r</u>esponse (UPR). The first observation of what would later be described as the UPR came from the increase in expression of BiP and Grp94 due to accumulation of misfolded proteins in the ER (295).

The mammalian UPR works through the concerted effects of three signaling branches generated by three ER membrane protein sensors, <u>i</u>nositol-<u>r</u>equiring protein <u>1</u> (IRE1), <u>a</u>ctivating <u>t</u>ranscription <u>f</u>actor <u>6</u> (ATF6), and <u>p</u>rotein kinase RNA-like <u>ER</u> <u>k</u>inase (PERK). Being sensors in the ER membrane, each of these proteins will be able to sense a stress signal either in the ER lumen or its membrane, and react with a response in the cytosol (296). Their single or combined activation can lead to multiple cellular phenotypes working to restore and maintain ER proteostasis, namely through reducing the load of proteins entering the organelle, enlarging the volume of the ER by synthesis of new membrane, increasing the expression of pro-folding chaperones and folding enzymes in the ER, but also upregulating the expression of ERAD machinery, in order to deal with accumulation of misfolded proteins. Lastly, if ER stress is maintained, the UPR will trigger cell-death, protecting the whole organism, at the expense of single cells (297).

IRE1 is a single-pass membrane kinase and RNase, and the most conserved and well characterized UPR sensor. In its resting state, IRE1 is expressed as a monomer in the ER membrane with its ER luminal N-terminal domain stabilized by BiP binding through recruitment via ERdj4 (298,299). Its activation is dependent on BiP dissociation, and either unfolded protein or lipid bilayer stress. These will lead IRE1 to oligomerize, and trans-autophosphorylate its cytosolic domain (89,300,301), resulting in the activation of its endonuclease activity and consequent splicing of XBP1 mRNA, to produce, after ligation, the spliced form of XBP1, XBP1s (302). XBP1s encodes a transcription factor that can bind <u>ER</u> <u>s</u>tress response <u>e</u>lements (ERSEs) in the nucleus, upregulating the expression of several ER pro-folding enzymes and chaperones, ERAD machinery, as well as enzymes involved in lipid biosynthesis (296). Furthermore, activated IRE1 has also been shown to cleave ER-localized mRNA transcripts, thus lowering the burden of non-essential secretory protein synthesis (303).

On another branch, ATF6 is maintained in an either monomeric or disulfide linked oligomeric inactive state in the ER, through binding of inhibitory partners such as BiP. Its activation is triggered by accumulation of unfolded proteins in the ER, dislocation of BiP, binding to ERp18, and export to the Golgi upon stress (304,305). There it can encounter two membrane-embedded proteases, site 1, and site 2 proteases (S1P, and S2P) which will sequentially cleave off the luminal and transmembrane domains of ATF6, respectively (306). This cleavage triggers the release of its cytosolic N-terminal domain which can act as a transcription factor similarly to XBP1s, and has been implied in the upregulation of BiP, Grp94, PDI, and CCAAT enhancer binding protein homologous protein (CHOP) (307).

Lastly, PERK is an ER resident kinase, which similarly to IRE1 oligomerizes and autophosphorylates in response to protein unfolding and lipid bilayer stress. This form of the kinase can also phosphorylate the eukaryotic translation initiation factor 2 α (eIF2α). This phosphorylation leads to a decrease in overall protein translation by inhibiting a guanine NEF form converting eIF2 to its active form, which will ultimately result in reduced initiation of protein translation (308). eIF2 inhibition conversely triggers the expression of ATF4, which upregulates the expression of different targets, including XBP1 and CHOP (309).

CHOP plays an important role in case ER stress is not remedied, as part of the cellular proapoptotic machinery. Its expression as a transcription factor can activate or downregulate a multitude of pro- and antiapoptotic pathways. Namely through inhibition of certain members of the B cell lymphoma 2 (BCL2) family, mitochondria get permeabilized and release cytochrome c, an apoptosis-inducing factor to the cytosol, resulting in cell death (310,311). CHOP can also act on apoptosis by promoting the biogenesis of Ero1, resulting in the increase of reactive oxygen species in the ER and consequently the cytosol (312).

Lastly, it is worth mentioning that all the pathways described rely on relatively slow responses to ER stress, all involving transcription and translation of new proteins, which may reveal itself inappropriate to deal with scenarios of acute stress. In fact, cells have also evolved mechanisms to deal with ER stress in a smaller time scale, dependent on PTM rather than gene expression. Homooligomers of BiP have been shown to form, and since oligomerization occurs via the canonical substrate interaction pocket, this keeps the chaperone in an inactive form. An acute increase in the amount of unfolded proteins can

trigger de-oligomerization of BiP, allowing the chaperone to stabilize substrate proteins (313,314). AMPylation of BiP is another mechanism to regulate the activity and availability of its chaperoning functions (315). In a scenario where BiP is not necessary, the chaperone can be AMPylated by an ER enzyme, rendering it inactive. Spikes in protein synthesis in the ER, or protein misfolding can be rapidly handled by de-AMPylation of BiP, without the need to activate the much lengthier response of the UPR (316). An additional example was recently uncovered for PDI and the secretory family with sequence similarity 20 C (Fam20C) kinase. Upon ER stress Fam20C was found to rapidly and reversibly phosphorylate PDI, leading the enzyme to lose oxidoreductase activity. Instead, PDI gains chaperoning activity, stabilizing unfolded peptides and protecting them against aggregation, an activity which seems to be prioritized during acute protein folding stress (317).

3. Connexin proteins as a model

Connexins (Cx) are a group of pore-forming transmembrane proteins expressed in a variety of organisms and virtually every mammalian cell type. Humans express 21 types of connexin proteins and mutations in at least 10 of them are known to be involved in disease (318,319). To date there are five subtypes (α, β, γ, δ, and ε) of connexins known, based on their sequence identity and length of their cytoplasmic tail (Fig. 9). In terms of their nomenclature, connexins are named (i) based on their molecular weight (e.g. Cx23 for 23 kDa) (ii) based on their subtype and order of discovery (e.g. Cx23 can also be named Cxε1, with the respective gene being *GJE1*).

Connexins can assemble into hexamers, and assembly can take place in the ER or all the way to the *trans*-Golgi, depending on the type of connexin, and its expression levels. In general terms, the higher the connexin expression level, the earlier in the secretory pathway assembly can take place (320,321). Once hexamers (connexon, hemichannel, HC) reach the plasma membrane, they are able to dock head-to-head onto another hexamer in an opposing membrane, forming the gap junction intercellular communication (GJIC). The name "gap" came from the appearance of a 2-4 nm space between the two cells joined by GJIC, when seen via electron microscopy (322).
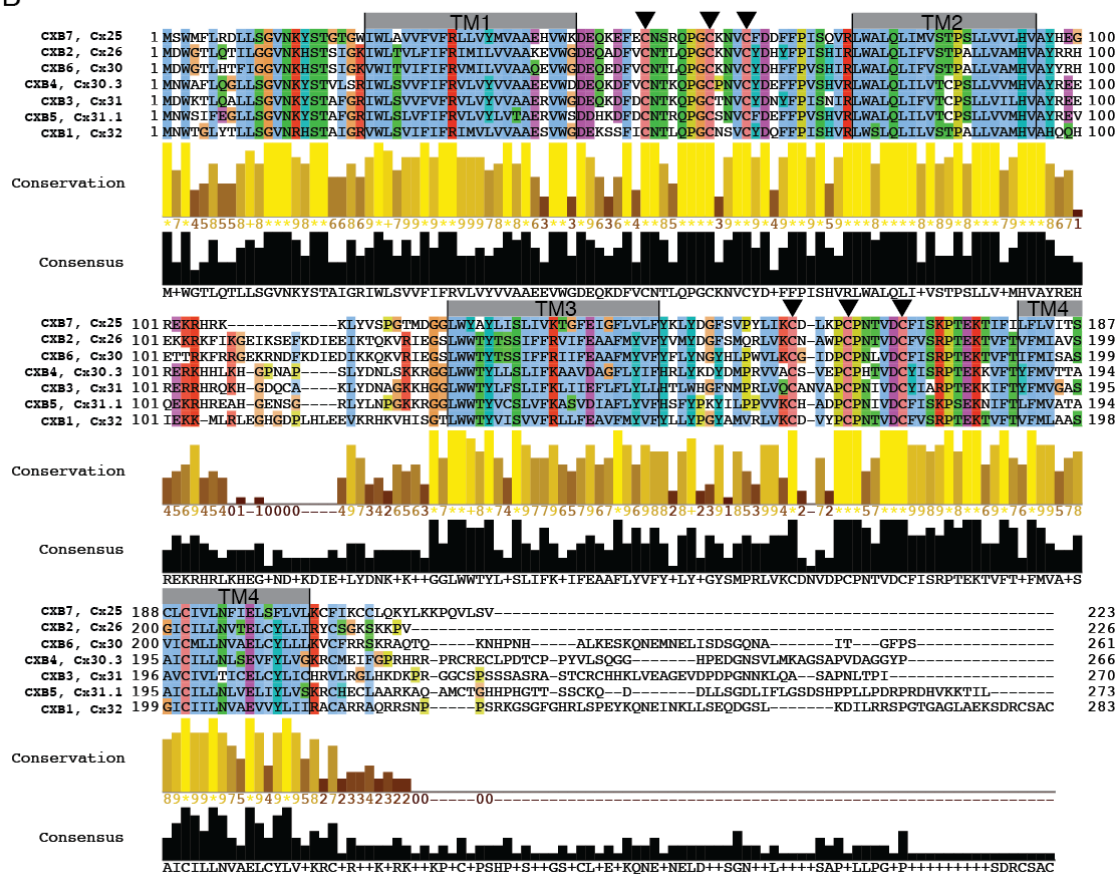
GJIC can move small hydrophilic metabolites (such as glucose), second messengers (cAMP, IP$_3$), and ions (K$^+$) across cytoplasms with different connexins showing different selectivity and permeability towards different solutes

(323). Molecular weight is also a limiting factor for GJIC transport since solutes
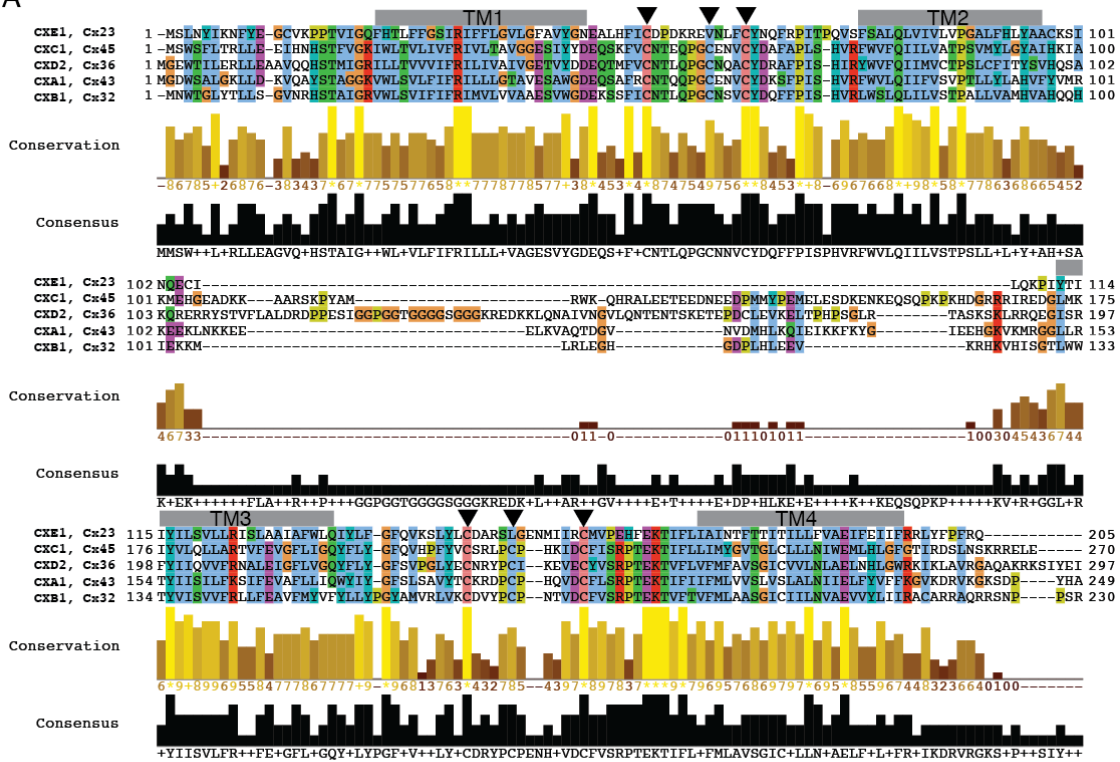
(figure legend in the next page)

Figure 9: Sequence conservation among members of the connexin family (**A**) Alignment of connexins from different subtypes, showing sequence conservation is not well kept among different connexin subtypes. TM segments are indicated on top of the sequence. The C-terminal region was cropped for simplicity. (**B**) Sequence alignment of connexins from the β family. Sequence conservation is maintained throughout most of the proteins, excluding the cytoplasmic loop 2 (between TM2 and TM3) and the C-terminal of the proteins. Alignments are colored according to Perseus (324).

bigger than 1 kDa are not transported. As such, connexins play a vital role in enabling electrical and chemical coupling between neighboring cells effectively allowing cell growth, synchronization, and differentiation (325-327).

Given the differential expression according to cell type, not all connexins are expressed in the same tissues even though its likely a given cell is expressing more than one type of connexin (326). As such, HC may be found with only one type of connexin (homomeric), or more than one type of connexin protomer (heteromeric HC). The same principle can be seen when HC dock into GJIC – these can also be homotypic or heterotypic according to the assembly of the same or different HC, respectively. Interestingly not all HC combinations are possible, and their matching seems to be tightly associated with the subtype of connexin (328,329).

Several hundred GJIC can come together side-by-side in patches of the plasma membrane forming physiologically relevant gap junction (GJ) plaques. Assembly of these is regulated by e.g. actin and zonula occludens 1 (ZO-1), and it has been postulated that, at least for some connexins, e.g. Cx43, integration into a plaque can only occur from the plaque periphery, with endocytosis from the center, all constrained by restricted mobility throughout the plaque (330,331). While in the plasma membrane, plaques can be internalized, forming double membrane vesicles with patches or intact GJ plaques – annular gap junctions – occasionally including HC of neighboring cells. While their degradative fate has been postulated, some doubt remains whether these structures can also mediate connexin and/or gap junction plaque recycling back to the plasma membrane (Fig. 10) (332).

Connexin degradation can also be achieved by ERAD (via polyubiquitination) or plasma membrane internalization of either connexins, connexons, or GJ plaques resulting in either lysosomal, autophagosomal, and proteasomal mediated degradation (via monoubiquitination) (333-335).

a. Connexins structural features and elements

Connexins are all multipass TM proteins, made up of four TM segments, with both their N- and C-termini exposed to the cytosolic side of the membrane, i.e. their first TM segment has a type II (N_{in}-C_{out}) topology (336,337), and even though membrane topology has not been explicitly investigated for all members of the connexin family, to date no other orientation has been found (338). Other orientations indeed are unlikely given the high homology and sequence identity/conservation of most connexin proteins, especially around their TM regions and extracellular domains (Fig. 9) (339).

One of the first roles attributed to the N-terminal domain of Cx proteins (approximately the first twenty amino acid residues) was its significance for voltage-dependent gating of the channels (340,341) and was thus postulated to be placed close to, or even be a part of the GJIC pore. Later NMR work on N-terminal peptides of Cx26 and Cx32 have shown the first 10 amino acid residues to form a helical structure, usually termed N-terminal helix (NTH), followed by a flexible region created by the conserved Gly12 which would allow NTH to insert into the aqueous channel pore and interact with the first TM segment (342,343). Cryo EM studies later showed that a plug like density in the central pore of Cx26 hemichannels was lost in an NTH deletion mutant of the protein (344), fortifying the idea of this helix acting as a plug in gap junctions. Resolving Cx26 and Cx46/50 structures confirmed this placement, and attributed it to hydrophobic interaction between Cx26 W3 and M34 of a neighboring protomer (345,346) while the structure of Cx31.3 hemichannels placed the NTH at the cytoplasmic
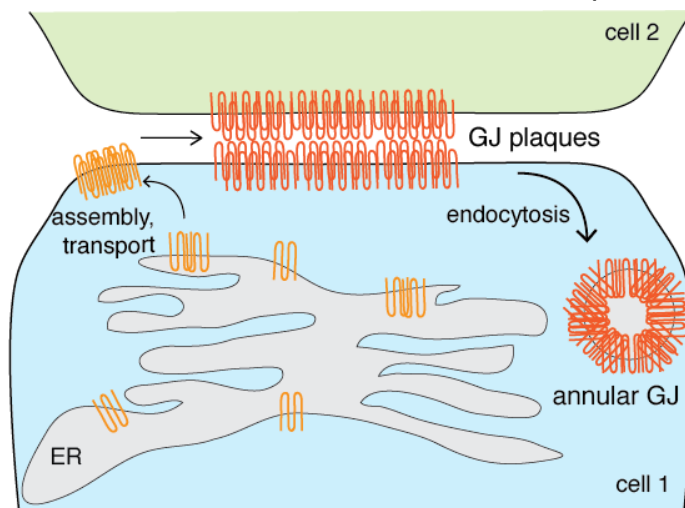

Figure 10: Simplified view of GJ plaque assembly and endocytosis. Connexins traffic from the ER to the plasma membrane, where connexons can assemble side-by-side, forming plaques with a connexon from a neighboring cell. Plaques can be endocytosed as a whole, or partially, forming annular GJ in the cytosol.

entrance of the channel, covering the pore (347). In the latter study the authors purified and resolved HC as opposed to GJIC, which they speculate to be in a partially closed state.

Through <u>s</u>ubstituted <u>c</u>ysteine <u>a</u>ccessibility <u>m</u>ethod (SCAM) performed on Cx46 and Cx32/Cx46 chimeric hemichannels the first transmembrane segment of connexins, TM1, was attributed as the pore lining segment (348,349) and this was mostly confirmed with the Cx26 and Cx46/50 gap junction channels structures (345,346). TM1 is naturally tilted which makes the pore narrow from the cytoplasmic to the extracellular side, from a diameter of 40 Å to 14 Å, on a conformation that is presumed (but not confirmed) to be open (350,351).

Structurally speaking, the first <u>extra</u><u>c</u>ellular domain (EC1, also termed loop 1) starts with a parahelix (structurally similar to a 3_{10} helix). Together with the NTH, this domain was described as being involved in channel ion selectivity and conductance (352,353) in part due to the conservation of its negative charges in the TM1/EC1 boundary, which are able to form a negative charged path in the pore. Additionally, an arrangement of twelve EC1 domains (six from each hemichannel) form the inner half the extracellular portion of the gap junction channels (354).

The second transmembrane domain, TM2, partially faces the pore of the channel but to a lesser extent than TM1 (345). Together with the NTH and TM1 this TM segment appears to be a hotspot in Cx46/50 for mutations causing cataracts indicating the underlying functional relevance of these domains (346). A conserved proline residue, Pro87, produces a kink in the helix, and when mutated to a Leu in Cx26 is known to affect channel voltage gating and, when mutated in Cx32, cause human disease (355,356). Furthermore, the cryo-EM structure of Cx31.3 has shown extensive interactions between TM2 and the NTH placed in the cytosolic entrance of the channel (347). These are hydrophobic in nature and span residues from T95 to W103. Another point of contention on the relative positioning of NTH in regards to TM1 vs. TM2 comes from the fact that only half of the human Cx proteins show conservation in these NTH-interacting TM2 residues. This raises the question if NTH-TM2 is maintained according to sequence conservation, or as mentioned previously, is dependent on a HC vs. GJIC organization.

The α-helix of TM2 extends further into the cytosol together with TM3. Between the two segments, Cx26 has eleven positively charged residues in this area that constitutes the entrance to the channels pore, and are thought to contribute to Cx26 preferential permeation to anions (354). TM3 was initially thought to be the pore lining segment for connexin proteins due to being to only truly amphipathic TM segment (357,358). Additional SCAM and cryo-EM based molecular modeling work have appeared to confirm this (359,360), later to be discredited by a plethora of experiments and the first crystal structure of Cx26. Interestingly, despite being the least conserved TM segment in connexin proteins, TM3 plays an important role in inter-protomer interactions for both Cx32 (361) and Cx43 (362). Solving Cx26 structure mostly attributed this to an "aromatic face" composed of aromatic amino acid residues every third to fourth position on this helix that stabilizes protomer interaction (345).

Bridging TM2 and TM3 is the intracellular loop (ICL, also termed loop 2) which is mostly though to be disorder since its structure was never solved. This loop is mostly thought to have regulatory functions (363) since its lack of conservation among connexin proteins could have implications in channel selectivity and permeability.

The second extracellular domain (EC2, also termed loop 3) is structurally composed of two β-sheets, one of which runs anti-parallel to the β-sheet in EC1. This loop contains three highly conserved cysteine residues that bridge EC1 (also containing three conserved Cys residues) and EC2 together (364,365). Publication of the Cx26 structure has placed EC2 as forming the outside wall of the connexon, facing the lipid bilayer. Additionally, given its position, it was found to be relevant for docking of hemichannels from two opposing membranes via hydrogen bonding with conserved residues in EC1 (345,366).

The fourth TM segment, TM4 is also considerably tilted in Cx26 contributing to the overall bigger area of the channel on the cytosolic side (345), and together with TM3 and ECL2 are the domains of connexins facing the lipid bilayer.

Similarly to the ICL, the C-terminal domain (CTD) of connexins is mostly disordered and was never structurally resolved outside biophysical studies performed in membrane tethered TM4/CTD constructs which found connexins of the α isotype (e.g. Cx43) to be more enriched in α-helical structure than other

connexin subtypes (367). It is the most heterogeneous domain of connexin proteins both in size and in sequence, and the main hub for post-translational modifications as well as binding partners, from cytoskeleton proteins to regulatory kinases (338). It is abundantly phosphorylated (with the exception of Cx26 for having a very short CTD (368)) which becomes specially relevant for CTD structure (369) and consequent interaction with different binding partners responsible for intracellular trafficking, gating, turnover, among others (370,371). Acetylation of the CTD was also recently found to play a role in Cx32 mediated cell proliferation through a GJIC independent function (372).

b. Connexins function and regulation

Connexin activity at the plasma membrane can usually be described as the activity of either nonjunctional, unopposed HC, or as the one of a GJIC, mediated by HC docking. In the first case, connexin HC activity is measured as the exchange of metabolites from the cytosol to the extracellular space and vice-versa, while in the second, GJIC activity refers to metabolite transfer between two cells. In general terms, there is a need for GJIC to remain open and maintain metabolic synchronization, and for HC to remain close until docking as avoid intracellular metabolite leaking into the extracellular space, even though there are exceptions to this (e.g. Cx26 HC can be found open under basal conditions) (373,374). Regardless of this, channel activity is a highly regulated and connexin type-dependent event, with special relevance on cell growth, differentiation, and death.

Despite different connexin presenting different ionic and molecular selectivity, and conductance rates, they all present voltage dependent gating, usually described as either transjunctional gating (V_j gating, or fast V_j gating) or loop (slow) gating. The first corresponds to fast (in the few ms range) transition to or from an open state to a subconductance state (also termed substate), in which conductance can vary from 5 to 40% of that of a fully open channel. The substate is thought to be important in maintaining electric and ionic coupling between cytoplasms while decoupling molecular signaling (375). The voltage gating sensor seems to be located at the NTH for most connexin proteins, with possible involvement of the TM1/ECL1 border. The role of the NTH in V_j gating became clear through mutagenesis: Cx26, with an Asp at position 2, had its V_j

gating polarity reversed in D2R and D2K mutants, now reaching the substate when the cytoplasm becomes negative (340). As such, the general rule for connexin V_j gating seems to be that connexins with net neutral or negative charges in the NTH (such as Cx26) reach substates upon depolarization, while net positive charges in the NTH (such as Cx32) close into substates with membrane hyperpolarization (inside potential is negative) (375,376).

The second type of voltage dependent gating, loop-gating is thought to involve a series of slower, step-wise conformational changes leading to a fully closed state. Loop-gating-driven channel closure is thought to be the reason for HC closure at basal conditions (377). Studies for this type of gating have been less clear, but some seem to point towards narrowing of the pore via TM1/ECL1 movement (378-380). Molecular dynamic simulations have postulated that, in a voltage-driven way, this TM1/ECL1 region has its electrostatic and van der Walls networks reorganized, resulting in the protrusion of the ECL1 parahelix into the pore (381). Left to clarify is how these models of loop-gating balance out with the established role of the extracellular region of connexins in assembly and docking (382).

The first gating mechanism for connexins was proposed to be based on the sliding of protomers along the pore axis line, i.e. an open connexon would have each connexin subunit tilted in the membrane, and upon calcium stimulus, each subunit would slide and align with the perpendicular axis of the membrane, closing the channel (383,384). While at this point connexins were still to be identified and cloned, some years later the first report on actual HC gating was gained from oocyte death via swelling when unless cells were kept in a high extracellular $[Ca^{2+}]$ ($[Ca^{2+}]_o$) solution (385). This meant that, for the studied Cx46, high $[Ca^{2+}]_o$ would induce HC closure. By resolving the X-ray structure of Cx26 (un)bound to calcium, it became apparent Ca^{2+} ions coordinate with negatively charged residues in the TM1/ECL1 boundary between two protomers, leading to small conformational changes around the binding site. Thus, calcium-dependent closure of GJIC was revealed to not be dependent on drastic structural rearrangements, such as narrowing of the channel pore, but rather due to the creation of an electrostatic barrier – in a Ca^{2+} bound state the pore shows an almost entirely positive electrostatic surface potential (386,387). This should be

enough to hinder permeation to cations in Cx26, but remains to be elucidated how anion transporting HC (such as Cx32) have their gated affected by Ca^{2+}.

Intracellular pH was also described early as a regulator of GJIC activity. Early reports had pointed towards amphibian GJIC closing upon decrease of intracellular pH, through a presumed direct effect of protonation on connexins, and not via an intermediate (388,389). Even though sensitivity to pH varies among connexins (e.g. Cx32 is one of the most pH-insensitive connexins), it is mostly accepted that virtually all of the connexin subtypes expressed in different cell types are uncoupled via cytosolic acidification (390,391). Via the use of connexin chimeras, this same study also attributed the pH sensitive domain to the ICL of the proteins, which was also later extended to positive charges in the beginning of the Cx32 CTD domain (392). Further studies on Cx43 have also shown acidification triggered uncoupling to happen through the CTD, via a mechanism proposed to stem from a particle-receptor, "ball and chain" model, in which protonated CTD associated with the ICL of Cx43, gating the channel (393).

Various other stimuli and PTMs affect GJIC, such as phosphorylation by mitogen-activated protein kinase (MAPK) or protein kinase C (PKC), known to decrease channel opening probability, which can also be observed with a decrease in the oxidation level of the cytosol such as what happens in metabolic inhibition conditions (374).

c. CMT1X

Cx32, GJβ1 is a 283 amino acid residue connexin encoded by the *GJB1* gene located at the Xq13.1 locus in humans (394). The protein is expressed in liver as well as myelin forming cells of the peripheral (Schwann cells) and central (oligodendrocytes) nervous systems (395,396). Both Schwann cells and oligodendrocytes are myelinated cells who wrap around axons in the nervous system thereby insulating them though an increase in both the membrane resistance and conduction velocity of electrical signals throughout the axon (397).

In myelinated cells, Cx32 is mostly found in areas of non-compact myelin, which compared to compact myelin, do not present such tight spiraling of the membrane. These non-compact areas include the paranodal area, bordering the nodes of Ranvier, as well as the Schmidt-Lanterman incisures, areas of

expanded cytoplasm within the compact myelin (398,399). Schwann cells rely on areas of non-compact myelin mostly for organelle maintenance, since these are excluded from areas of compact myelin, dedicated to the transmission of electric signals (397). Given the tight wrapping and extended cytoplasmic length of Schwann cells and oligodendrocytes (which can reach the 4 mm in length), Cx32 plays a fundamental role (especially in the PNS) in the radial transport of metabolites across different layers of the Schwann cell cytoplasm (in which their thickness is as big as 4 µm) (399).

Over 450 mutations in *GJB1* are known to cause X-linked Charcot-Marie-Tooth disease (CMT1X), the first human disease linked to a connexin protein (394,400). CMT1X is the second most common form of CMT, accounting for 10 to 20% of its cases. CMT is the most common hereditary neuropathy with a prevalence of ca. 30:100,000 (401).

Cx32 mutants are known to show a multitude of cellular phenotypes, from reduced or absent Cx32 synthesis, to intracellular retention, and non-functional or dysfunctional GJ channels (400). In males, symptoms usually start in the second decade of life and include progressive axon loss and demyelination resulting in distal muscle weakness. Furthermore, peripheral nerve inflammation seems to lead to reduced conductivity in these nerves, resulting in distal muscle atrophy and sensory loss. CMT1X is traditionally termed an X-linked dominant disease, since females can still be affected by the disease, though usually with later and milder symptoms onset (397,402,403). In *GJB1* knockout mice, axonal abnormalities (including cytoskeleton changes and impaired transport of synapse associated proteins) were found to precede demyelination (404). Furthermore, in the same transgenic mouse models demyelination can be observed at 3 months of age, where myelin thins out and shows abnormal "onion bulb" formations (405,406).

In conclusion, most of the data regarding CMT1X etiology come from the physiological effects of Cx32 mutants on myelination and overall tissue homeostasis. On the other hand, the possible involvement of protein quality control on Cx32 and their relevance for disease remain poorly elucidated.

Aims

The ER is responsible for the synthesis and folding of soluble and membrane proteins of the secretory pathway. Since both synthesis and folding are prone to a different array of errors, cells had to evolve machineries and mechanisms to deal with possible faulty proteins. When it comes to single pass membrane proteins, TM segment misintegration is one of the possible topogenesis-based blunders membrane proteins may face. In the case of the TCR α, TM misintegration is handled in the ER lumen by BiP, and its targeting for ERAD is taken care of via Hrd1 (69).

As such, the first aim of this study was to decipher if the same misintegration phenotype could be found in multipass TM proteins. This was supported by the notion that ca. 25% of TM helices in multipass proteins are unstable in the lipid bilayer, when analyzed in isolation (63). Since apolar-to-polar missense mutations in TM segments are often associated with human disease (407), we decided this type of mutation would be a good starting point to examine possible misintegration phenotypes. As a model, we focused on Cx32, a four TM segment membrane protein, known to cause human disease when mutated (394). The second major aim was to understand the physiological consequences of misintegration, by means of subcellular expression, and degradation kinetics. And finally, to decipher if the same quality control machinery acting on single pass TM protein misintegration could be found in our system.

While investigating misintegration phenotypes, we observed that several Cx32 mutants produce a second, faster-migrating immunoblot species, when compared to the wild type protein. As such, the second part of this work focuses on the characterization of this species. We presumed its origin stemmed from proteolytical cleavage, and sought to find out which protease could be responsible for its production, and what would be the trigger for cleavage. To conclude, we decided to investigate the effects and interaction of this species with the full-length version of Cx32.

All in all, we hope the results from this work can be expanded to other membrane proteins, and have brought to light new insights into membrane protein folding and quality control.

Materials and Methods

1. DNA, siRNA, and antibodies

Human Cx32, PMP22 cDNA, and C_L/Cx32-TMS were obtained from Origene. Human Cx26 cDNA was obtained from GPCF (DKFZ-ZMGH, Heidelberg). Human His$_6$-tagged Hrd1 constructs, as well as rodent BiP were kindly gifted by Prof. Dr. Linda Hendershot (St. Jude Children Research Hospital, TN, USA). Human V5-tagged gp78 was kindly gifted by Prof. Dr. Zai-Rong Zhang (Shanghai Institute of Organic Chemistry, Shanghai, China). Ligation into appropriate mammalian expression vectors (pSVL (Amersham) or pcDNA3.1 (Addgene)) and introduction of N- and C-terminal tags were carried out with T4 ligase (Promega). Introduction of point mutations, and all other tagging was performed by mutagenesis PCR using a Pfu polymerase (Promega). All constructs were sequenced prior to use (Eurofins Genomics).

siRNAs were selected from *Silencer* ® Select siRNA (Thermo Fischer Scientific) as follows: EMC5 (s41129), EMC10 (s49611), *SPCS1* (s226239), *SPCS2* (s18920), *SPCS3* (s34132). Antibodies used, dilutions and applications are present in the table below.

Target	Company, catalog no.	Application	Dilution
BiP	Cell Signaling, C50B12	IB	1:250
BiP (murine)	(408)	IB	1:1000
CANX	Biozol, BLD-699401	IB	1:1000
C_L	Southern Biotech, 1060-01	IB	1:250
Cx32	Sigma-Aldrich, C3595	IB	1:500
EMC10	(Abcam, ab181209	IB	1:10000
EMC4	Abcam, ab184544	IB	1:10000
EMC5	Abcam, ab174366	IB	1:250
FLAG	Sigma-Aldrich, F7425	IB	1:500
FLAG	Sigma-Aldrich, F1804	IF	1:500
GAPDH	Santa Cruz, sc-365062	IB	1:1000
HA	Biozol, BLD-901514	IB	1:1000
His$_6$, HRP-conjugated	Sigma-Aldrich, 11965085001	IB	1:3000
Hsc70	Santa Cruz, sc-7298	IB	1:1000
Mouse IgG	Santa Cruz, sc-516102	IB	1:10000
Mouse IgG, Texas Red-conjugated	Thermo Fischer, PA1-28626	IF	1:300

PDI, Alexa Fluor 488-conjugated	Cell Signaling, 5051	IF	1:50
PDIA6	Proteintech, 18233-1-AP	IB	1:1000
Rabbit IgG	Santa Cruz, sc-2357	IB	1:10000
Rat IgG	Biozol, BLD-405405	IB	1:10000
SPC12	Proteintech, 11847-1-AP	IB	1:500
SPC18	Proteintech, 14753-1-AP	IB	1:500
SPC22/23	Santa Cruz, sc-377334	IB	1:100
SPC25	Proteintech, 14872-1-AP	IB	1:1000
Ubiquitin	Santa Cruz, sc-8017	IB	1:500
V5	Abcam, ab27671	IB	1:1000

2. Mammalian cell culture

293T (ECACC), COS-7 (ECACC), and NF1 (ATCC) cells were cultured in DMEM (Sigma-Adrich) containing 10% FBS (Gibco), and 1% antibiotic/antimycotic solution (Sigma-Aldrich), in a humidified 5% CO_2 atmosphere at 37° C.

siRNA transfection was carried out for 48 h using 25-50 nM siRNA and RNAiMAX (Thermo Fischer Scientific), according to manufacturer instructions. Transient DNA transfections were performed via chemical transfection (293T) or electroporation (COS-7, NF1). 293T were transfected with Genecellin (Bulldog Bio) 24 h after seeding, according to manufacturer instructions. In case of co-transfection, the amount of DNA would be split equally unless the vectors used had different strength promoters where a ratio of 3:1 (weaker promoter vector:stronger promoter vector) would be used. For COS-7 and NF1 cells were split the day prior to transfection. Electroporation was carried out with a X2 Gemini electroporator (BTX) according to manufacturer instructions and protocol for COS-7, and SK-N-MC protocol for NF1 cells.

Incubations with reagents were carried out by dilution in pre-warmed medium, and incubation of cells for the relevant time prior to lysis. VCP/p97 inhibition was carried out with 2.5 µM (O/N) or 5 µM (3 h) CB-5083 (Selleckchem). Translational arrested was performed with 50 µg/mL CHX (Sigma-Aldrich). Disulfide reduction and UPR induction were carried out with 10 mM DTT (Sigma-Aldrich). Proteasomal inhibition was carried out with 2 µM (O/N) or 10 µM (3 h)

MG132 (Sigma-Aldrich). UPR induction was carried with 5 µg/mL tunicamycin (Sigma-Aldrich) for 6 h.

3. Mammalian cell lysates and Immunoprecipitation

All lysate handling was performed on ice, at 4° C, or with ice-cold solutions unless otherwise stated. Typically, prior to lysis cells were washed twice with PBS (Sigma-Aldrich) and lysed in the appropriate amount of NP-40 lysis buffer (50 mM Tris-HCl pH 7.5, 150 mM NaCl, 0.5% (w/v) NaDOC, 0.5% (v/v) NP-40 substitute, 1X protease inhibitors). Samples were centrifuged for 15 min at 15,000g and the supernatant was added to 4X Laemmli buffer containing 20% ß-ME (Sigma-Aldrich). For samples where membrane proteins were to be analyzed, lysates were incubated for 30 min at 37° C, while lysates for analysis of soluble proteins were boiled at 95° C for 5 min.

To assess and maintain formation of oxidized species, cells were instead washed and lysed in the presence 20 mM NEM (Sigma-Aldrich), added to the PBS and lysis buffer, respectively. After centrifugation, lysates were added to Laemmli buffer either containing 20 mM NEM (non-reducing) or 5% ß-ME (reducing). For analysis of gap-junction plaque formation, cells were washed, lysed, and centrifuged as usual. The pellet fraction containing the possible gap-junction plaque forming fraction of protein was solubilized for 10 min at 95° C in 50 mM Tris-HCl (Sigma-Aldrich) pH 6.8, 2% (w/v) SDS (Sigma-Aldrich). The solubilized pellets were then supplemented with lysis buffer up to the original volume of lysis, followed by a 15 min centrifugation at 15,000g. Supernatants containing the gap junction plaque forming connexin fraction were supplemented with Laemmli containing ß-ME, and incubated, as described above. Protein N-glycosylation assessment was performed resorting to EndoH (New England Biolabs) and/or PNGase F (New England Biolabs) mediated N-deglycosylation, according to manufacturer instructions.

Protein retrotranslocation was assessed by semi-permeabilizing cells after PBS washes as described elsewhere (289). Briefly, semi-permeabilization was carried out for 5 min in buffer containing 0.015% (v/v) digitonin (Sigma-Aldrich), followed by scraping the cells into a tube. A small aliquot was taken for a total fraction control sample, and mixed with 2X NP-40 lysis buffer. The remainder of the cell suspension was centrifuged at 15,000g for 5 min, and cytosolic proteins

were taken from the supernatant and supplemented with Laemmli, as described above. Membrane proteins were solubilized from the pellet fraction with NP-40 lysis buffer for 5 min on ice, followed by a 20,000*g* centrifugation for 10 min. Supernatant were taken and supplemented with Laemmli as described above.

Samples intended for immunoprecipitation were either lysed in NP-40 lysis buffer or, when membrane-embedded interactions were under study, digitonin lysis buffer (50 mM Tris-HCl pH 7.5, 150 mM NaCl, 1% (w/v) digitonin, 1X protease inhibitors). For BiP co-immunoprecipitations apyrase (Sigma-Aldrich) was added to the NP-40 lysis buffer. Immunoprecipitation of target proteins was carried out by adding 1-2 µg of antibody to the lysates and rotating samples for 2 h, followed by 1 h rotation with Protein A/G agarose beads (Thermo Fischer Scientific). Alternatively, for FLAG immunoprecipitations, FLAG M2 Affinity gel (Sigma-Aldrich) was used for 3 h. Beads were washed three times in either NP-40 wash buffer (50 mM Tris-HCl pH 7.5, 400 mM NaCl, 0.5% (w/v) NaDOC, 0.5% (v/v) NP-40 substitute) or digitonin wash buffer (50 mM Tris-HCl pH 7.5, 150 mM NaCl, 0.5% (w/v) digitonin). Proteins destined for MS were washed twice more in detergent-free wash buffer. Proteins were eluted with 2X Laemmli buffer supplemented with ß-ME and incubated at either 37° or 95° C as described above.

4. Immunoblot

Proteins were separated by SDS-PAGE in a Tris-Glycine system (Biorad), and blotted onto a methanol (Sigma-Aldrich) activated PVDF membrane (Biorad) at 4° C O/N. Membranes were blocked for 3-5 h in 5% skimmed milk (Sigma-Aldrich), 0.1% Tween-20 (Biorad) in TBS (50 mM Tris-HCl pH 7.5, 150 mM NaCl), and incubated O/N with primary antibody diluted in blocking milk. The following day, membranes were washed three times with TBS and TBS-T (TBS, 0.1% Tween-20), incubated with HRP-conjugated secondary antibody (Santa Cruz), and washed thrice more. Chemiluminescence was detected in a Fusion 6 Pulse Imager (Vilber Lourmat) using Amersham ECL Prime (Thermo Fischer Scientific).

5. Mass spectrometry

After immunoprecipitation, proteins to be analyzed by MS were digested and eluted from the beads, and sample desalted and purified as described elsewhere (409). Nanoflow LC MS/MS analysis were performed with an UltiMate 3000 Nano HPLC (Thermo Fischer Scientific) system, coupled to an Orbitrap Fusion mass spectrometer (Thermo Fischer Scientific). Peptides were loaded on an Acclaim C18 PepMap100 75 µm ID × 2 cm trap column with 0.1% TFA, then transferred to an Acclaim C18 PepMap RSLC, 75 µm ID × 50 cm, 0.1% FA analytical column heated at 50° C, and separated. Peptides were ionized using an EASY-ETD/IC source. Full scan (MS1) acquisition (scan range of 300–1500 m/z) was performed in the orbitrap at a resolution of 120,000 and with an automatic gain control ion target value of 2e5. Isolation was performed in the quadrupole using a window of 1.6 m/z. Fragments were generated using HCD (collision energy: 30%). The MS2 automatic gain control target was set to 1e4 and a maximum injection time for the ion trap of 50 ms was used (with inject ions for all available parallelizable time enabled). Fragments were scanned with the rapid scan rate.

MS raw files were analyzed with MaxQuant (410) with a protein database containing human sequences (downloaded May 2017 from Uniprot, taxonomy ID: 9606).

6. Immunofluorescence

To determine target protein intracellular localization, electroporated COS-7 were used. 48 h after transfection cells were washed twice with pre-warmed PBS, followed by fixation in glyoxal (Sigma-Aldrich) as described elsewhere (411). Cells were permeabilized and epitopes blocked for 15 min in 2.5% BSA (Sigma-Aldrich), 0.1% Triton X-100 (Biorad) in PBS. Primary antibodies were incubated for 2 h at RT, followed by three PBS washes, and 1 h secondary antibody incubation, followed by one PBS wash. 1 µg/mL DAPI (Sigma-Aldrich) in PBS was used to briefly stain nuclei, and the samples were then again washed three times with PBS, and mounted with mounting medium (Ibidi). Imaging was performed on a DMi8 CS Bino inverted widefield fluorescence microscope (Leica) with the appropriate filters, and analysis was performed with LAS X (Leica). For

signal deconvolution, z-stacks were taken and exported to Huygens Essential (Scientific Volume Imaging).

7. Structural modeling and sequence analysis

Cx32 structural modelling was performed with iTasser (412) by using the F chain of Cx26 X-ray structure as a template (PDB ID: 2zw3). Cx32 and Cx26 share 49% and 71% sequence identity and conservation, respectively. Superimposed model and X-ray structure had an overall RMSD of 0.72 Å. The modeled protomer was then structurally aligned to the hexameric structure of Cx26, and the resulting modeled Cx32 hexamer was energy minimized using Yasara Structure (413).

Potential revertant mutants on Cx26 and Cx32 were assessed and modeled on the X-ray Cx26 structure (PDB ID: 2zw3) and the generated Cx32 hemichannel model. Disease-causing point mutants were simulated and energy minimized in Yasara Structure, and the resulting models were manually queried for potential compensatory mutants, followed by a new energy minimization step. Cartoon depictions of protein models were performed on Chimera (UCSF) (414).

Sequence alignments were performed in Clustal Omega (EMBL-EBI) (ebi.ac.uk/Tools/msa/clustalo/), and analyzed in Jalview (415). ΔG_{app} for TM segment insertion was performed with DGpred (dgpred.cbr.su.se/). TM segment predictions were performed in either DGpred (63), or TOPCONS (topcons.cbr.su.se/) (416).

Non-canonical signal peptide prediction was performed by retrieving the FASTA sequences of proteins with a transmembrane annotation from UniprotKB, and running them through the SignalP 3.0 (cbs.dtu.dk/services/SignalP-3.0) (417), SignalP 4.1 (cbs.dtu.dk/services/SignalP-4.1) (418), and TMHHM servers (cbs.dtu.dk/services/TMHMM). Sequences were filtered by their SignalP D-score, based on the threshold value of each SignalP version. The TMHMM server was used to filter for multispanning membrane proteins having their first TM segment in a type II orientation, and in their first 70 aa. Proteins with at least one type II TM1 prediction, from a full protein scan or a scan with just the first seventy amino acids of the protein, were included. The list of 442 proteins was then filtered for

expression on the secretory pathway and absence of annotated signal peptide (both annotations taken from UniprotKB).

8. Quantification and statistical analysis

Immunoblots were quantified using Bio1D (Vilber Lourmat). Fractions of glycosylated or cleaved species were calculated by dividing the concerned species by the sum of the intensity of the different species. Co-immunoprecipitation values were calculated by normalizing the amount of co-immunoprecipitated protein to the amount of immunoprecipitated protein in the same samples. Relative poly-ubiquitination was calculated by subtracting the background signal from mock controls, relative to each treatment and transfection. CHX decays were calculated by normalizing the intensity at each time point to the intensity of the sample with no CHX incubation (t = 0 h). Half-life calculation were done by logarithmically linearizing the CHX decays and finding the intersection of this line to ln(0.5).

Statistical analysis for MS data was performed in Perseus (324). Proteins identified only by site, reverse hits or potential contaminants were removed. LFQ intensities were log2 transformed. Data were then filtered for at least two valid values in at least one replicate group. Then, missing values were imputed from normal distribution. The replicate groups were compared via a two-sided, two-sample Student's t test. Enrichment values and corresponding −log10 *P* values were plotted.

All other statistical analysis was performed using Prism (GraphPad) using two-tailed Student's *t* tests. Statistical significance was set at *P* < 0.05.

Results

1. A network of chaperones prevents and detects failures in membrane protein lipid bilayer integration

a. Disease-causing mutants cause Cx32 TM segment misintegration

Membrane protein integration and topogenesis are two molecular processes prone to failure, which means that in order for cellular homeostasis to be maintained, they must be tightly controlled and regulated. Among the different challenges membrane proteins face, stability of TM segments within the membrane is one of them, since approximately 25% of all TM helices, when analyzed individually, are predicted to be unstable in the hydrophobic environment of the lipid bilayer (63). The main reason for this intrinsic instability is the presence of polar or charged amino acid residues within these segments, the same type of residues that present the highest degree of conservation among TM proteins and their TM segments (419,420). A common strategy to circumvent the problem of instability is achieving intramembrane packing through TM-TM interactions – polar or charged residues will be hidden from the hydrophobic acyl chains through interaction with amino acid residues in neighboring helices, either in the same or on a partner protein. In case this fails, previous reports have pointed towards slipping of TM segments into the ER lumen in single-pass TM proteins (68,69). However, when it comes to multipass TM proteins, reports on TM misintegration seem to be confined to transient, co-translational events, where translation of downstream TM segments guarantees full TM insertion (64,66,421).

Cx32 is a four TM segment membrane protein with both its N- and C-termini facing the cytosol (Fig. 11A). We became interested in the protein since we predicted one of its TM segments (TM2) to be unstable in the membrane, and mutants all throughout the protein are known to cause CMT1X (Fig. 11A) (394). Since TM misintegration has been observed for single-pass proteins, we were interested if the same would occur with the Cx32 TM segments. Towards this, we generated a model of hexameric Cx32 (Fig. 11B) based on the crystal structure of Cx26 (345), and decided to focus on CMT1X-causing mutants that, while embedded in the membrane, cause a predicted instability for their TM segment

in the hydrophobic interior of the membrane (Fig. 11B). The mutants were selected throughout the four TM segments of Cx32, with sidechains facing distinct structural elements (e.g. the lipid bilayer or the center of the protomer), and their apolar-to-polar character increases their instability as seen by the increase in their ΔG_{app} for membrane integration (dgpred.cbr.su.se, (63)) (Fig. 11A).

In order to assess if TM misintegration could occur for any of these mutants, we took advantage of the fact glycosylation occurs only in the ER lumen (143) and is easily assessed via immunoblot. Since Cx32 has a naturally occurring glycosylation sequon in its N-terminal tail ([2]NWT[5]), we individually equipped wild type and mutant proteins with glycosylation sites in the remaining loops and C-
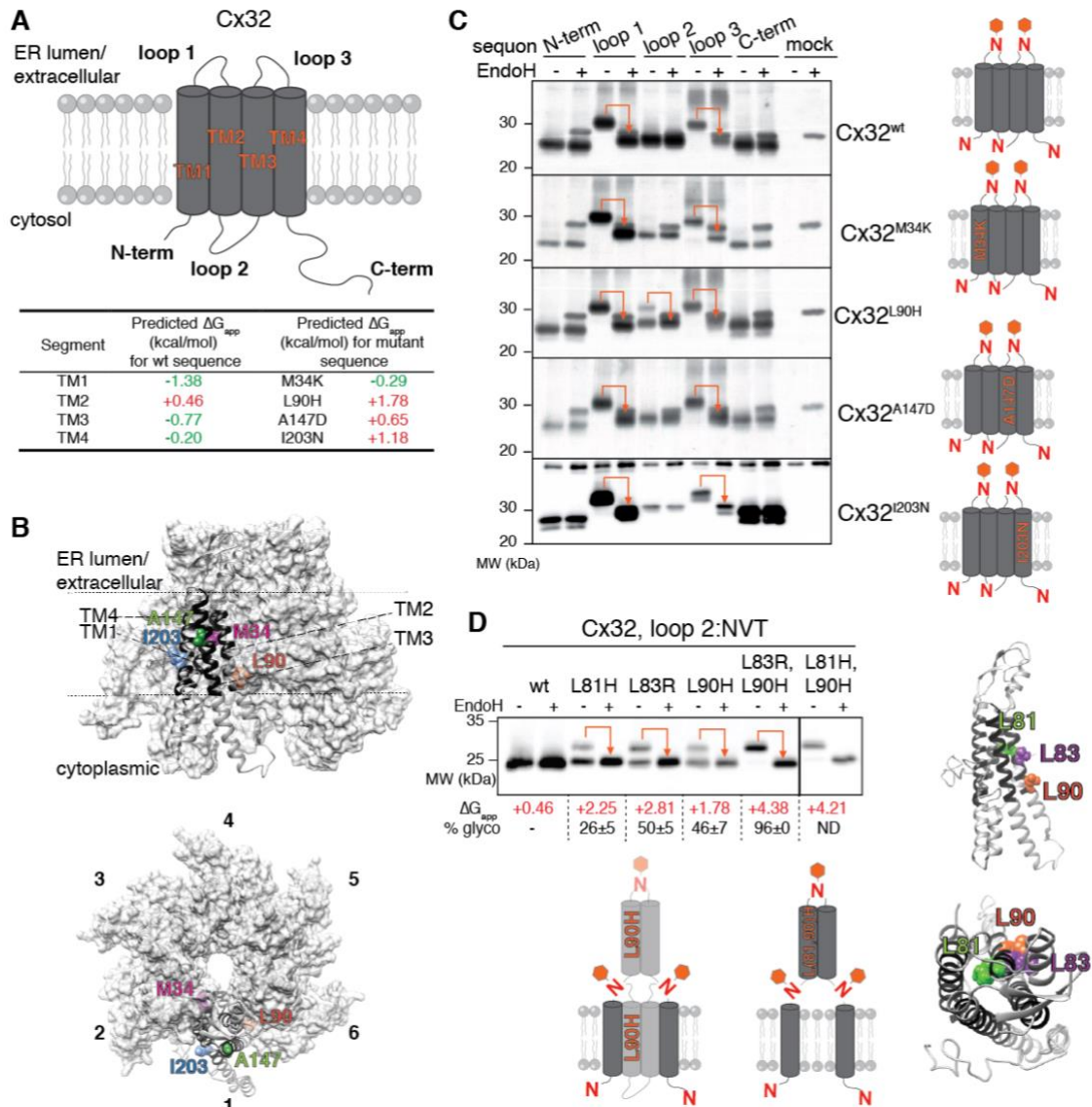
(figure legend in the next page)

Figure 11: Cx32 mutants lead to TM segments misintegration. (**A**) Top, schematic of Cx32 integration in the membrane, and table with ΔG_{app} for each wild type TM segment. Numbers in green indicate favorable integration, and in red unfavorable integration. CMT1X-causing mutants and respective ΔG_{app} are also shown. (**B**) Side and top view of the modeled Cx32 hexamer shown with surface filling. The four mutants presented in (A) are shown in the model, colored. TM segments are colored black and labeled in the side view of the model. Individual hexamers are numbered in the top view of the model. (**C**) Cx32^{wt} and mutants with glycosylation sequons in the indicated sites were transfected into 293T, lysed and treated with EndoH as indicated. Orange arrows indicate sugar digest by the enzyme and represent ER lumen exposure of a given loop. Models for properly integrated mutants are shown on the right. (**D**) The indicated mutants in TM2 were treated as described in (C). ΔG_{app} and fraction of glycosylated species are shown below the immunoblot. A modeled monomer is shown on the right side with side and top views, presenting the location of the three studied TM2 mutants. On the bottom side two models for partial and complete misintegration with example mutations in TM2. ND, not determined.

terminal tail (Fig. 11C). This way, anytime Cx32 exposes one of these regions to the ER lumen, glycosylation can occur and protein topology can be inferred. We proved assay functionality by confirming the previously published topology of Cx32^{wt}, where loop 1 and loop 3 are in the ER luminal face of the membrane, and the remaining loops on the cytoplasmic side (Fig. 11C) (337). Furthermore, while most mutants showed complete integration of their TM segments, this was only partially true for Cx32^{L90H} (Fig. 11C). For this TM2 mutant, a fraction of the protein shows glycosylation in loop 2, as confirmed by EndoH glycosidase treatment. This means that both TM2 and TM3 in Cx32^{L90H} are partially misintegrated, while the remaining TM segments (TM1 and TM4) show complete membrane integration (Fig. 11C). The wild type sequence of TM2 is predicted to not be inserted favorably in the membrane, when analyzed in isolation (Fig. 11A), which led us to infer small perturbations in this segment appeared to be enough for TM slipping to occur. To test this idea, we mutated Cx32 twice more with CMT1X-causing mutants in TM2, both once again destabilizing of TM helix membrane integration (Fig. 11D). For these, Cx32^{L81H} and Cx32^{L83R}, a subpopulation of Cx32 where both TM2 and TM3 were not integrated could again be detected (Fig. 11D), establishing TM2 as hot-spot for mutations leading to failed Cx32 topogenesis. Importantly, the three TM2 mutants were spread out throughout TM2, facing different sides of the TM helix (Fig. 11D).

Of note, at this point we could not detect quantitative glycosylation of our loop 2 reporter. This could be either due to (i) partial, not complete misintegration of TM2 and TM3 – i.e. there would be a $Cx32^{L90H}$ (and the other TM2 mutants) sub-population in which topogenesis was not compromised or, (ii) intrinsic failure of our sequon to be fully glycosylated, e.g. due to steric hinderance. To test if one of these hypotheses was correct, we decided to simultaneously equip TM2 with two destabilizing mutants – in this scenario algorithm prediction of TM integration completely misses the TM character of this sequence (data not shown). For these newly created double mutants, $Cx32^{L81H,L90H}$ and $Cx32^{L83R,L90H}$, glycosylation of the reporter site on loop 2 was now almost complete (Fig. 11D), meaning that it should be permanently exposed to the ER lumen according to our steady state analysis, and arguing for only partial misintegration of the single mutants in TM2.

b. Misintegrated Cx32 mutants are subject to ERAD

Having established TM2 (and consequently TM3) as a segment prone to misintegration upon mutation, we next wondered what the intracellular fate of these mutants would be. Towards this end, we tagged $Cx32^{wt}$, $Cx32^{L81H}$, $Cx32^{L90H}$, and double mutant, $Cx32^{L81H,L90H}$ with a C-terminal FLAG tag and electroporated COS-7 cells with said constructs. When immunofluorescence was performed, the intracellular location of $Cx32^{wt}$ was similar to that in previously published reports (422), arguing that C-terminally tagging Cx32 with FLAG does not hamper its trafficking or assembly (Fig. 12A). In these cells, while some intracellular retention can be observed, gap-junction plaques can be seen in cell-cell boundaries (Fig. 12A). These consist of ensembles of thousands of gap junction channels packed side-to-side, known to be physiologically relevant Cx32 supramolecular assemblies (332). The presence of these gap junction plaques could also be confirmed through a detergent insolubility assay: upon cell lysis, gap junction plaques will aggregate into a NP-40-insoluble pellet. Solubilization of this pellet by heating in 2% SDS-containing buffer and immunoblotting, we could clearly detect $Cx32^{wt}$ (Fig. 12B), arguing, together with the immunofluorescence data, for proper gap junction plaque assembly of the epitope-tagged $Cx32^{wt}$.
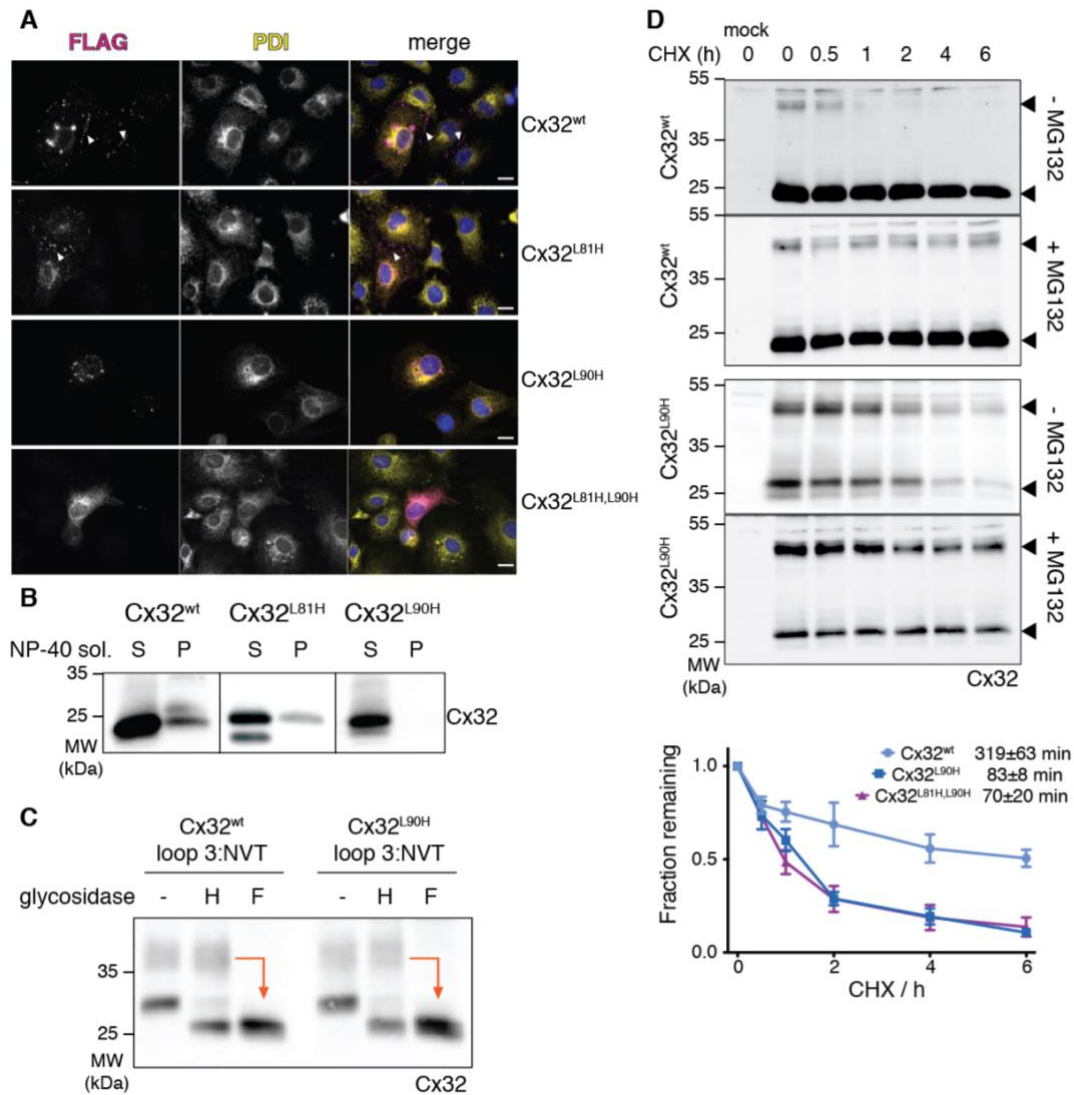
Figure 12: Misintegrated Cx32 is retained in the ER intracellularly and sent to ERAD. (**A**) FLAG-tagged Cx32 constructs were electroporated into COS-7 cells and connexin expression determined by immunofluorescence, in magenta. White arrowheads indicate gap junction plaque formation. PDI was used as an ER marker, in yellow. Nuclei are stained blue. Scale bars correspond to 20 μm. (**B**) 293T were transfected with the indicated constructs and lysed in NP-40 buffer. After centrifugation pellets were solubilized (P) and Cx32 immunoblotted in both the pellet and soluble (S) fractions. (**C**) 293T lysates with the indicated constructs expression were digested with either EndoH (H) or PNGaseF (F). Orange arrows indicate digestion of complex modified sugars. (**D**) Representative immunoblots and quantification of degradation kinetics of the indicated constructs in the presence of CHX. Arrowheads in the immunoblots indicate dimeric and monomeric forms of Cx32. Decays correspond to the sum of monomeric and dimeric species (indicated with arrowheads) for the samples without addition of MG132. The degradation of Cx32^{L81H,L90H} is shown in the graph only, together with the half-lives of the plotted constructs. Graph is shown as mean±SEM, N>3.

The same type of assembly could be observed for Cx32^{L81H}, but strikingly, while Cx32^{L90H} still did form punctae-like structures, there was no evidence for cell-cell boundary gap junction plaques (Fig. 12A), which could also be confirmed through the detergent-insolubility assay described above (Fig. 12B). We additionally noticed, through our glycosylation reporter system, that adding the NVT sequon on the third loop of Cx32^{L90H} gave rise to Golgi complex modified sugars which could only be digested with PNGase F, and not EndoH (Fig. 12C). These data point towards at least marginal traversing of Cx32^{L90H} through the Golgi, and against complete ER retention. Interestingly, by causing the topology to be fully compromised with our double mutant, Cx32^{L81H,L90H}, we could also completely retain this mutant in the ER (Fig. 12C). Taken together with partial ER escape from our partially misintegrated mutants, we can speculate that the misintegrated fraction of Cx32^{L81H} and Cx32^{L90H} is most likely ER retained.

Since we detected intracellular trafficking defects of our (partially) misintegrated mutants when compared to Cx32^{wt} (Fig. 12A), we decided to test if they would be recognized by the degradation machinery of the cell. Through CHX chases we could show that, while the wild type protein was mostly stable, with a half-life of ca. 5-6 h (Fig. 12D), our partially misintegrated, assembly-incompetent mutant, Cx32^{L90H}, showed a severely reduced half-life, at ca. 80 min, a decay that was mostly reversed by inhibiting the proteasome with MG132 (Fig. 12D). The same increase in degradation rate was seen for Cx32^{L81H,L90H}, showing a half-life of ca. 70 min (Fig. 12D). Thus, both the intracellular retention and the increased degradation rates seem to point towards the presence of mammalian machinery to deal with aberrant TM segment misintegration in multipass membrane protein.

c. Misintegrated Cx32 is recognized by a network of chaperones

As previously mentioned, the TM segments of single-pass membrane proteins may slip from the membrane into the ER lumen if their structure formation fails, e.g. due to failed intramembrane assembly (69). In these cases, the ER Hsp70 chaperone BiP can intervene to chaperone these mostly unstructured, hydrophobic TM segments. We thus wondered if the same can be found in our misintegrated Cx32 system. When we immunoprecipitated FLAG tagged Cx32^{wt}, Cx32^{L81H}, Cx32^{L90H} we could detect BiP binding to all of these

constructs (Fig. 13A). Since the wild type protein only has its loop 1 and loop 3 exposed to the ER lumen, we hypothesize some unstructured elements may be temporarily present in these until assembly can occur. We could also convincingly observe that both our partially misintegrated mutants co-immunoprecipitated significantly more BiP (Fig. 13A). Due to the fact BiP binds moderately hydrophobic peptides (169), we hypothesized that binding could be occurring directly via one of the misintegrated helices. To test this hypothesis, we adapted a previously described reporter system (69), in which an ER targeting, BiP-inert antibody C_L domain was fused to a Cx32 TM segment, followed by a glycosylation
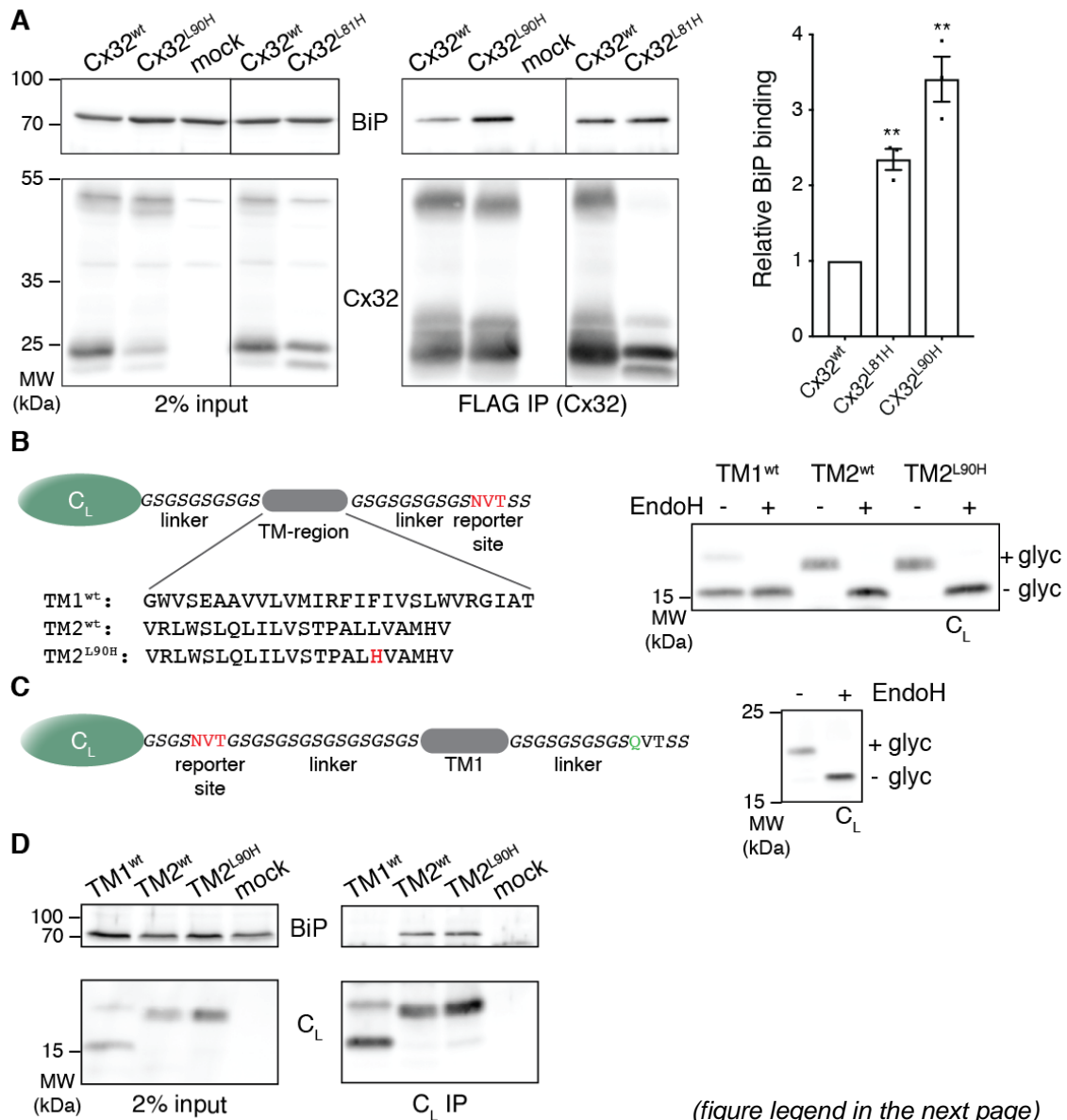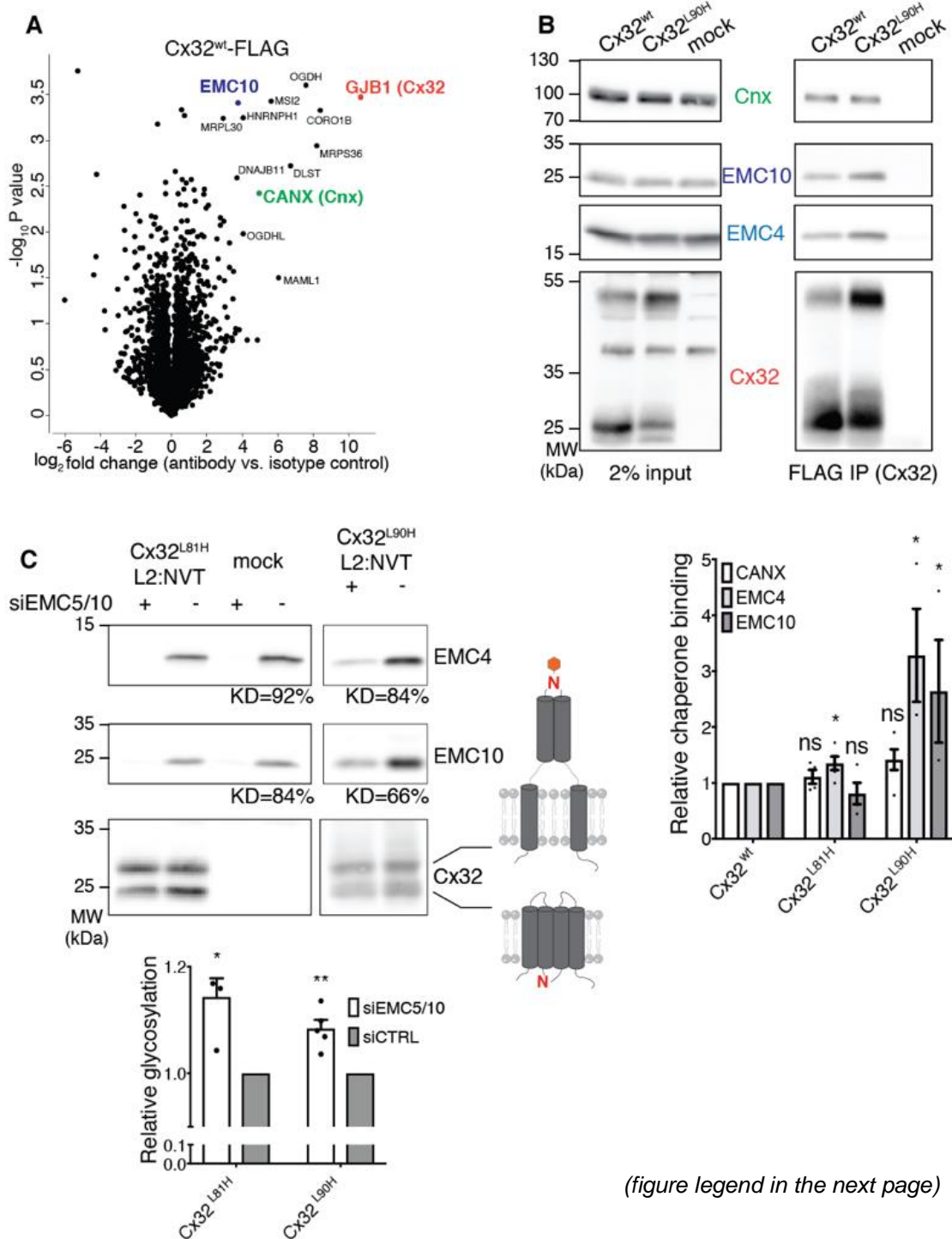

(figure legend in the next page)

Figure 13: BiP recognizes misintegrated TM segments. (**A**) The indicated FLAG-tagged Cx32 constructs were transfected together with murine BiP in 293T, and pulled down from cell lysates. Representative immunoblots from both input controls and immunoprecipitations are shown, together with quantification of relative BiP binding, on the right. Bar graphs are shown as mean±SEM, N=3. **, P value < 0.01. (**B**) Schematic of the construct containing a C_L domain and TM helix with sequence of the indicated TM segments. In red is the reporter site to assess integration. On the right, representative immunoblot for the different TM segment construct, with(out) preceding EndoH digest. (**C**) Schematic of the construct used to assess correct orientation of the inverted TM1 sequence. The glycosylation reporter site (in red) was placed downstream of TM1, and the original site seen in (B) was mutated (in green). On the right, immunoblot of 293T cells transfected with this construct, lysed, digested with EndoH, and immunoblotted for the C_L domain. (**D**) The constructs used in (B) were co-transfected with murine BiP into 293T cells, and immunoprecipitated. A representative immunoblot from the BiP interaction with each construct is shown.

sequon to monitor the TM segment integration (Fig. 13B). When Cx32 TM1 was applied to the system, we could detect very little glycosylation of our reporter site, indicating TM1 was integrated almost entirely (Fig. 13B). Of note, our TM1 sequence had to be inverted so the segment had the wild type orientation in the membrane, and we confirmed this inversion did not lead to altered TM segment topology (Fig. 13C). On the other hand, both wild type and mutated (L90H) C_L-TM2 constructs were almost fully misintegrated, slipping to the ER lumen, as seen by the nearly complete glycosylation of the C-terminal reporter site (Fig. 13B). This agrees with the ΔG_{app} for TM2 membrane integration (Fig. 11A), and tells us that in the context of full-length Cx32, TM2 integration in the membrane is most likely dependent on the presence of other Cx32 TM segment(s). Additionally, when assessing BiP binding to these constructs, while C_L-TM1 showed barely detectable BiP co-immunoprecipitation, both C_L-TM2^{wt} and C_L-TM2^{L90H} co-immunoprecipitated BiP (Fig. 13D), indicating that the chaperone is able to recognize the misintegrated TM segment and that these are most likely unstructured, based on BiP preferential binding propensities (169).

Having characterized BiP binding to Cx32^{L90H}, we decided to take a proteomics-based approach to identify other factors that could be involved in the quality control of Cx32. Towards this end we made use of our FLAG tagged constructs, immunoprecipitated them from 293T in mild digitonin buffer to maintain possible TM-TM interactions intact, and performed affinity-enrichment

mass spectrometry experiments (Fig. 14A). One of the most interesting hits resulting from this approach was the identification of the ER chaperone CANX (Fig. 14A). CANX is one of the most abundant chaperones in the mammalian ER and its canonical role is the recognition of sugar moieties in ER glycosylated proteins, as a means to assess protein folding in this organelle (151). Interestingly, Cx32 is not a glycoprotein which makes a possible calnexin

(figure legend in the next page)

Figure 14: Cx32 is recognized by different ER membrane chaperones. (**A**) Volcano plot resulting from AE-MS performed from the immunoprecipitation of Cx32^{wt}-FLAG in mild digitonin buffer from transfected 293T cells, against immunoprecipitation with an IgG control antibody. Cx32 is highlighted in red. In green and blue are the identified chaperone characterized further. Names correspond to Uniprot gene name. (**B**) FLAG-tagged Cx32 constructs were immunoprecipitated and interaction with endogenous CANX, EMC4, and EMC10 was detected. Quantification of the degree of interaction for the different Cx32/chaperone pairs is shown below. Bar graph represents mean±SEM, N>3. (**C**) The EMC was destabilized through siRNA-mediated knockdown in 293T cells, and Cx32 with a glycosylation topology reporter on loop 2 (red "N") was transfected. Levels of average knockdown are shown. On the right side, schematics on the topology of each species in the immunoblot. Quantification of relative glycosylation is shown below in the bar graph showing mean±SEM, N>3. ns, not significant; *, P value < 0.05; **, P value < 0.01

chaperoning role to be independent of its canonical lectin activity. In order to confirm the chaperone as a true-positive from our AE-MS, we co-immunoprecipitated endogenous CANX by pulling down FLAG-tagged Cx32 as previously described (Fig. 14B). We could once again preserve CANX interaction with both Cx32^{wt} and the partially misintegrated mutants, and while there was a tendency for Cx32^{L90H} to bind more calnexin, this difference in binding was not significant (Fig. 14B).

One other interesting hit we detected in our AE-MS experiments was EMC10 (Fig. 14A). EMC10 is part of the ten-membered ER membrane protein complex, a complex recently reported to play a role in different aspects of membrane protein biogenesis, particularly in the insertion of TM segments with low hydrophobicity (75,79,90). This sparked our interest since our Cx32 variants have this distinguishing feature. We started by demonstrating EMC10 binding to all Cx32 variants (Fig. 14B), and by extending our co-immunoprecipitation studies, we could also detect binding to the EMC4 subunit (Fig. 14B). As was the case for interaction with BiP, both EMC subunits were preferentially enriched upon pulldown of partially misintegrated Cx32 variants.

The different roles ascribed to the EMC in TM segment insertion have been mostly placed in its cytoplasmic activity, i.e. low hydrophobicity TM segments in the cytosol getting inserted into the ER membrane by means of the complex (423). We became interested if the same could happen in our system where the misintegrated TM segment is in the ER lumen. To test this idea, we took

advantage of our glycosylation reporter system to measure integration, and towards this, we decided to destabilize the EMC via siRNA induced knockdown (Fig. 14C). Previous work has described both the EMC5 and EMC6 to be central to the stability of the whole complex, since destabilizing either of these can disrupt the complex for the most part (76,79). Hence, we decided to use EMC5 and EMC10 siRNAs (in order to guarantee EMC10 knockdown, the interaction partner we had detected in AE-MS) and compared the levels of Cx32 TM2 and TM3 integration against the use of a control siRNA. Despite a small effect, a reproducible increase in misintegration could be detected for both Cx32^{L81H} and Cx32^{L90H} when the EMC was knocked down (Fig. 14C), corroborating our theory in which the complex can aid TM segment insertion, possibly even on the ER luminal side.

d. Misintegrated Cx32 ERAD is handled by gp78

Given the preferential binding of our misintegrated mutants to quality control machinery in the form of BiP and the EMC (Fig. 13A, 14B), and the fact we could see a significant increase in the degradation rate of Cx32^{L90H} when comparing it to Cx32^{wt} (Fig. 12D), we became interested in the E3 ubiquitin ligase responsible for the clearance of misintegrated membrane proteins. We focused mostly on the ER resident Hrd1 and gp78 which have been vastly implied in ERAD-L and ERAD-M (424). In order to assess if one of the two had a role in the disposal of faulty Cx32, we cloned dominant negative RING mutants for both, Hrd1^{C291S} and gp78^{C341S,C378S} (270,425). When these were individually co-transfected with Cx32^{L90H}, Hrd1^{C291S} showed a modest effect in stabilizing the mutant, while gp78^{C341S,C378S} showed a considerably stronger effect (Fig. 15A). In order to determine if the stabilization we observed was due to the E3 ubiquitin ligase activity of gp78, we co-transfected 293T cells with Cx32^{L90H} and gp78^{wt},

gp78$^{C(341,378)S}$, or mock plasmid, and inhibited the proteasome in order to allow ubiquitinated protein to accumulate. After this, we immunoprecipitated Cx32^{L90H} and detected ubiquitinated proteins (Fig. 15B). Co-transfection of our RING mutant gp78 led to no significant increase in the levels of ubiquitinated Cx32 upon MG132 treatment, which could be observed seen for gp78^{wt} co-transfection (Fig. 15C). Taken together, we could show that Hrd1, and even more so gp78 plays a role in clearing the cell of misintegrated Cx32 via ERAD.

Figure 15: gp78 handles misintegrated Cx32^{L90H} ERAD. (**A**) Decay of Cx32^{L90H} co-transfected with the indicated gp78 constructs, or a mock plasmid, assessed via CHX chase. Graphs are shown as mean±SEM, N>3. *, P value < 0.05 for gp78^{C314S,C378S} vs mock transfection; #, P value < 0.05 for Hrd1^{C291S} vs mock transfection (**B**) 293T co-transfected with the indicated construct pairs were incubated with MG132 or DMSO as a control for 6 h, followed by FLAG immunoprecipitation and immunoblotting of the indicated proteins. (**C**) Quantification of (B). Bar graphs are shown as mean±SEM, N=4. ns, not significant; **, P value < 0.01.
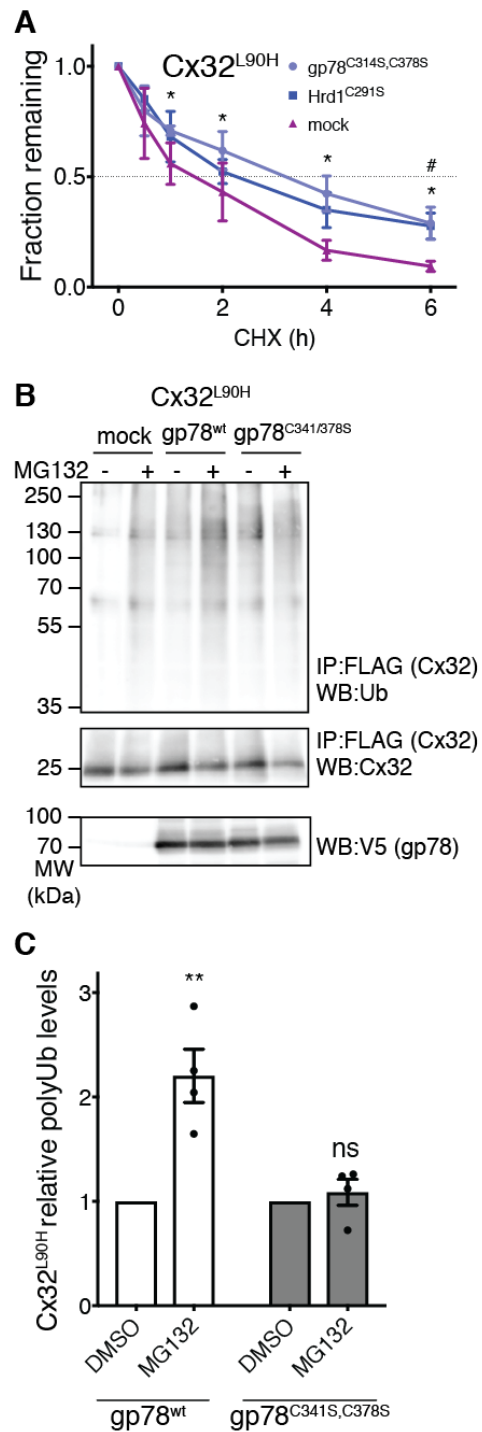
2. The endoplasmic reticulum signal peptidase acts as a quality control enzyme for membrane proteins

a. Disease-causing connexin mutants are processed in their N-terminal region

When studying the different CMT1X-causing mutants, we showed how membrane embedded mutations may lead to problems in TM helix integration, and how this is recognized and handled by ER quality control mechanisms. At the same time, we observed that several of our CMT1X mutants showed an aberrant running behavior when analyzed via immunoblotting (Fig. 16A). In order to expand our repertoire of studied connexins, we decided to additionally look into two membrane-embedded deafness-causing mutants of Cx26 (GJß2), $Cx26^{R32H}$ and $Cx26^{I203K}$, located in TM1 and TM4 respectively. Similar to what we observed for Cx32, these mutants also showed an

Figure 16: Connexins are cleaved in their N-terminal. (**A**) Schematic of Cx32 membrane integration, disulfide formation pattern, and localization of membrane and luminal mutants. A representative immunoblot for the indicated constructs is shown below. Arrowheads represent the two species, wild type like and aberrant (**B**) Same as in (A) for Cx26. Hsc70 was used as a loading control. (**C**) NF1 cells were electroporated with the indicated Cx32 mutants, and lysates immunoblotted. Arrowheads indicate the two Cx32 species seen in 293T cells. (**D**) Connexin constructs were FLAG tagged in either termini, transfected into 293T cells, and immunoblotted with either Cx32 and FLAG antibodies (for Cx32 mutants), or only a FLAG antibody (for Cx26).
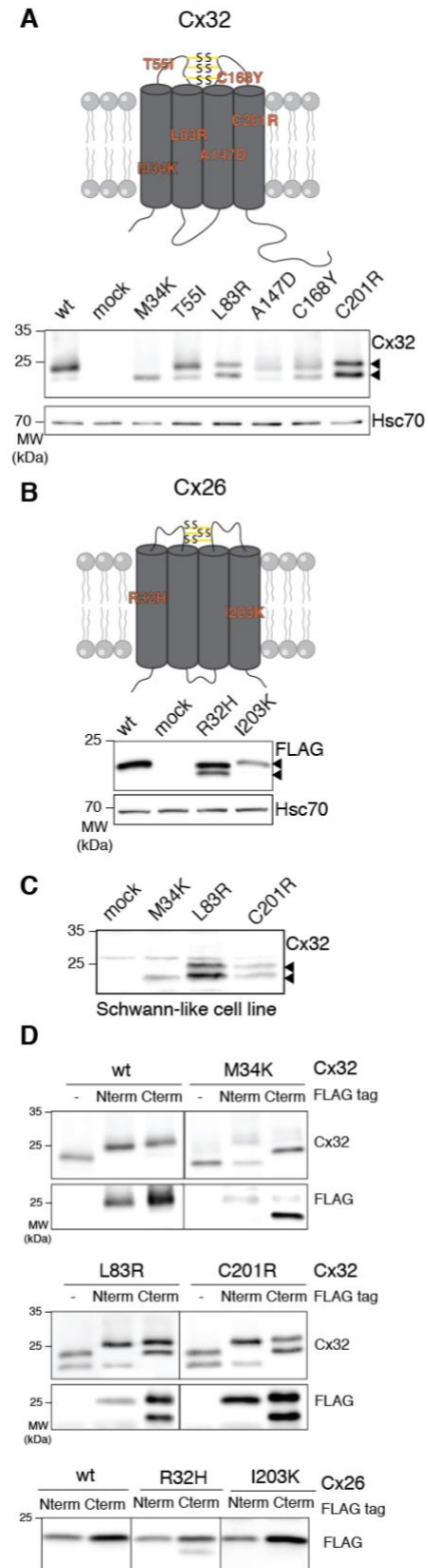
aberrant SDS-PAGE running behavior (Fig. 16B). While most of the wild-type protein would migrate at its expected size, these mutants led to the appearance of a faster migrating species, either exclusively (Cx32^{M34K}), or together the typical wildtype like species. Importantly, the same running behavior was seen when Cx32 was transfected into NF1 cells (Fig. 16C), a precursor of the human Cx32-expressing Schwann cell line, arguing that such phenotype would also be found in CMT1X patients affected by any of these mutations. Having excluded glycosylation and incomplete disulfide reduction on Cx32 as possible origins of the second species (data not shown), we decided to focus on proteolysis as a possible cause. To accomplish this, we equipped wild type protein and mutants with a FLAG tag in either of their termini, transfected these into 293T cells, and blotted the constructs with either a Cx32 or a FLAG antibody (Fig. 16D). When analyzing the Cx32 blots we could clearly see the decrease in mobility for the FLAG tagged upper band. However, the faster migrating species on the N-terminally tagged mutants migrated at the same height as the faster migrating, untagged band (Fig. 16D), thus confirming and mapping cleavage to the N-terminal of Cx32.

b. SPC cleaves cryptic cleavage sites in mutant connexins

Given the size of the cleaved connexin species when compared to that of the full-length protein, we assumed N-terminal cleavage would likely be occurring around TM1. This TM segment has a type II topology (N_{in}/C_{out}) for all known connexin proteins (426) which would be one of the prerequisites for SPC mediated proteolysis (427). This complex is abundant in the ER and is responsible for the juxtamembrane cleavage of signal peptides in membrane proteins, and especially, soluble proteins of the secretory pathway (427). Furthermore, expressing Cx32^{C201R} in different knockout cell lines for distinct ER intramembrane proteases did not lead to a change in the presence of cleavage product (data not shown). Different algorithms have been trained to identify the presence of signal peptides in proteins, so we made use of one of these, SignalP 4.1 (418), to check if a signal peptide would be predicted. When analyzing the sequence of Cx32, the SignalP 4.1 algorithm identified three cleavage sites, with a predicted low probability, after Cx32 TM1, consistent with the role of this segment as a signal anchor (Fig. 17A). Given the proximity to the threshold

probability for cleavage given by the algorithm, and the fact that if SPC-mediated cleavage was occurring, it would not be through a canonical pathway (see its dependency on mutations located as far as Cx32 last TM segment), we decided to follow this route.

It has been previously described that, similar to other proteases, SPC cleavage depends on the presence of looped regions around the cleavage site of the substrate (428). Since SignalP 4.1 predicted cleavage to occur between A39/A40, A41/E14 (scoring the highest cleavage provability), and G45/D46 (scoring the lowest) (Fig. 17A), we hypothesized that promoting α-helical structure around this stretch, by effectively extending TM1, would hamper SPC mediated cleavage. By doing this on Cx32^{M34K} (Cx32^{M34K,} TM1^{ext}), we could completely block the cleavage phenotype (Fig. 17C). Additionally, by a new
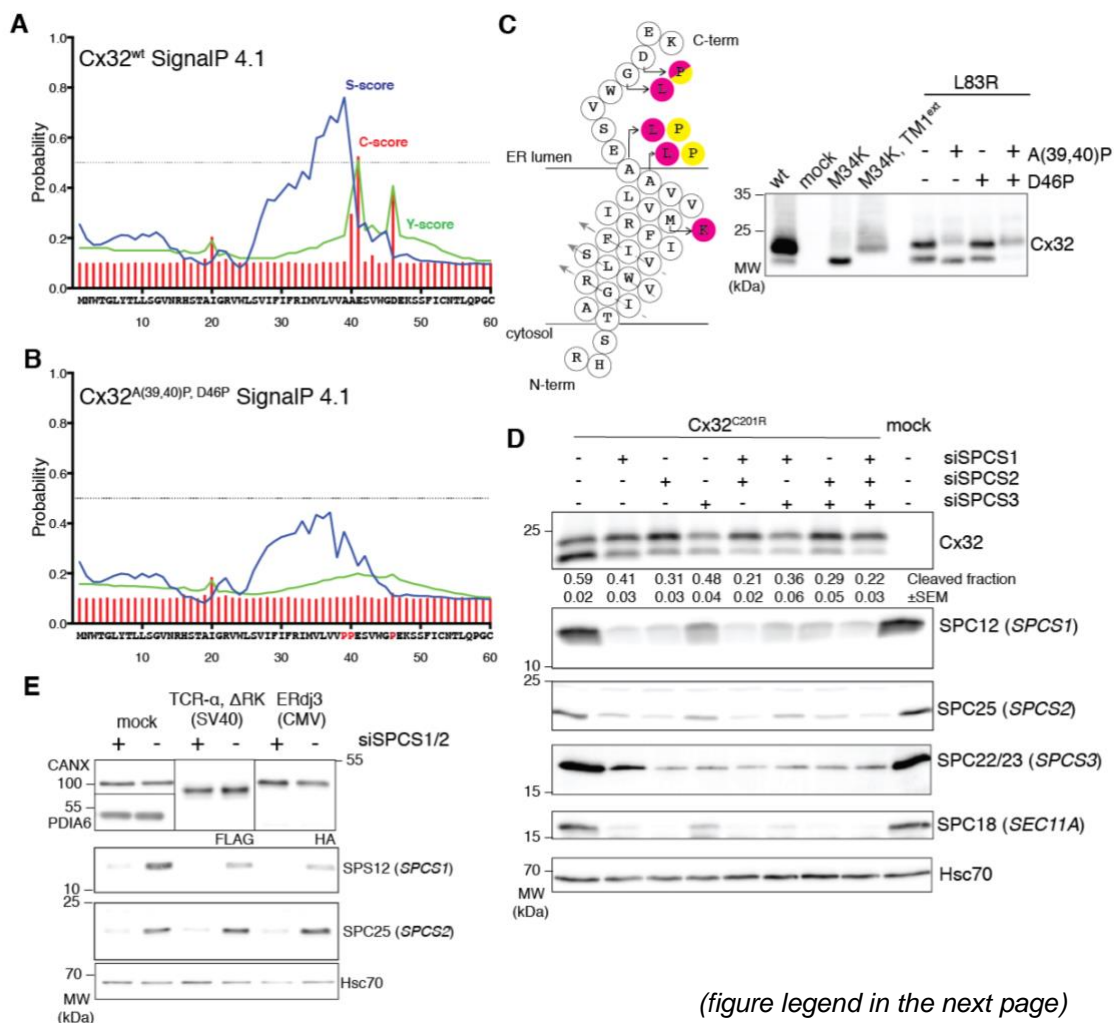
Figure 17: Cx32 is processed by the SPC. (**A**) SignalP 4.1 plots Cx32^{wt}. The C-score determines the probability that cleavage occurs before a given amino acid residue. The S-score

determines the probability of a given sequence being a signal peptide, and the Y-score combines the C-score with the slope of the S-score. The first 70 amino acids of Cx32 are shown. (**B**) Same as (A), for Cx32$^{A(39,40)P,D46P}$ (**C**) Schematic of Cx32 TM1 with arrows depicting the orientation of the sequence. Mutants used to revert cleavage are shown, colored pink for usage in the context of Cx32^{M34K}, and yellow for usage in the context of Cx32^{L83R}. A representative immunoblot is shown on the right, resulting from the transfection of the indicated constructs into 293T. "M34K, TM1^{ext}" refers to the extension of TM1 in the context of Cx32^{M34K}. (**D**) The auxiliary subunits of the SPC were knocked down from 293T via siRNA, and Cx32^{C201R} was transfected into these cells. Representative immunoblots for Cx32 as well as the SPC subunits are shown. Average cleavage and SEM are shown under the Cx32 immunoblot. N>3. (**E**) 293T were depleted of the SPC as in (D) and transfected with the indicated constructs. TCR-α, ΔRK, under the control of a weak SV40 promoter, a version of the TCR-α lacking Arg and Lys residues in its TM segments, guaranteeing stable membrane insertion (69). ERdj3 was under the control of a strong CMV promoter. Immunoblots for endogenous CANX and PDIA6 (soluble) are shown in mock transfected cells. Hsc70 served as a loading control.

analysis on SignalP 4.1 we realized that exchanging key residues to Pro led to a prediction of no-cleavage (Fig. 17B). These Pro residues were mutated onto Cx32^{L83R}, once again completely blocking our cleavage phenotype, and effectively converting our seemingly non-canonical Cx32 signal peptide to a signal anchor (Fig. 17C). Interestingly, the Pro replacement for the first predicted cleavage site (Cx32$^{A(39,40)P,L83R}$) leads to an electrophoretic mobility shift of its cleaved fragment, consistent with a new cleavage site around D46 (Fig. 17C).

Since replacement of structural elements in Cx32 is not enough to determine the identity of the responsible protease, we decided to switch our attention to the relationship between SPC expression and connexin mutant cleavage. The mammalian SPC is composed of five subunits – two catalytical (SPC18 and SPC21, encoded by *SEC11A* and *SEC11C*, respectively), and three auxiliary (SPC12, SPC22/23, and SPC25, encoded by *SPCS1*, *SPCS3*, and *SPCS2*, respectively) subunits (Fig. 17C) (93,104,427). We decided to resort to siRNA-mediated knockdown of the auxiliary subunits, alone or in combination, in an attempt to confirm SPC as the responsible protease, and to try to pinpoint which of the subunits is responsible for cleavage. Of note, the biological roles of the auxiliary subunits still remain ill-defined. Transfecting Cx32^{C201R} into 293T cells with individual or combined knockdown of the auxiliary SPC subunits showed us a reversal in the cleavage phenotype (Fig. 17D), with an increase in full-length protein and concomitant decrease in the cleaved species intensity,

convincingly confirming SPC as the responsible protease for Cx32 cleavage. Interestingly we also found that, akin to other membrane protein complexes (79,429), knockdown of either one of the three auxiliary subunits would lead to destabilization of the remaining complex subunits, where *SPCS2* knockdown seemed to lead to the highest degree of destabilization (Fig. 17D). Unfortunately, for this reason we could not define an individual subunit of the SPC responsible for targeting connexins to cleavage. Interestingly, despite reduction in overall SPC levels, we observed no effect on precursor processing on an array of canonical substrates of the SPC, regardless if they were endogenously expressed or not, or if they were a membrane or soluble substrate (Fig. 17E).

c. Misfolding triggers SPC mediated cleavage

Having proven SPC mediated cleavage of our Cx32 mutants, we became interested in the reason for this to occur to such an extent. Given the different nature and location of the mutants along two different proteins, Cx26 and Cx32, our data argue for a general principle underlying SPC cleavage that cannot be attributed to changes in cleavage sites themselves. One of the characteristics common to the cleaved proteins was the presence of missense mutations in structurally critical parts of the protein, such as the TM segments or disulfide bonds (such is the case for Cx32^{C168Y}) (Fig. 16A). When we decided to analyze the intracellular expression of our mutants by immunofluorescence in COS-7 cells, we found most to be ER-retained (Fig. 18A, B), and seemingly not present in wild type-like gap junction plaques, which could also be confirmed by our detergent-insolubility assay (Fig. 18C, D). Since one of the reasons for protein retention in the ER is misfolding, we hypothesized this could be in the basis for cleavage. We speculated that if this was the case we could in principle reduce the amount of cleavage by correcting connexin misfolding. Towards this end we took a revertant based approach – corrector mutants which should, in principle, be able to ameliorate misfolding through e.g. charge compensation. Our
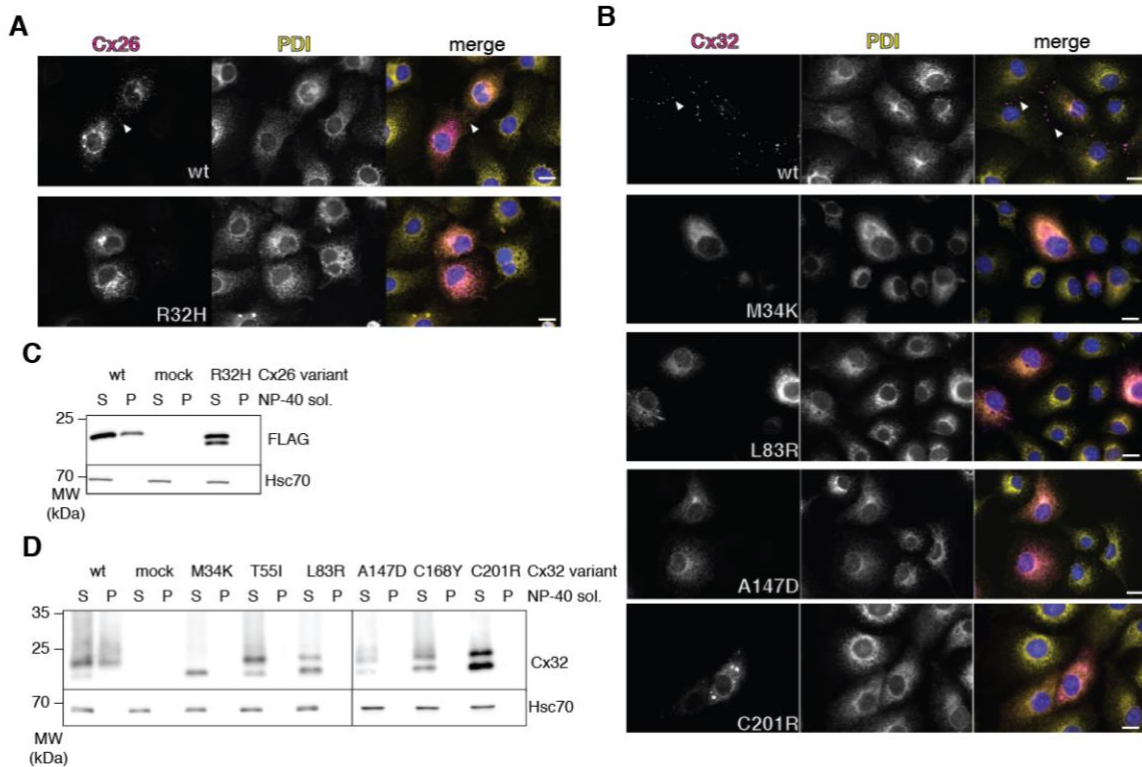
Figure 18: Processed connexin mutants are retained in the ER. (**A**) Immunofluoresnce of COS-7 cells transfected with the indicated Cx26 FLAG-tagged constructs, detected in magenta. PDI was used as an ER marker, in yellow, and nuclei were stained and are shown in blue. White arrowheads refer to gap junction plaque formation. Scale bars correspond to 20 µm. (**B**) Same as in (A), for Cx32 mutants. (**C**) The different Cx26 constructs were transfected into 293T, cells were lysed in NP-40 containing buffer and centrifuged. The resulting pellet (P) was solubilized and both this and the soluble (S) fractions were immunoblotted for Cx32. (**D**) Same as in (C), for Cx32 constructs. (**D**) Same as in (B) for Cx32 constructs. Hsc70 was used as a loading control.

hypothesis was that these would decrease the degree of cleavage. Cx26 provided a good avenue to take this kind of approach since a crystal structure is available (345). Focusing on Cx26^{R32H} we speculated that in this scenario, E147 (located on Cx26 TM3) was left unpaired in the membrane, where in Cx26^{wt} it can interact with R32 (Fig. 19A). Therefore, we computationally devised that replacing the Glu by an Ala would resolve this in the context of Cx26^{R32H}. By generating Cx26^{R32H,E147A}, modeled to stabilize the helical bundle in the membrane (Fig. 19B), we could partially reverse the cleavage of Cx26^{R32H} (Fig. 19C). A similar approach, this time based on charge stabilization, was taken for Cx32^{M34K} and Cx32^{C201R}, based on analysis of newly generated structural models for each mutant (Fig. 19D, E). In the first case we engineered Cx32^{M34K,V38E} (where E38 can act as a potential charge stabilizer in the same TM helix) (Fig. 19D) as a
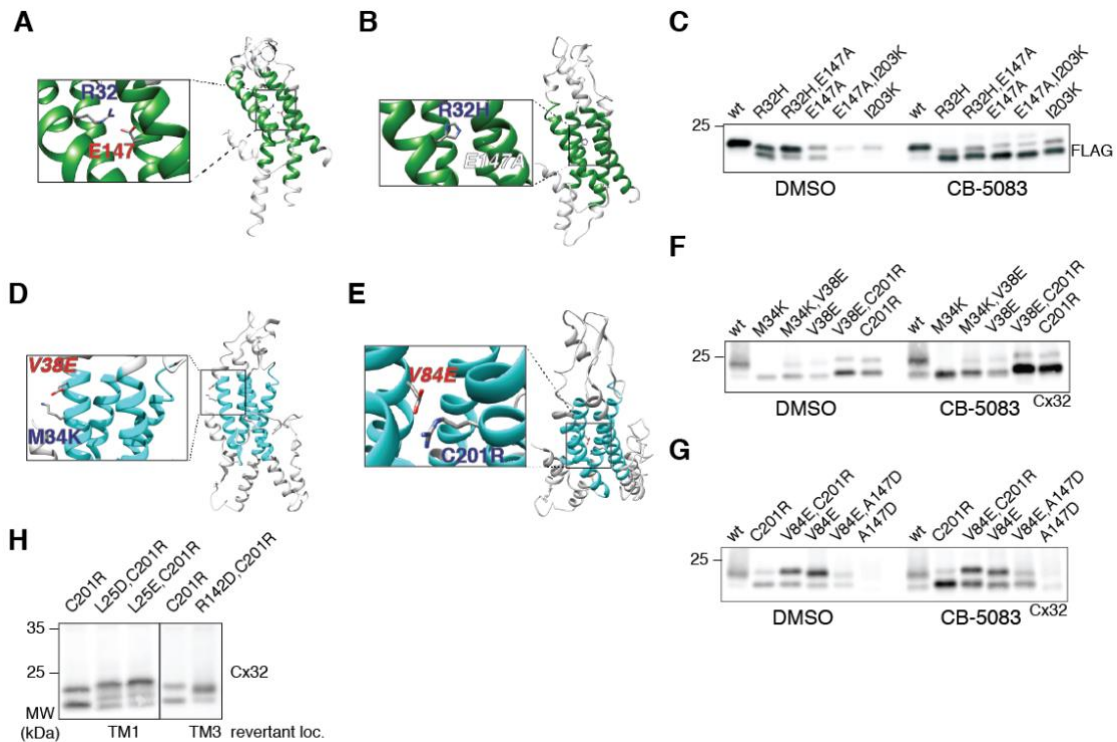
Figure 19: Connexin revertants decrease SPC-mediated cleavage. (**A**) Structure of Cx26^{wt} (345), with inlet showing interaction between R32 and E147, shown as sticks, colored by atom. Transmembrane segments are colored green. (**B**) Same as in (A), for modeled Cx26^{R32H,E147A}. (**C**) Representative immunoblot of revertant expression in DMSO- or CB-5083-treated 293T. Controls for the effect of revertants on cleavage are also shown on the same immunoblot. (**D**) Same as in (A) for Cx32^{M34K,V38E}. (**E**) Same as in (A) for Cx32^{C201R,V84E}. Cx32 transmembrane helices are colored cyan. (**F**) Same as in (C) for the Cx32^{M34K,V38E} revertant. (**G**) Same as in (C) for Cx32^{C201R,V84E} revertant. (**H**) Immunoblot showing different Cx32^{C201R} revertants and their TM segment location.

possible revertant, and for Cx32^{C201R} we speculated that introducing V84E in TM3 could also ameliorate the intramembrane fold (where charge compensation would be stemming from different TM helices) (Fig. 19E). Alike the reversal on Cx26 cleavage, we could now also observe stabilization of the full-length protein with concomitant reduction in the cleaved fraction (Fig. 19F, G). Not only this, but most of our revertant mutants were destabilizing when analyzed in isolation (e.g. Cx32^{V38E}) (Fig. 19F), and in some cases would further increase cleavage (through presumably increasing misfolding) of unrelated, structurally apart mutants (e.g. Cx32^{V38E,C201R}) (Fig. 19F), pointing towards the specificity of the observed effect. In order to be certain the effects we were observing were due to a reversal in the cleavage phenotype, and not preferential ERAD of one species over the other, we incubated our 293T cells with the VCP/p97 inhibitor, CB-5083,

to guarantee connexin proteins would not be extracted from the membrane and degraded. In agreement with our previous data, the revertants led to a stabilization of the full-length species (Fig. 19C, F, G), arguing the effect we observed in our initial steady state analysis was not due to e.g. preferential degradation of the cleaved species. Moreover, we could extend the repertoire of Cx32^{C201R} full-length stabilizing revertants to other Cx32 TM helices with different amounts of success (Fig. 19H). This gave us a very good indication that indeed misfolding was at the basis of cleavage, since improving it via protein engineering seemed to revert the cleavage phenotype in our selected mutants.

Likewise, since ameliorating folding led to a reduction in cleavage, we envisioned that by worsening misfolding we could further increase SPC mediated cleavage, as seemed to be the case for some revertant pairing (e.g. Cx32^{V38E,C201R}). Connexin proteins contain three well conserved disulfide bonds, bridging both their extracellular loops, and whose role is mostly thought to be in

(figure legend in the next page)

76
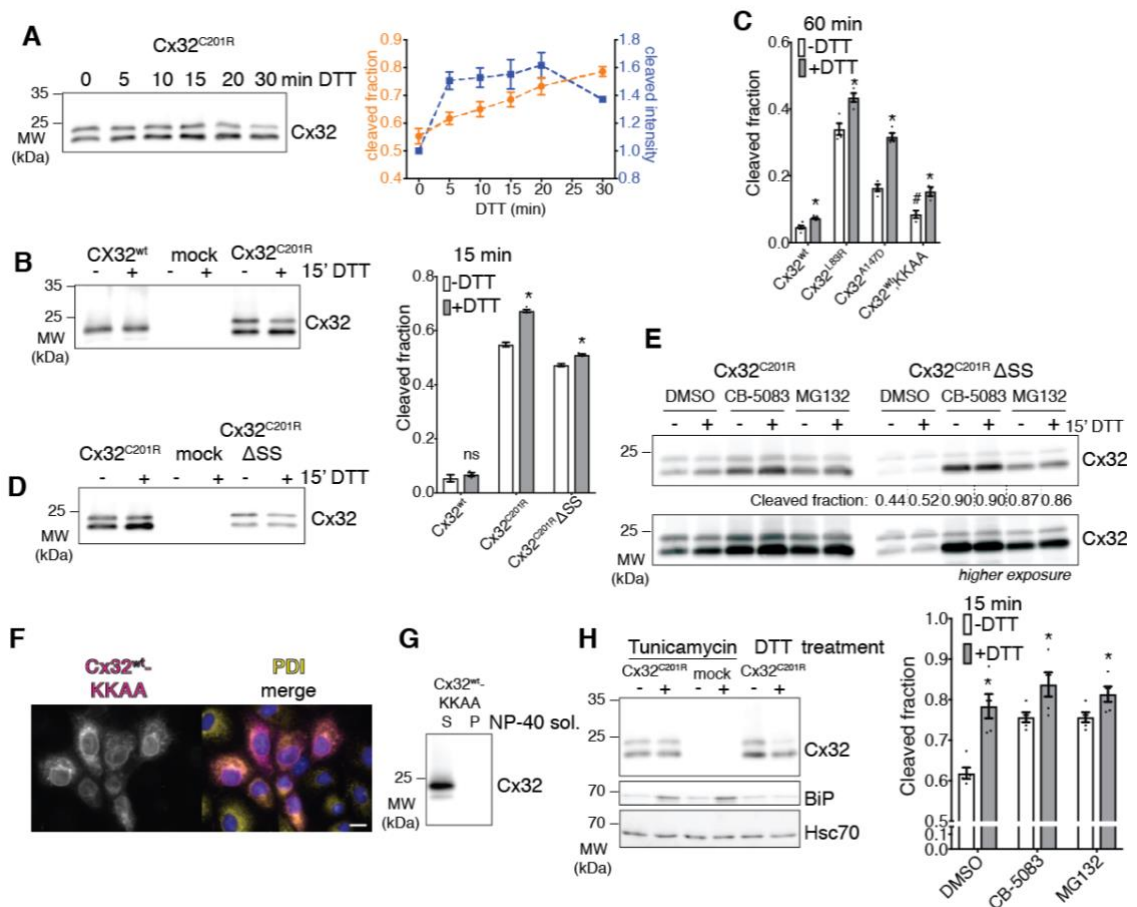
Figure 20: Destabilization of Cx32 folding further triggers SPC-mediated processing. (**A**) Cx32^{C201R} was transfected into 293T, and cells were incubated for the indicated time with 10 mM DTT pre-lysis. A representative blot is shown, together with its quantification on the right. Data points refer to mean±SEM, N=3. (**B**) The indicated constructs were transfected into 293T, and cells were incubated with 10 mM DTT for 15 min pre-lysis. A representative Cx32 immunoblot is shown, together with its quantification in the right. Bar graphs are shown as mean±SEM, N>3. (**C**) 293T were transfected with the indicated constructs and incubated with 10 mM DTT for 1 h before lysis. Quantification is shown in the bar graph as mean±SEM, N>3. (**D**) As in (B) with the indicated constructs. Quantification for Cx32^{C201R} ΔSS is shown in (B). (**E**) Cx32^{C201R} with and without disulfide forming cysteines was transfected into 293T cells. Cells were incubated for 3 h with CB-5083, MG132, or DMSO as a vehicle control, followed by a 15 min incubation with 10 mM DTT. A higher exposure blot is shown due to the low signal of DMSO treated Cx32^{C201R} ΔSS samples. The amount of cleaved fraction from one experiment is shown below the top Cx32 blot. Graph below refers to Cx32^{C201R} cleavage with treatments indicated. Data are shown as mean±SEM, N=5. (**F**) Cx32^{wt}-KKAA was electroporated into COS-7 cells, and its cellular expression was determined via immunofluorescence, in magenta. PDI was used as an ER marker, in yellow, and nuclei are shown in blue. Scale bar corresponds to 20 μm. (**G**) 293T were transfected with Cx32^{wt}-KKAA and lysed in NP-40 buffer. The insoluble fraction was solubilized (P) and Cx32 was immunoblotted in this fraction and the NP-40 soluble one (S). (**H**) 293T transfected with the indicated constructs were treated with tunicamycin for 6 h, or DTT for 1 h. After lysis the samples were immunoblotted for the indicated proteins. Hsc70 served as a loading control. ns, not significant; #, P value < 0.05 for comparison of Cx32^{wt}-KKAA with Cx32^{wt}, both without the addition of DTT; *, P value < 0.05.

stabilizing connexon assembly between two membranes and hence, GJIC function (365,430). To test if inducing misfolding further in our disease-causing mutants would also promote further cleavage, we made use of connexin disulfides and their susceptibility to reduction through DTT incubation, thus generating misfolding in vitro. A DTT incubation time as short as 5 min prior to lysis was enough to produce a concomitant increase in both the intensity of the cleaved species, as well as its relative fraction (Fig. 20A), and an incubation of 15 min produced a significant increase on Cx32^{C201R} cleavage, while marginally affecting Cx32^{wt} (Fig. 20B). Interestingly, an incubation time longer than 20 min resulted in a decrease of intensity for the cleaved species, in what we assume is the start of the effect DTT has on protein translation arrest (431). Nonetheless, longer incubations of up to 1 h produced strong changes for all of our studied mutants, but due to translation shutoff induced by DTT, and overall lower protein

levels, analysis of these adds a layer of confounding factors (Fig. 20C). Removal of all disulfide-forming cysteines from Cx32^{C201R} (Cx32^{C201R} ΔSS) precluded most of the effect DTT had on the disulfide-forming Cx32^{C201R}, arguing for a specific effect of the compound on disulfide reduction and ensuing misfolding (Fig. 20B, D).

One of the drawbacks our experimental setup could face was preferential ERAD of full-length protein (as described above), induced even by short DTT incubation times. To control for this possibility, we took advantage of the VCP/p97 inhibitor, CB-5083, and the proteasome inhibitor, MG132, and incubated transfected 293T for 3 h with either one, or DMSO as a vehicle control. After this, we included 10 mM DTT in the cell medium for the standard 15 min. Even with inhibition of these two pathways, we could still see a conversion of full-length protein into cleaved protein, arguing that the effect of DTT we see by immunoblot is not based on preferential ERAD of full-length protein (Fig. 20E). Once again, this conversion was largely lost in Cx32^{C201R} ΔSS, despite the absence of other experimental replicates.

In regards to the cleavage inducing behavior of DTT, we could also observe a significant but modest effect in Cx32^{wt}. We expected Cx32^{wt} to be susceptible to DTT-induced cleavage, but given our steady state approach, that the majority of protein had already escaped the ER, where the SPC is expressed. By adding a cytosolic di-lysine ER retention motif to the C-terminal of Cx32^{wt} (Cx32-KKAA), the protein became retained (Fig. 20F), unable to form gap junction plaques (Fig. 20G), and more sensitive to the effect of DTT (Fig. 20C).

Finally, since DTT is an established activator of the UPR (431), and this pathway is surely expected to be activated at longer incubation times of e.g. 1 h, we used another UPR inducer, the glycosylation inhibitor tunicamycin, to test if UPR activation could trigger connexin cleavage. Importantly, Cx32 is not glycosylated, so any observed effect would be directly due to ER stress and not changes in Cx32 glycosylation status. Although tunicamycin efficiently triggered the UPR as seen by the increase in BiP expression, no change in the levels of cleaved Cx32 was observed (Fig. 20H), further arguing for structural destabilization-induced cleavage of Cx32.

d. Cleaved connexins are ER-retained and sent to ERAD

The fact some cleaved mutants seemed to be able to leave the ER and form higher order complexes, such as the observation of punctae for $Cx32^{C201R}$ (Fig. 18B), we questioned if this type of phenotype could be due to bypassing of ER quality control ,due to assembly of cleaved with full-length protein.

To investigate possible interaction between the two fractions of protein, we made use of our N-terminally FLAG-tagged $Cx32^{C201R}$, in which the affinity tag will only be present in the full-length protein, and not in its cleaved counterpart. By immunoprecipitation the FLAG-tagged full-length $Cx32^{C201R}$ we could convincingly co-purify the cleaved fraction of the mutant (Fig. 21A). To confirm and expand this result, we cloned a truncated version of $Cx32^{wt}$, missing its first 46 amino acid residues, which we confirmed to be ca. 90% efficiently inserted in the ER membrane through the use of topology reporter sequons (Fig. 21B), as described previously. Next, by cloning a C-terminal HA tag to our truncated construct, and by once again resorting to the C-terminally FLAG-tagged $Cx32^{wt}$, we expressed both constructs, together or in isolation, in 293T cells. We then immunoprecipitated each variant, and through immunoblot sought to detect the other one (Fig. 21C), to confirm if interaction would be maintained. Furthermore, we decided to control for eventual post-lysis interaction by making use of two lysates transfected with each construct individually, and mixing them post-lysis. We could clearly find that regardless of the immunoprecipitated protein, we could always detect interaction with the other, expect for when the samples were mixed post-lysis, demonstrating intracellular interaction (Fig. 21C). Besides this, in cells where only ΔTM1-Cx32-HA was transfected, the immunoprecipitation assay also revealed that the truncated protein can self-assemble, showing the cleaved mutant is not inherently unable to assemble with itself or the full-length protein (Fig. 21C).

Due to this interaction and possible assembly phenotype, we continued to wonder if cleaved Cx32 escaping the ER would be due to the possible interaction with full-length protein. If escape was bound to the presence of uncleaved protein, we devised a way to exclusively express SPC-generated, fully cleaved Cx32 mutants. Since $Cx32^{M34K}$ presumably behaves like a canonical, co-translational substrate, showing quantitative cleavage (Fig.12 A), we figured combining this mutation with $Cx32^{L83R}$ or $Cx32^{C201R}$, would generate fully processed variants of

79

the mutants. Propitiously, since K34 is expressed in TM1, its presence would be excluded from the cleaved protein. In fact, expression of these two new double mutants led to a pattern of quantitative cleavage (Fig. 21D), and once these mutants were FLAG-tagged, immunofluorescence showed a more convincing ER retained signal (Fig. 21E), and arguing for hetero assembly-driven escape from quality control.

Despite this apparent escape from ER quality control, the stability of any of our cleavage-prone mutants was severely decrease when the protein was
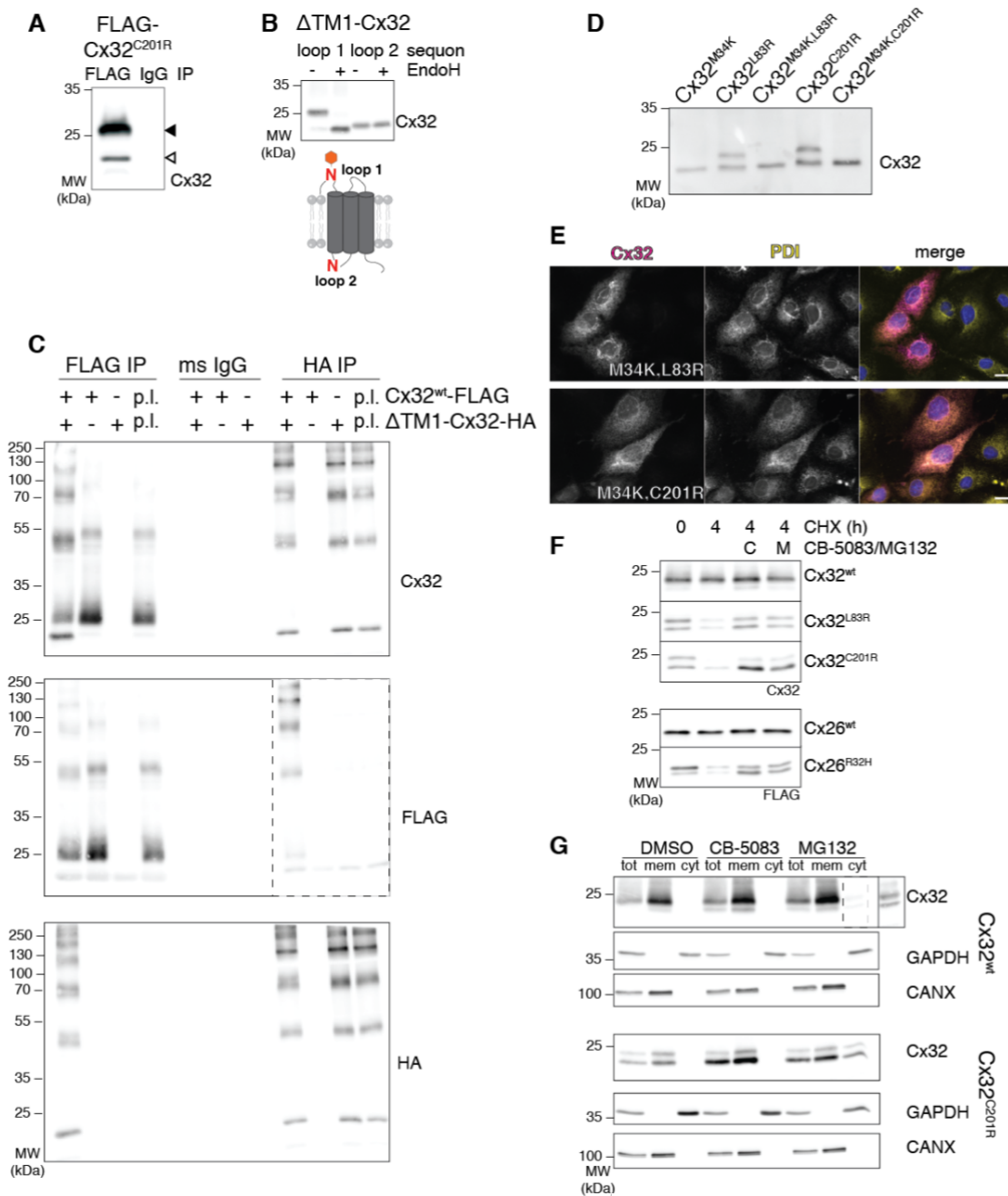
(figure legend in the next page)

Figure 21: Hetero assembles of Cx32 may shield processed protein from ER retention. (**A**) 293T were transfected with N-terminally FLAG-tagged Cx32^{C201R} and full-length protein was purified (black arrowhead). Representative immunoblot showing co-immunoprecipitation of cleaved product (white arrowhead). A immunoprecipitation with non-immune IgG were used as a control. (**B**) A truncated version of Cx32 (ΔTM1) with sequons in loop 1 and 2 (red "N") was transfected into 293T cells, which were then lysed and digested with EndoH, as seen in the Cx32 immunoblot. A cartoon below shows the correct orientation of the truncated variant. (**C**) Full-length FLAG-tagged Cx32^{wt} and truncated HA-tagged Cx32^{wt} were transfected together or alone into 293T. Both proteins were individually immunoprecipitated via their C-terminal tags and samples were immunoblotted with the indicated antibodies. A mouse (ms) IgG antibody was used as a control. Lysates from single transfections were mixed post-lysis (p.l.) and immunoprecipitated with the indicated antibodies to control for post-lysis interaction. A higher exposure inlet for the FLAG immunoblot samples resulting from HA immunoprecipitation is shown. (**D**) Representative immunoblot of 293T transfected with the indicated Cx32 mutants. (**E**) COS-7 were electroporated with the indicated Cx32 constructs and their cellular localization determined via immunofluorescence. Scale bars correspond to 20 μm. (**F**) The indicated constructs were transfected into 293T, and cells were incubated 4 h before lysis with CHX with(out) CB-5083 or MG132 co-incubation. Representative blots are shown. (**G**) Cx32 expressing 293T were incubated with the indicated compounds for 3 h, and cells were semi-permeabilized in low percent digitonin buffer. Total (tot), membrane (mem), and cytosolic (cyt) fractions were collected and samples immunoblotted for the indicated proteins. Tot fraction represents half the relative amount of the other two fractions. GAPDH served as a cytosolic control, and CANX as a membrane control. A higher exposure of cytosolic Cx32^{wt} treated with MG132 is shown on the right side of the respective blot.

immunoblotted after CHX incubation, and the stabilization seen with VCP/p97 or proteasome inhibitors made a strong case towards these being ERAD substrates (Fig. 21F). However, despite a slight delay in the decay of the cleaved species, we detected no major differences in the half-life of full-length and processed connexins (data not shown). What we could detect was a seeming preferential stabilization of processed Cx32^{C201R} and Cx26^{R32H}, particularly after incubation with CB-5083, but also after proteasome inhibition (Fig. 21F). The most reflexive and natural explanation is preferential extraction (and proteasomal degradation) of processed products, even though our CHX chase data does show major differences in the decay of the two species (data not shown). The other hypothesis, relevant for VCP/p97 inhibition, is that by blocking retrotranslocation, we reach a scenario in which extraction-ready misfolded proteins start accumulating in the ER membrane (regardless of processing phenotype), which

would lead to eventual SPC-mediated cleavage, and hence accumulation of processed species. The other possible conclusion is that cleavage works as a physiologically relevant prerequisite for extraction, in a scenario where less TM segments in a polypeptide chain would need to be removed at once.

To test this last hypothesis, we repeated the inhibition of both VCP/p97 and the proteasome, and semi-permeabilized Cx32 transfected 293T cells in order to fraction cytosolic and membrane fractions. For Cx32^{C201R}, the inhibition of the proteasome showed us both full-length and cleaved fractions populating the cytoplasm (Fig. 21G), meaning there is no strict SPC cleavage requirement for Cx32^{C201R} extraction. For Cx32^{wt} however, we could observe a preferential enrichment for the cleaved species in the cytosol when compared to the membrane bound protein (Fig. 21G). Of note, we did not account for lysosomal degradation, from the plasma membrane, which will likely be more relevant for the degradation of full-length protein. This means that at least for the wild type protein, protein extraction from the ER and degradation in the cytosol seem to be preferential for the cleaved fraction, which does not seem to apply for Cx32^{C201R} where both species populate the cytosol and membrane to a similar degree.

e. Cryptic cleavage sites are abundant in the human membranome

Having observed misfolding-triggered SPC cleavage of connexins, and the physiological consequences of such processing, we decided to investigate if cryptic signal peptides and cleavage sites may be present in other secretory proteins. We considered that one of the hallmarks for such proteins would be to have a signal anchor where some features for a signal peptide could still be detected, either in what would be the h- or the c-region, such as misfolding would
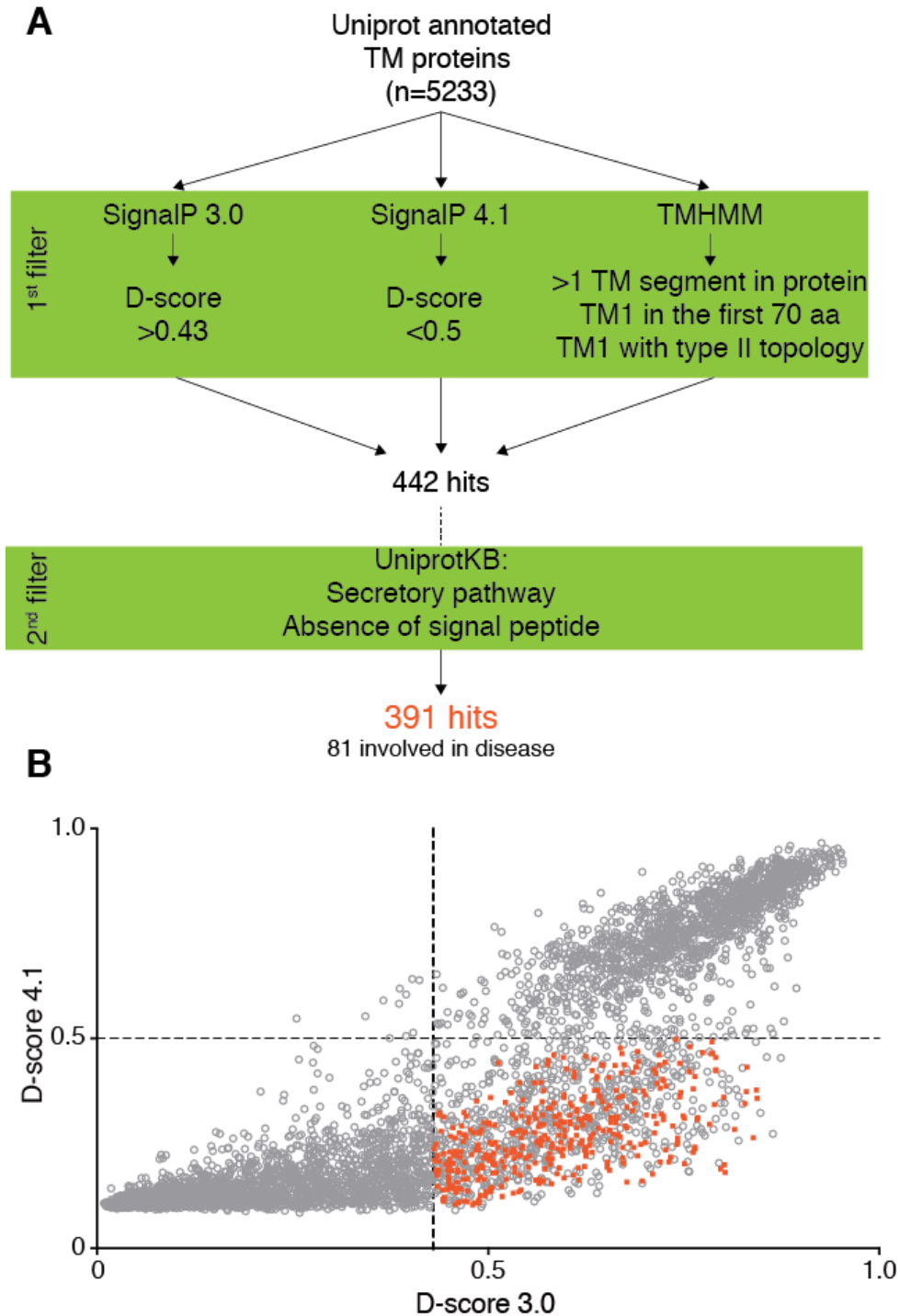
Figure 22: Cryptic cleavage site in the human proteome. (**A**) Flowchart of the strategy used for the identification of possible cryptic signal peptides in the human proteome. (**B**) Graphic representation of the D-score obtained from different versions of the SignalP algorithm. Positive hits from (A) are shown in orange.

trigger recognition by the SPC and cleavage. Towards this, we went back to the SignalP servers and made use of the fact version 4.1 had been developed to decrease the number of false-positive signal peptide predictions done by version

3.0 (418). We thus conceived that the group of signal peptides attributed in SignalP 3.0, that would later be rejected in SignalP 4.1 could make up the group of proteins whose signal anchors are on the verge of becoming signal peptides upon misfolding. To address this, we teamed up with Prof. Dr. Marius Lemberg and Andrea Zanotti (Universität Heidelberg, Heidelberg, Germany), fetched every FASTA sequence from the human membranome (as annotated in UniprotKB, 5233 proteins), and submitted the first 70 amino acids of these to both SignalP version 3.0 and 4.1. Based on their SignalP D-score, the SignalP numerical value used to decide between a positive or negative prediction, we picked the proteins to which a signal peptide was attributed in SignalP 3.0, but lost this attribute in the refinements made for SignalP 4.1. Additionally, proteins were filtered to include only those with a type II TM1 (based on the TMHMM server (cbs.dtu.dk/services/TMHMM)). The resulting list of 442 proteins was further filtered to exclude proteins not expressed in the secretory pathway (based on Uniprot KB), and finally proteins to which a signal peptide had been annotated (also based on UniprotKB) (Fig. 22A). At the end, we obtained a list of 391 proteins, 81 of which have been implicated in human disease (Fig. 22B). This set of proteins (approximately 7% of the human membranome) can now be used to study if the same misfolding-triggered SPC cleavage is commonly observed in humans, what consequences does it have in other human diseases, and try to understand the implication of having cryptic cleavage sites left in secretory proteins.

Discussion

1. Misintegration of TM segments in multipass TM proteins

Folding, assembly and quality control have historically been at the backside of connexin biochemical research. Detailed work has been done with regards to the function and regulation of connexins. However, subcellular and molecular work has been lacking when it comes to the etiology of connexinopathies. Even though phenotypes such as mutant connexin intracellular retention have been previously observed, these never got the same detailed characterization as the work done on channel electrophysiology (363,422,432). By focusing on the phenotypes and machinery acting Cx32 mutants, we managed to uncover previously uncharacterized protein biology.

Since an abundance of membrane integrated, unstable TM segments has been reported in multipass membrane proteins (63), the identification of stabilizing elements and quality control measures for faulty misintegration phenotypes has become of interest. Cx32 is an attractive target to study these phenomena since one out of its four TM segments exhibits exactly this lack of propensity for membrane integration (Fig. 11). We found that TM2 is indeed especially prone for misintegration by single disease-causing point mutants. Concerning the etiology of CMT1X this becomes an important point: the protein shows defects in trafficking (Fig. 12), TM2 and TM3 are relevant for channel gating (355), and they also participate in the entrance to the GJ pore (354). All this features makes us speculate GJIC activity would be compromised, even if misintegrated protein reached the plasma membrane. While previously published work has reported the relevance of TM3 for inter-protomer interactions (361), we could not detect any abrogation in Cx32 assembly in our misintegrated mutants (data not shown). Hence, on the therapeutic side of CMT1X, membrane stabilization of these mutants would be an relevant approach, supposing that the channel properties of e.g. Cx32^{L90H} would not be altered in a fully integrated topology.

The observation that upon TM2 mutation, not only TM2 but also TM3 become misintegrated brings interesting hypothesis to the table. One of these is the possibility that TM4 has a strong propensity for a type I orientation, thus forcing TM3 to be exposed to the ER lumen. However, the existence of proteins

with dual topology indicates that a strict membrane orientation is not always the rule, and such is true for a gap junction interacting protein, ductin (433). On the other hand, it has been shown in different systems that TM segment "frustration" can occur. One stable TM segment can be forced to misintegrate due to strong orientational preference of another TM segment, or alternatively, when hydrophilic segments are forced into the membrane due to high orientation preference from a subsequent TM segment (434,435). Analysis of the charge distribution in Cx32 shows approximately the same absolute difference in flanking charge distribution between the N- and C-terminal of TM3, and the C-terminal of both TM3 and TM4 (data not shown). As such, TM3 seems to favor a type II orientation with the degree of tendency TM4 shows for a type I, meaning TM3 misintegration should not be stemming from TM4. The other hypothesis for TM3 misintegration comes from the possibility that TM3 may be the main contributor for TM2 integration, which notably cannot insert in the membrane in isolation (Fig. 13B). As discussed, since unstable TM segments must be stabilized in the membrane, in principle, by other TM segments, it becomes interesting to observe the caveat that this favorable interaction in topogenensis, may also lead to incorrect TM segment misintegration.

2. Cellular handling of misintegrated proteins

Our data on subcellular expression and degradation kinetics (Fig. 12) showed that misintegrated connexin can be recognized by quality control mechanisms. Furthermore, we could show complete ER retention of the fully misintegrated double mutant Cx32^{L81H,L90H}, arguing that the more drastic the misintegration phenotype, the more pronounced ER retention becomes (Fig. 12A, 21E). As such, membrane protein misintegration is a phenotype cells have evolved to detect, in agreement with what has been reported in single-pass proteins, and more recently in multipass complexes (69,71).

In our first study we could identify three main chaperones acting on Cx32 (Fig. 13, 14). CANX seems to indiscriminate between Cx32^{wt} and Cx32^{L90H}, so membrane topology may not be at the center of the recognition mechanism of this chaperone. However, it is important mentioning the lectin-independent binding of the chaperone to Cx32. Even though interaction with CANX has been occasionally observed for other non-glycosylated substrates (436,437), the

molecular basis (such as mode and timing of interaction) have yet to be elucidated, as well as its possible role in quality control.

The EMC was another interaction partner we were able to identify, which curiously has been previously shown to interact with CANX (438). As discussed previously, this chaperoning complex has a binding preference for hydrophilic TM segments (77). Even though we did not use the C_L-TM2 construct to assess direct binding to the EMC, one can expect the interaction with the complex to be centered around this TM segment. While most reports have shown co-translational interaction of the EMC with its substrates, one can assume that, in our co-immunoprecipitation experiments, such transient interactions would not be detected without resorting to e.g. crosslinkers, and that in fact stabilization by the EMC can occur even after a client substrate has left the ribosome and Sec61. Another important observation was that only EMC4 and EMC10 out of tested membrane-embedded subunits showed interaction. While we do not discard the possibility that this could be due to experimental shortcomings, it has been reported that these two subunits, together with EMC7 form the "peripheral EMC" (90). EMC7 and EMC10 have also been described as two of the three subunits with large ER luminal domains, where one would expect a post-translational interaction to be taking place (90). However, by solving the structure of the mammalian EMC, it has been shown that only one of the two predicted TM segments for EMC4 is inserted in the membrane, which would position a previously unidentified portion of the EMC4 in the ER lumen (74). Left to be validated is if the complex has an insertase activity when faced with ER luminal TM segments, or if its mode of recognition can also be centered around unpaired integrated segments. Finally, in terms of the EMC function and assembly, it would be interesting to test the possibility that EMC sub-complexes may be formed to deal with the multifaceted array of substrates the complex possesses (90). Alternatively, the same type of subcomplexes can also be responsible for the different functions of the EMC – from chaperoning, to insertion, to perhaps ERAD targeting.

On the luminal side of the ER membrane, BiP was also found to preferentially interact with our partially misintegrated mutants, and more specifically misintegrated TM2. Given the binding preference of the chaperone (439), this points towards gain of disordered structure of misintegrated TM2. Its

stabilization of such a TM segment should give enough time to the protein to try and insert the segment back into the ER membrane, likely through action of the EMC, effectively connecting the luminal and membrane-embedded quality control systems (Fig. 13, 14). While the recognition of unstable TM segments by the EMC seems to be coded in the complex itself, BiP recruitment to its substrates is usually dependent on ERdj proteins. Since we co-purified ERdj3 through our AE-MS approach, it would be interesting to investigate if this is the ERdj protein recruiting BiP to misintegration scenarios, perhaps through its ability to directly bind misfolded clients (440).

It would also be interesting to elucidate if other membrane proteins with unstable TM segments use the same group of chaperones, and perhaps through radioactive labeling and cross-linking, to establish an order of events for chaperoning, that our steady state approach cannot discern. The same is true for the process of misintegration itself, since the scenario in which two different protein populations leave the translocon with different topologies cannot be discriminated from the one in which one fully (mis)integrated population of Cx32 is first synthesized, with subsequent TM2/TM3 (mis)integration.

Even though we only sought after chaperoning for misintegrated TM2, TM3 itself will certainly work as an anchor for quality control, and eventually ERAD, machinery. When analyzed in the context of the C_L constructs, C_L-TM3 is completely integrated (data not shown), and thus inert to BiP. However, in the context of full-length, mutated Cx32, while TM2 has further lost hydrophobic properties (when compared to wild type protein), TM3 is still a classical TM segment. Additionally, the same reports that attributed TM3 to the pore of hexameric connexins due to its amphipathic nature, could hint towards its lateral association with the lipid bilayer (357), and possible loss of the speculated interaction between TM2 and TM3.

3. ERAD of misintegrated Cx32

ERAD of Cx32 is mediated via gp78 (Fig. 15), which has been implicated in the ubiquitination of several different membrane proteins (441). Additionally, an interesting link between the EMC and gp78 has been found before, where UBAC2 (the link between gp78 and UBXD8) was seen to interact with different EMC subunits (73), thus hinting to the attractive possibility that the EMC and gp78 are

intertwined in the chaperoning and possible degradation of terminally misintegrated membrane proteins.

Several of the substrates for gp78 are ERAD-M substrates, i.e. with degrons in the plane of the ER membrane (441). In our scenario, both (mis)integrated fractions of the protein are expected to contain degrons in the membrane, either be it via the presence of a destabilizing mutation in the case of integrated protein, or via the presence of most likely unpaired TM helices (TM1 and TM4) in the misintegrated fraction of protein. Since our experimental system cannot discriminate between preferential gp78 targeting of one species over the other, we can only infer that since both species have the same degradation rate (data not shown) they may be handled by the same degradation pathway, albeit different modes of recognition are surely to be expected. Additionally, a previous study has shown that membrane bound ERAD-L substrates are still targeted to degradation by gp78, so while one would expect the dependency for this E3 to be lost without its membrane anchoring TM1 and TM4, this cannot be said for full-length misintegrated Cx32 (222).

Lastly it is important to note that while we did detect a halting in both degradation and ubiquitination of mutant Cx32, our results were obtained by overexpressing a dominant negative mutant of the E3. Overexpressing of another ER E3 ligase has been shown to completely alter assembly complex characters (442), and even circumvent the need for an E3 ligase associated complex to assemble (247). On the other hand, knockdowns are often not sufficient to the detection of a stabilizing effect, either from a relative expression of E3 versus substrate, or due to cellular adaptation, and knockout approaches have been found to be compensated for through chromosomal duplication (246). All in all, while Cx32 degradation makes use of gp78, it is important to note that different strategies should be used, and that surely, out of the 25 ER E3 ligases, the degradation pathway for this protein is not solely dependent on one of them.

4. Misfolding triggered cleavage

The SPC was one of the first ER membrane protein complexes to be purified and fully characterized. Work done with canonical substrates and viral proteins (119,121,428) have made the bulk of the research into the SPC, and outside of that, experimentation into the SPC has been mostly static.

Our early work with Cx32 mutants has shown us the appearance of a faster migrating species for several different mutants. Despite differences in the degree at which this species appeared in our different mutants, its presence became, for the most part, a normal output from an immunoblot.

By first characterizing the nature of the faster migrating species we could show it resulted from N-terminal cleavage in both Cx32 and Cx26 (Fig. 16). Through an array of sequence engineering approaches and SPC knockdown data, we could prove that this complex was in fact acting on connexins (Fig. 17D). The fact that SPC could cleave off the TM1 in a sub-population of connexins was not the most surprising fact, since this could be an example of an inefficient signal peptide (443). What was surprising was the fact cleavage was clearly happening post-translationally, or more precisely, post-translocationally, such as mutations in the last transmembrane segment were promoting cleavage of the first forty amino acid residues in Cx32.

One interesting result from yeast correlated the ER targeting pathway taken by a protein with the properties of its signal sequence, and found that for a lot of signal peptides, an SRP-independent route was taken (38), which was mostly explained due to the reduced hydrophobicity signal peptides usually show in comparison to signal anchors (444). While in our system the tendency for signal peptide conversion is able to stem from downstream structural elements, it is also worth mentioning the SRP can engage with a translating ribosome before a signal sequence emerges (445). It would be interesting if a similar mechanism would occur for mammalian systems.

Additionally, it was very surprising to see protein misfolding could trigger SPC-mediated cleavage. Given the different nature and location of our cleaved mutants, we assumed there could be no better unifying characteristic between them besides misfolding, since it was clear we were not affecting, e.g. a cleavage site. In fact, thanks to the Cx26 structure (345), and the model for hexameric Cx32 we generated, we could identify different amino acid residues that could stabilize our mutants in the membrane. Through this approach we could see a steady state decrease in the amount of cleaved protein, pointing towards a misfolding based trigger (Fig. 19). On the reverse side, it was also interesting to observe that further injuring folding could have the reverse effect. By reducing disulfide bonds in cells, and thus misfolding connexins, we could clearly see an increase in the amount

of cleaved protein, in a scenario where we were adding insult to injury (Fig. 20). Two other curious results come out from our DTT experiments: the observation that by retaining Cx32^{wt} in the ER we could promote cleavage (Fig. 20C), pointing towards the eventual misfolding triggered by the prolonged expression of a membrane protein in this organelle; and the fact that at least in steady state levels, disulfide-less Cx32^{C201R} has its expression severely reduced, pointing towards the stabilizing effect disulfides can have on this protein (Fig. 20D, E).

On the side of the SPC, one important aspect to consider is if the complex is generally recognizing misfolding, and functioning as a quality control enzyme, similar to what happens with the SPP (229,446). An alternative hypothesis would be that despite the different location of our mutants, the cleavage site is always becoming unstructured, and thus prone to cleavage. In this scenario one cannot assume that all misfolding leads to SPC-mediated processing, but only cryptic signal peptide- and cleavage site-destabilizing misfolding. Several lines of evidence towards this exist: first, while not correcting misfolding, we can clearly inhibit it by engineering the cleavage site with Pro residues, or by extension of the alpha-helical character of TM1 (Fig. 17C). Second, while the data were not presented, we also characterized the topology of several of our cleaved mutants, and found that by adding Gly- and Ser-rich unstructured linkers, flanking a glycosylation sequon to Cx32^{C201R} loop 1 (around the cleavage site) we could observe full cleavage of the mutant (data not shown). While this is not true for other mutants (e.g. Cx32^{L83R}, not shown), it points towards the importance of having the cleavage site unstructured, and may partially explain why we could not find any cytosolic mutants showing the same degree of cleavage (data not shown). The mechanisms by which SPC can recognize these faulty proteins can now be extended and better characterized with the list of possible substrates we obtained from our bioinformatics approach (Fig. 22). Additionally, one could investigate if these types of sites are evolutionarily conserved in membrane proteins. On the one hand, their presence can be considered deleterious, since it will lead to truncated variants of a protein. On the other hand, the possibility that these sites also function as folding sensors, or indicator, is attractive, given their possible abundance in the membranome.

The other major question coming out of this work is the properties of the SPC itself. As is with different membrane protein complexes, single subunit destabilization resulted in lower levels of the whole complex (Fig. 17D), and as such we could never attribute specific roles for specific subunits. Perhaps by making use of systems with purified components in liposomes this could be achieved, where different sub-complexes could in principle be obtained. Interestingly we could not detect any abrogation of processing of SPC canonical substrates, which could just mean even at knockdown levels, the catalytic subunits are still plenty abundant for this canonical role, or that the auxiliary subunits, destabilized at a greater level in our knockdown conditions (Fig. 17D), play a major role in recognition of non-canonical substrates. The general role for the SPC auxiliary subunits also needs to be further characterized, especially on its possible and relevant interplay with ERAD, since a recent study has placed SPCS2 in close proximity to the Hrd1 complex, which would be an interesting player, bridging misfolded protein cleavage with ERAD (266).

5. Cleaved proteins are assembly competent

The observation that cleaved Connexins can still self-assemble and are not excluded from assembly with full-length variants (Fig. 21), brings into question the type of quality control exerted on cleaved Cx32. Added to the fact cleaved protein shows virtually the same decay as its unprocessed counter-parts (data not shown), it seems as though quality control mechanisms could have converged to handle both cleaved and full-length misfolded Cx32. This is somewhat corroborated by the fact we find the same relative fraction of Cx32^{C201R} species in the cytosol and in the membrane when the proteasome is inhibited (Fig. 21G). This may be explained through a common pathway that handles full-length protein with a destabilizing mutation in the membrane (in which the likely degron comes from the Cys to Arg mutation), as well as the same protein without a TM segment (from which the degron can come both from the missing helix, or from the still present Cys to Arg mutation). The case for Cx32^{wt} becomes then more puzzling due to the apparent preferential extraction of cleaved protein from the ER. In part this can resemble the phenotype of misintegration, given the

unpairing of TM segments. In this case, a degron should only be present after the removal of TM1, meaning this protein would be preferentially extracted. However, the stable expression of cleaved Cx32^{M34K} (Fig. 16A) tells us a wild type-like, cleaved protein can still be expressed at detectable levels on a cell lysate. The presumption that copies of processed Cx32^{wt} are removed faster than those of processed Cx32^{M34K} remains to be elucidated. Also to clarify further, is the possibility that the phenotype of extracted Cx32^{wt} could be corrected once lysosomal degradation from the plasma membrane is taken into account.

When considering assembly of the two fractions, and reiterating likely ER escape of Cx32^{C201R}, precluded by expression of fully cleaved mutant, one wonders if assembly can thus hide structural elements meant to be recognized. Since TM1 faces the GJ pore in assembled channels, its absence would expose new TM segments to this new "pore", and one can anticipate this to be recognized. Other assembly architectures could in principle still be formed, shielding the lack of TM1, but is also important remembering the exclusion of cleaved protein from gap junction plaques (Fig. 18C, D). It remains to be factually demonstrated if assembly inhibits ER retention of processed mutants or not, and if so, if Golgi (235,447) or plasma-membrane associated quality control (448,449) act on this selective exclusion of these faulty variants from higher connexin assembles.

6. Concluding remarks

Throughout this work we characterized how different mutations in the same polypeptide chain can lead to multitude of topological and processing-related defects in transmembrane proteins.

One group of mutants shows that mutations in TM2 of Cx32 make the protein especially prone for misintegration, leading to the exposure of two TM segments to the ER lumen. As is for single-pass membrane proteins, cells have evolved means to recognize and handle such aberrant topogenesis. At a co-translational level, the EMC has been found to chaperone these TM segments, which are naturally unstable in the lipid bilayer, and insert them into the ER membrane. We found two EMC subunits interacting preferentially with partially misintegrated Cx32, arguing for a more stable interaction that goes beyond a co-translational mode, while also finding an increase in the levels of misintegrated

Cx32 when the levels of EMC were reduced. Exposure of these segments to the ER lumen can be recognized and chaperoned by BiP, while gp78 is able to ultimately send these faulty proteins to degradation.

Another group of transmembrane mutants leads to non-canonical cleavage by the SPC. We found that misfolding acts as a trigger for post-translational cleavage, since by ameliorating, or worsening, the misfolding phenotype we could decrease, or increase, the relative amount of SPC-processed protein, respectively. We could also show that both fractions of protein are still able to interact, leading cleaved protein to leave the ER to some extent, while converting them to a fully-processed form seems to preclude any sort of ER escape.

Taken together these studies demonstrate the complexity and refinement of the ER quality control systems. And they also highlight the economy of quality control since luminal chaperones (BiP), and a protease normally used for signal peptide cleavage (SPC), can play an important role in membrane protein quality control. Since membrane protein misfolding comes in different flavors, so does the way the organelle can recognize and deal with these (Fig. 23). While we could contribute to the understanding of the delicate balance between pro-folding quality control, and the inescapable decision for protein processing or polyubiquitination, further detailing into the workings of the quality control and degradation machineries found in the mammalian ER will certainly surprise us and redefine postulates in cellular and molecular biology.
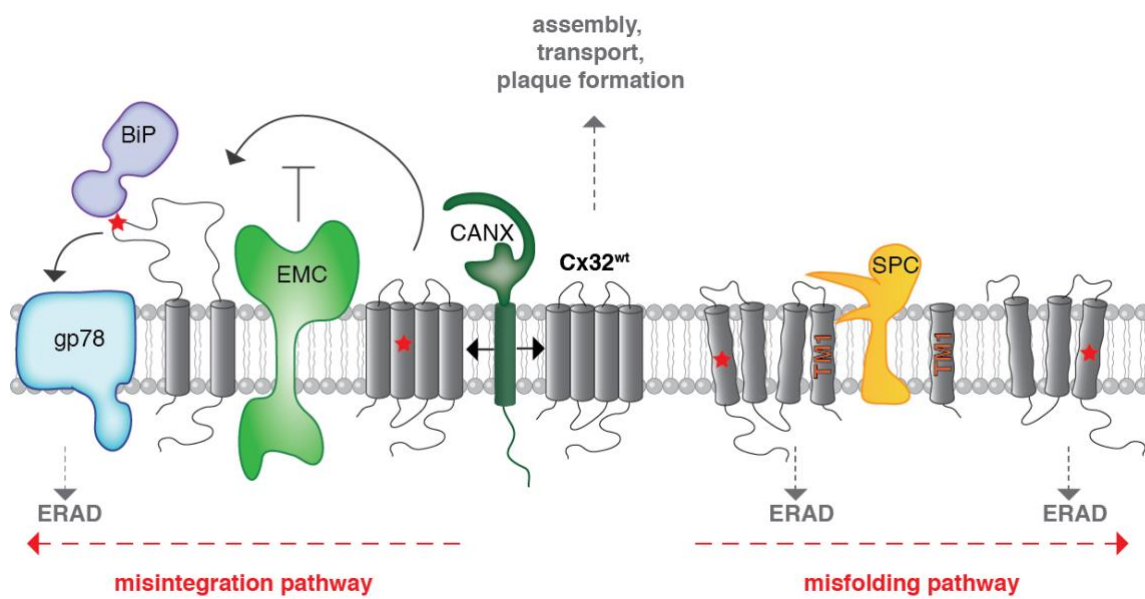
Figure 23: A model for the different ways to quality control and degrade a faulty membrane protein. On the left the machineries used to chaperone and degrade misintegrated Cx32. On the right, a model on the proteolytical decision towards misfolded Cx32.

References

1. Almen, M. S., Nordstrom, K. J., Fredriksson, R., and Schioth, H. B. (2009) Mapping the human membrane proteome: a majority of the human membrane proteins can be classified according to function and evolutionary origin. *BMC Biol* **7**, 50
2. Gamerdinger, M., Hanebuth, M. A., Frickey, T., and Deuerling, E. (2015) The principle of antagonism ensures protein targeting specificity at the endoplasmic reticulum. *Science* **348**, 201-207
3. Gamerdinger, M., Kobayashi, K., Wallisch, A., Kreft, S. G., Sailer, C., Schlomer, R., Sachs, N., Jomaa, A., Stengel, F., Ban, N., and Deuerling, E. (2019) Early Scanning of Nascent Polypeptides inside the Ribosomal Tunnel by NAC. *Mol Cell* **75**, 996-1006 e1008
4. Chartron, J. W., Hunt, K. C., and Frydman, J. (2016) Cotranslational signal-independent SRP preloading during membrane targeting. *Nature* **536**, 224-228
5. Walter, P., and Blobel, G. (1980) Purification of a membrane-associated protein complex required for protein translocation across the endoplasmic reticulum. *Proc Natl Acad Sci U S A* **77**, 7112-7116
6. Walter, P., and Blobel, G. (1982) Signal recognition particle contains a 7S RNA essential for protein translocation across the endoplasmic reticulum. *Nature* **299**, 691-698
7. Krieg, U. C., Walter, P., and Johnson, A. E. (1986) Photocrosslinking of the signal sequence of nascent preprolactin to the 54-kilodalton polypeptide of the signal recognition particle. *Proc Natl Acad Sci U S A* **83**, 8604-8608
8. Voorhees, R. M., and Hegde, R. S. (2015) Structures of the scanning and engaged states of the mammalian SRP-ribosome complex. *Elife* **4**
9. Gilmore, R., Walter, P., and Blobel, G. (1982) Protein translocation across the endoplasmic reticulum. II. Isolation and characterization of the signal recognition particle receptor. *J Cell Biol* **95**, 470-477
10. Keenan, R. J., Freymann, D. M., Stroud, R. M., and Walter, P. (2001) The signal recognition particle. *Annu Rev Biochem* **70**, 755-775
11. Halic, M., and Beckmann, R. (2005) The signal recognition particle and its interactions during protein targeting. *Curr Opin Struct Biol* **15**, 116-125
12. Simon, S. M., and Blobel, G. (1991) A protein-conducting channel in the endoplasmic reticulum. *Cell* **65**, 371-380
13. Crowley, K. S., Liao, S., Worrell, V. E., Reinhart, G. D., and Johnson, A. E. (1994) Secretory proteins move through the endoplasmic reticulum membrane via an aqueous, gated pore. *Cell* **78**, 461-471
14. Mothes, W., Prehn, S., and Rapoport, T. A. (1994) Systematic probing of the environment of a translocating secretory protein during translocation through the ER membrane. *EMBO J* **13**, 3973-3982
15. Martoglio, B., Hofmann, M. W., Brunner, J., and Dobberstein, B. (1995) The protein-conducting channel in the membrane of the endoplasmic reticulum is open laterally toward the lipid bilayer. *Cell* **81**, 207-214
16. Gogala, M., Becker, T., Beatrix, B., Armache, J. P., Barrio-Garcia, C., Berninghausen, O., and Beckmann, R. (2014) Structures of the Sec61 complex engaged in nascent peptide translocation or membrane insertion. *Nature* **506**, 107-110
17. Voorhees, R. M., Fernandez, I. S., Scheres, S. H., and Hegde, R. S. (2014) Structure of the mammalian ribosome-Sec61 complex to 3.4 A resolution. *Cell* **157**, 1632-1643
18. Hamman, B. D., Hendershot, L. M., and Johnson, A. E. (1998) BiP maintains the permeability barrier of the ER membrane by sealing the lumenal end of the translocon pore before and early in translocation. *Cell* **92**, 747-758
19. Voorhees, R. M., and Hegde, R. S. (2016) Structure of the Sec61 channel opened by a signal sequence. *Science* **351**, 88-91
20. Park, E., and Rapoport, T. A. (2011) Preserving the membrane barrier for small molecules during bacterial protein translocation. *Nature* **473**, 239-242
21. Voorhees, R. M., and Hegde, R. S. (2016) Toward a structural understanding of co-translational protein translocation. *Curr Opin Cell Biol* **41**, 91-99
22. Gorlich, D., and Rapoport, T. A. (1993) Protein translocation into proteoliposomes reconstituted from purified components of the endoplasmic reticulum membrane. *Cell* **75**, 615-630
23. Voigt, S., Jungnickel, B., Hartmann, E., and Rapoport, T. A. (1996) Signal sequence-dependent function of the TRAM protein during early phases of protein transport across the endoplasmic reticulum membrane. *J Cell Biol* **134**, 25-35
24. Rapoport, T. A., Li, L., and Park, E. (2017) Structural and Mechanistic Insights into Protein Translocation. *Annu Rev Cell Dev Biol*
25. Tamborero, S., Vilar, M., Martinez-Gil, L., Johnson, A. E., and Mingarro, I. (2011) Membrane insertion and topology of the translocating chain-associating membrane protein (TRAM). *J Mol Biol* **406**, 571-582
26. Chen, Q., Denard, B., Lee, C. E., Han, S., Ye, J. S., and Ye, J. (2016) Inverting the Topology of a Transmembrane Protein by Regulating the Translocation of the First Transmembrane Helix. *Mol Cell* **63**, 567-578
27. Hartmann, E., Gorlich, D., Kostka, S., Otto, A., Kraft, R., Knespel, S., Burger, E., Rapoport, T. A., and Prehn, S. (1993) A tetrameric complex of membrane proteins in the endoplasmic reticulum. *Eur J Biochem* **214**, 375-381
28. Pfeffer, S., Dudek, J., Schaffer, M., Ng, B. G., Albert, S., Plitzko, J. M., Baumeister, W., Zimmermann, R., Freeze, H. H., Engel, B. D., and Forster, F. (2017) Dissecting the molecular organization of the translocon-associated protein complex. *Nat Commun* **8**, 14516
29. Wiedmann, M., Goerlich, D., Hartmann, E., Kurzchalia, T. V., and Rapoport, T. A. (1989) Photocrosslinking demonstrates proximity of a 34 kDa membrane protein to different portions of preprolactin during translocation through the endoplasmic reticulum. *FEBS Lett* **257**, 263-268
30. Nguyen, D., Stutz, R., Schorr, S., Lang, S., Pfeffer, S., Freeze, H. H., Forster, F., Helms, V., Dudek, J., and Zimmermann, R. (2018) Proteomics reveals signal peptide features determining the client specificity in human TRAP-dependent ER protein import. *Nat Commun* **9**, 3765

31. Fons, R. D., Bogert, B. A., and Hegde, R. S. (2003) Substrate-specific function of the translocon-associated protein complex during translocation across the ER membrane. *J Cell Biol* **160**, 529-539

32. Li, X., Itani, O. A., Haataja, L., Dumas, K. J., Yang, J., Cha, J., Flibotte, S., Shih, H. J., Delaney, C. E., Xu, J., Qi, L., Arvan, P., Liu, M., and Hu, P. J. (2019) Requirement for translocon-associated protein (TRAP) alpha in insulin biogenesis. *Sci Adv* **5**, eaax0292

33. Kriegler, T., Kiburg, G., and Hessa, T. (2020) Translocon-Associated Protein Complex (TRAP) is Crucial for Co-Translational Translocation of Pre-Proinsulin. *J Mol Biol* **432**, 166694

34. Hann, B. C., and Walter, P. (1991) The signal recognition particle in S. cerevisiae. *Cell* **67**, 131-144

35. Schlenstedt, G., Gudmundsson, G. H., Boman, H. G., and Zimmermann, R. (1990) A large presecretory protein translocates both cotranslationally, using signal recognition particle and ribosome, and post-translationally, without these ribonucleoparticles, when synthesized in the presence of mammalian microsomes. *J Biol Chem* **265**, 13960-13968

36. Ng, D. T., Brown, J. D., and Walter, P. (1996) Signal sequences specify the targeting route to the endoplasmic reticulum membrane. *J Cell Biol* **134**, 269-278

37. Ngosuwan, J., Wang, N. M., Fung, K. L., and Chirico, W. J. (2003) Roles of cytosolic Hsp70 and Hsp40 molecular chaperones in post-translational translocation of presecretory proteins into the endoplasmic reticulum. *J Biol Chem* **278**, 7034-7042

38. Ast, T., Cohen, G., and Schuldiner, M. (2013) A network of cytosolic factors targets SRP-independent proteins to the endoplasmic reticulum. *Cell* **152**, 1134-1145

39. Shao, S., and Hegde, R. S. (2011) A calmodulin-dependent translocation pathway for small secretory proteins. *Cell* **147**, 1576-1588

40. Stefanovic, S., and Hegde, R. S. (2007) Identification of a targeting factor for posttranslational membrane protein insertion into the ER. *Cell* **128**, 1147-1159

41. Shao, S., Rodrigo-Brenni, M. C., Kivlen, M. H., and Hegde, R. S. (2017) Mechanistic basis for a molecular triage reaction. *Science* **355**, 298-302

42. Panzner, S., Dreier, L., Hartmann, E., Kostka, S., and Rapoport, T. A. (1995) Posttranslational protein transport in yeast reconstituted with a purified complex of Sec proteins and Kar2p. *Cell* **81**, 561-570

43. Lang, S., Benedix, J., Fedeles, S. V., Schorr, S., Schirra, C., Schauble, N., Jalal, C., Greiner, M., Hassdenteufel, S., Tatzelt, J., Kreutzer, B., Edelmann, L., Krause, E., Rettig, J., Somlo, S., Zimmermann, R., and Dudek, J. (2012) Different effects of Sec61alpha, Sec62 and Sec63 depletion on transport of polypeptides into the endoplasmic reticulum of mammalian cells. *J Cell Sci* **125**, 1958-1969

44. Brodsky, J. L., and Schekman, R. (1993) A Sec63p-BiP complex from yeast is required for protein translocation in a reconstituted proteoliposome. *J Cell Biol* **123**, 1355-1363

45. Zalisko, B. E., Chan, C., Denic, V., Rock, R. S., and Keenan, R. J. (2017) Tail-Anchored Protein Insertion by a Single Get1/2 Heterodimer. *Cell Rep* **20**, 2287-2293

46. Colombo, S. F., Cardani, S., Maroli, A., Vitiello, A., Soffientini, P., Crespi, A., Bram, R. F., Benfante, R., and Borgese, N. (2016) Tail-anchored Protein Insertion in Mammals: FUNCTION AND RECIPROCAL INTERACTIONS OF THE TWO SUBUNITS OF THE TRC40 RECEPTOR. *J Biol Chem* **291**, 15292-15306

47. Vilardi, F., Stephan, M., Clancy, A., Janshoff, A., and Schwappach, B. (2014) WRB and CAML are necessary and sufficient to mediate tail-anchored protein targeting to the ER membrane. *PLoS One* **9**, e85033

48. Wang, F., Chan, C., Weir, N. R., and Denic, V. (2014) The Get1/2 transmembrane complex is an endoplasmic-reticulum membrane protein insertase. *Nature* **512**, 441-444

49. Aviram, N., Ast, T., Costa, E. A., Arakel, E. C., Chuartzman, S. G., Jan, C. H., Hassdenteufel, S., Dudek, J., Jung, M., Schorr, S., Zimmermann, R., Schwappach, B., Weissman, J. S., and Schuldiner, M. (2016) The SND proteins constitute an alternative targeting route to the endoplasmic reticulum. *Nature* **540**, 134-138

50. Hassdenteufel, S., Johnson, N., Paton, A. W., Paton, J. C., High, S., and Zimmermann, R. (2018) Chaperone-Mediated Sec61 Channel Gating during ER Import of Small Precursor Proteins Overcomes Sec61 Inhibitor-Reinforced Energy Barrier. *Cell Rep* **23**, 1373-1386

51. Ast, T., and Schuldiner, M. (2013) All roads lead to Rome (but some may be harder to travel): SRP-independent translocation into the endoplasmic reticulum. *Crit Rev Biochem Mol Biol* **48**, 273-288

52. von Heijne, G. (2006) Membrane-protein topology. *Nat Rev Mol Cell Biol* **7**, 909-918

53. Skach, W. R. (2009) Cellular mechanisms of membrane protein folding. *Nat Struct Mol Biol* **16**, 606-612

54. Devaraneni, P. K., Conti, B., Matsumura, Y., Yang, Z., Johnson, A. E., and Skach, W. R. (2011) Stepwise insertion and inversion of a type II signal anchor sequence in the ribosome-Sec61 translocon complex. *Cell* **146**, 134-147

55. Goder, V., and Spiess, M. (2003) Molecular mechanism of signal sequence orientation in the endoplasmic reticulum. *EMBO J* **22**, 3645-3653

56. Denzer, A. J., Nabholz, C. E., and Spiess, M. (1995) Transmembrane orientation of signal-anchor proteins is affected by the folding state but not the size of the N-terminal domain. *EMBO J* **14**, 6311-6317

57. Heijne, G. (1986) The distribution of positively charged residues in bacterial inner membrane proteins correlates with the trans-membrane topology. *EMBO J* **5**, 3021-3027

58. von Heijne, G. (1989) Control of topology and mode of assembly of a polytopic membrane protein by positively charged residues. *Nature* **341**, 456-458

59. van Klompenburg, W., Nilsson, I., von Heijne, G., and de Kruijff, B. (1997) Anionic phospholipids are determinants of membrane protein topology. *EMBO J* **16**, 4261-4266

60. Hartmann, E., Rapoport, T. A., and Lodish, H. F. (1989) Predicting the orientation of eukaryotic membrane-spanning proteins. *Proc Natl Acad Sci U S A* **86**, 5786-5790

61. Goder, V., Junne, T., and Spiess, M. (2004) Sec61p contributes to signal sequence orientation according to the positive-inside rule. *Mol Biol Cell* **15**, 1470-1478

62. Hessa, T., Kim, H., Bihlmaier, K., Lundin, C., Boekel, J., Andersson, H., Nilsson, I., White, S. H., and von Heijne, G. (2005) Recognition of transmembrane helices by the endoplasmic reticulum translocon. *Nature* **433**, 377-381

63. Hessa, T., Meindl-Beinker, N. M., Bernsel, A., Kim, H., Sato, Y., Lerch-Bader, M., Nilsson, I., White, S. H., and von Heijne, G. (2007) Molecular code for transmembrane-helix recognition by the Sec61 translocon. *Nature* **450**, 1026-1030

64.   Lu, Y., Turnbull, I. R., Bragin, A., Carveth, K., Verkman, A. S., and Skach, W. R. (2000) Reorientation of aquaporin-1 topology during maturation in the endoplasmic reticulum. *Mol Biol Cell* **11**, 2973-2985

65.   Skach, W. R., Shi, L. B., Calayag, M. C., Frigeri, A., Lingappa, V. R., and Verkman, A. S. (1994) Biogenesis and transmembrane topology of the CHIP28 water channel at the endoplasmic reticulum. *J Cell Biol* **125**, 803-815

66.   Kanki, T., Sakaguchi, M., Kitamura, A., Sato, T., Mihara, K., and Hamasaki, N. (2002) The tenth membrane region of band 3 is initially exposed to the luminal side of the endoplasmic reticulum and then integrated into a partially folded band 3 intermediate. *Biochemistry* **41**, 13973-13981

67.   Tector, M., and Hartl, F. U. (1999) An unstable transmembrane segment in the cystic fibrosis transmembrane conductance regulator. *EMBO J* **18**, 6290-6298

68.   Shin, J., Lee, S., and Strominger, J. L. (1993) Translocation of TCR alpha chains into the lumen of the endoplasmic reticulum and their degradation. *Science* **259**, 1901-1904

69.   Feige, M. J., and Hendershot, L. M. (2013) Quality control of integral membrane proteins by assembly-dependent membrane integration. *Mol Cell* **51**, 297-309

70.   Carvalho, H. J. F., Del Bondio, A., Maltecca, F., Colombo, S. F., and Borgese, N. (2019) The WRB Subunit of the Get3 Receptor is Required for the Correct Integration of its Partner CAML into the ER. *Sci Rep* **9**, 11887

71.   Inglis, A. J., Page, K. R., Guna, A., and Voorhees, R. M. (2020) Differential Modes of Orphan Subunit Recognition for the WRB/CAML Complex. *Cell Rep* **30**, 3691-3698 e3695

72.   Jonikas, M. C., Collins, S. R., Denic, V., Oh, E., Quan, E. M., Schmid, V., Weibezahn, J., Schwappach, B., Walter, P., Weissman, J. S., and Schuldiner, M. (2009) Comprehensive characterization of genes required for protein folding in the endoplasmic reticulum. *Science* **323**, 1693-1697

73.   Christianson, J. C., Olzmann, J. A., Shaler, T. A., Sowa, M. E., Bennett, E. J., Richter, C. M., Tyler, R. E., Greenblatt, E. J., Harper, J. W., and Kopito, R. R. (2011) Defining human ERAD networks through an integrative mapping strategy. *Nat Cell Biol* **14**, 93-105

74.   Pleiner, T., Pinton Tomaleri, G., Januszyk, K., Inglis, A. J., Hazu, M., and Voorhees, R. M. (2020) Structural basis for membrane insertion by the human ER membrane protein complex. *Science*

75.   Chitwood, P. J., Juszkiewicz, S., Guna, A., Shao, S., and Hegde, R. S. (2018) EMC Is Required to Initiate Accurate Membrane Protein Topogenesis. *Cell* **175**, 1507-1519 e1516

76.   Volkmar, N., Thezenas, M. L., Louie, S. M., Juszkiewicz, S., Nomura, D. K., Hegde, R. S., Kessler, B. M., and Christianson, J. C. (2018) The ER membrane protein complex (EMC) promotes biogenesis of sterol-related enzymes maintaining cholesterol homeostasis. *J Cell Sci*

77.   Shurtleff, M. J., Itzhak, D. N., Hussmann, J. A., Schirle Oakdale, N. T., Costa, E. A., Jonikas, M., Weibezahn, J., Popova, K. D., Jan, C. H., Sinitcyn, P., Vembar, S. S., Hernandez, H., Cox, J., Burlingame, A. L., Brodsky, J., Frost, A., Borner, G. H., and Weissman, J. S. (2018) The ER membrane protein complex interacts cotranslationally to enable biogenesis of multipass membrane proteins. *Elife* **7**

78.   Tian, S., Wu, Q., Zhou, B., Choi, M. Y., Ding, B., Yang, W., and Dong, M. (2019) Proteomic Analysis Identifies Membrane Proteins Dependent on the ER Membrane Protein Complex. *Cell Rep* **28**, 2517-2526 e2515

79.   Guna, A., Volkmar, N., Christianson, J. C., and Hegde, R. S. (2017) The ER membrane protein complex is a transmembrane domain insertase. *Science*

80.   Ngo, A. M., Shurtleff, M. J., Popova, K. D., Kulsuptrakul, J., Weissman, J. S., and Puschnik, A. S. (2019) The ER membrane protein complex is required to ensure correct topology and stable expression of flavivirus polyproteins. *Elife* **8**

81.   Lin, D. L., Inoue, T., Chen, Y. J., Chang, A., Tsai, B., and Tai, A. W. (2019) The ER Membrane Protein Complex Promotes Biogenesis of Dengue and Zika Virus Non-structural Multi-pass Transmembrane Proteins to Support Infection. *Cell Rep* **27**, 1666-1674 e1664

82.   Bai, L., You, Q., Feng, X., Kovach, A., and Li, H. (2020) Structure of the ER membrane complex, a transmembrane-domain insertase. *Nature* **584**, 475-478

83.   Miller-Vedam, L. E., Brauning, B., Popova, K. D., Schirle Oakdale, N. T., Bonnar, J. L., Prabu, J. R., Boydston, E. A., Sevillano, N., Shurtleff, M. J., Stroud, R. M., Craik, C. S., Schulman, B. A., Frost, A., and Weissman, J. S. (2020) Structural and mechanistic basis of the EMC-dependent biogenesis of distinct transmembrane clients. *Elife* **9**

84.   O'Donnell, J. P., Phillips, B. P., Yagita, Y., Juszkiewicz, S., Wagner, A., Malinverni, D., Keenan, R. J., Miller, E. A., and Hegde, R. S. (2020) The architecture of EMC reveals a path for membrane protein insertion. *Elife* **9**

85.   Wideman, J. G. (2015) The ubiquitous and ancient ER membrane protein complex (EMC): tether or not? *F1000Res* **4**, 624

86.   Mateja, A., Szlachcic, A., Downing, M. E., Dobosz, M., Mariappan, M., Hegde, R. S., and Keenan, R. J. (2009) The structural basis of tail-anchored membrane protein recognition by Get3. *Nature* **461**, 361-366

87.   Anghel, S. A., McGilvray, P. T., Hegde, R. S., and Keenan, R. J. (2017) Identification of Oxa1 Homologs Operating in the Eukaryotic Endoplasmic Reticulum. *Cell Rep* **21**, 3708-3716

88.   Nepal, B., Leveritt, J., 3rd, and Lazaridis, T. (2018) Membrane Curvature Sensing by Amphipathic Helices: Insights from Implicit Membrane Modeling. *Biophys J* **114**, 2128-2141

89.   Halbleib, K., Pesek, K., Covino, R., Hofbauer, H. F., Wunnicke, D., Hanelt, I., Hummer, G., and Ernst, R. (2017) Activation of the Unfolded Protein Response by Lipid Bilayer Stress. *Mol Cell*

90.   Volkmar, N., and Christianson, J. C. (2020) Squaring the EMC - how promoting membrane protein biogenesis impacts cellular functions and organismal homeostasis. *J Cell Sci* **133**

91.   Kopec, K. O., and Lupas, A. N. (2013) beta-Propeller blades as ancestral peptides in protein evolution. *PLoS One* **8**, e77074

92.   Milstein, C., Brownlee, G. G., Harrison, T. M., and Mathews, M. B. (1972) A possible precursor of immunoglobulin light chains. *Nat New Biol* **239**, 117-120

93.   Evans, E. A., Gilmore, R., and Blobel, G. (1986) Purification of microsomal signal peptidase as a complex. *Proc Natl Acad Sci U S A* **83**, 581-585

94.   Shelness, G. S., Kanwar, Y. S., and Blobel, G. (1988) cDNA-derived primary structure of the glycoprotein component of canine microsomal signal peptidase complex. *J Biol Chem* **263**, 17063-17070

95.   Greenburg, G., Shelness, G. S., and Blobel, G. (1989) A subunit of mammalian signal peptidase is homologous to yeast SEC11 protein. *J Biol Chem* **264**, 15762-15765

96.   Shelness, G. S., and Blobel, G. (1990) Two subunits of the canine signal peptidase complex are homologous to yeast SEC11 protein. *J Biol Chem* **265**, 9512-9519

97.   Shelness, G. S., Lin, L., and Nicchitta, C. V. (1993) Membrane topology and biogenesis of eukaryotic signal peptidase. *J Biol Chem* **268**, 5201-5208

98.   Greenburg, G., and Blobel, G. (1994) cDNA-derived primary structure of the 25-kDa subunit of canine microsomal signal peptidase complex. *J Biol Chem* **269**, 25354-25358

99.   Kalies, K. U., and Hartmann, E. (1996) Membrane topology of the 12- and the 25-kDa subunits of the mammalian signal peptidase complex. *J Biol Chem* **271**, 3925-3929

100.   Dalbey, R. E., Lively, M. O., Bron, S., and van Dijl, J. M. (1997) The chemistry and enzymology of the type I signal peptidases. *Protein Sci* **6**, 1129-1138

101.   Auclair, S. M., Bhanu, M. K., and Kendall, D. A. (2012) Signal peptidase I: cleaving the way to mature proteins. *Protein Sci* **21**, 13-25

102.   Hedstrom, L. (2002) Serine protease mechanism and specificity. *Chem Rev* **102**, 4501-4524

103.   Ekici, O. D., Paetzel, M., and Dalbey, R. E. (2008) Unconventional serine proteases: variations on the catalytic Ser/His/Asp triad configuration. *Protein Sci* **17**, 2023-2037

104.   Bohni, P. C., Deshaies, R. J., and Schekman, R. W. (1988) SEC11 is required for signal peptide processing and yeast cell growth. *J Cell Biol* **106**, 1035-1042

105.   Gemmer, M., and Forster, F. (2020) A clearer picture of the ER translocon complex. *J Cell Sci* **133**

106.   Meyer, H. A., and Hartmann, E. (1997) The yeast SPC22/23 homolog Spc3p is essential for signal peptidase activity. *J Biol Chem* **272**, 13159-13164

107.   Antonin, W., Meyer, H. A., and Hartmann, E. (2000) Interactions between Spc2p and other components of the endoplasmic reticulum translocation sites of the yeast Saccharomyces cerevisiae. *J Biol Chem* **275**, 34068-34072

108.   Kalies, K. U., Rapoport, T. A., and Hartmann, E. (1998) The beta subunit of the Sec61 complex facilitates cotranslational protein transport and interacts with the signal peptidase during translocation. *J Cell Biol* **141**, 887-894

109.   Pfeffer, S., Burbaum, L., Unverdorben, P., Pech, M., Chen, Y., Zimmermann, R., Beckmann, R., and Forster, F. (2015) Structure of the native Sec61 protein-conducting channel. *Nat Commun* **6**, 8403

110.   Shaw, A. S., Rottier, P. J., and Rose, J. K. (1988) Evidence for the loop model of signal-sequence insertion into the endoplasmic reticulum. *Proc Natl Acad Sci U S A* **85**, 7592-7596

111.   von Heijne, G. (1985) Signal sequences. The limits of variation. *J Mol Biol* **184**, 99-105

112.   von Heijne, G. (1983) Patterns of amino acids near signal-sequence cleavage sites. *Eur J Biochem* **133**, 17-21

113.   Folz, R. J., Nothwehr, S. F., and Gordon, J. I. (1988) Substrate specificity of eukaryotic signal peptidase. Site-saturation mutagenesis at position -1 regulates cleavage between multiple sites in human pre (delta pro) apolipoprotein A-II. *J Biol Chem* **263**, 2070-2078

114.   Weihofen, A., Binns, K., Lemberg, M. K., Ashman, K., and Martoglio, B. (2002) Identification of signal peptide peptidase, a presenilin-type aspartic protease. *Science* **296**, 2215-2218

115.   Weihofen, A., Lemberg, M. K., Ploegh, H. L., Bogyo, M., and Martoglio, B. (2000) Release of signal peptide fragments into the cytosol requires cleavage in the transmembrane region by a protease activity that is specifically blocked by a novel cysteine protease inhibitor. *J Biol Chem* **275**, 30951-30956

116.   Robakis, T., Bak, B., Lin, S. H., Bernard, D. J., and Scheiffele, P. (2008) An internal signal sequence directs intramembrane proteolysis of a cellular immunoglobulin domain protein. *J Biol Chem* **283**, 36369-36376

117.   Lara, P., Tellgren-Roth, A., Behesti, H., Horn, Z., Schiller, N., Enquist, K., Cammenberg, M., Liljenstrom, A., Hatten, M. E., von Heijne, G., and Nilsson, I. (2019) Murine astrotactins 1 and 2 have a similar membrane topology and mature via endoproteolytic cleavage catalyzed by a signal peptidase. *J Biol Chem* **294**, 4538-4545

118.   Nilsson, I., Johnson, A. E., and von Heijne, G. (2002) Cleavage of a tail-anchored protein by signal peptidase. *FEBS Lett* **516**, 106-108

119.   Pene, V., Lemasson, M., Harper, F., Pierron, G., and Rosenberg, A. R. (2017) Role of cleavage at the core-E1 junction of hepatitis C virus polyprotein in viral morphogenesis. *PLoS One* **12**, e0175810

120.   Liljestrom, P., and Garoff, H. (1991) Internally located cleavable signal sequences direct the formation of Semliki Forest virus membrane proteins from a polyprotein precursor. *J Virol* **65**, 147-154

121.   Zhang, R., Miner, J. J., Gorman, M. J., Rausch, K., Ramage, H., White, J. P., Zuiani, A., Zhang, P., Fernandez, E., Zhang, Q., Dowd, K. A., Pierson, T. C., Cherry, S., and Diamond, M. S. (2016) A CRISPR screen defines a signal peptide processing pathway required by flaviviruses. *Nature* **535**, 164-168

122.   Watson, P., and Stephens, D. J. (2005) ER-to-Golgi transport: form and formation of vesicular and tubular carriers. *Biochim Biophys Acta* **1744**, 304-315

123.   Barlowe, C., Orci, L., Yeung, T., Hosobuchi, M., Hamamoto, S., Salama, N., Rexach, M. F., Ravazzola, M., Amherdt, M., and Schekman, R. (1994) COPII: a membrane coat formed by Sec proteins that drive vesicle budding from the endoplasmic reticulum. *Cell* **77**, 895-907

124.   Kuehn, M. J., Herrmann, J. M., and Schekman, R. (1998) COPII-cargo interactions direct protein sorting into ER-derived transport vesicles. *Nature* **391**, 187-190

125.   Glick, B. S., and Luini, A. (2011) Models for Golgi traffic: a critical assessment. *Cold Spring Harb Perspect Biol* **3**, a005215

126.   Mironov, A. A., and Beznoussenko, G. V. (2019) Models of Intracellular Transport: Pros and Cons. *Front Cell Dev Biol* **7**, 146

127.   Ohtsubo, K., and Marth, J. D. (2006) Glycosylation in cellular mechanisms of health and disease. *Cell* **126**, 855-867

128.   Schekman, R., and Orci, L. (1996) Coat proteins and vesicle budding. *Science* **271**, 1526-1533

129.   Jackson, L. P., Lewis, M., Kent, H. M., Edeling, M. A., Evans, P. R., Duden, R., and Owen, D. J. (2012) Molecular basis for recognition of dilysine trafficking motifs by COPI. *Dev Cell* **23**, 1255-1262

130.   Brauer, P., Parker, J. L., Gerondopoulos, A., Zimmermann, I., Seeger, M. A., Barr, F. A., and Newstead, S. (2019) Structural basis for pH-dependent retrieval of ER proteins from the Golgi by the KDEL receptor. *Science* **363**, 1103-1107

131.   Wilson, D. W., Lewis, M. J., and Pelham, H. R. (1993) pH-dependent binding of KDEL to its receptor in vitro. *J Biol Chem* **268**, 7465-7468

132.   Wu, M. M., Llopis, J., Adams, S., McCaffery, J. M., Kulomaa, M. S., Machen, T. E., Moore, H. P., and Tsien, R. Y. (2000) Organelle pH studies using targeted avidin and fluorescein-biotin. *Chem Biol* **7**, 197-209
133.   Hanulova, M., and Weiss, M. (2012) Membrane-mediated interactions--a physico-chemical basis for protein sorting. *Mol Membr Biol* **29**, 177-185
134.   Borgese, N. (2016) Getting membrane proteins on and off the shuttle bus between the endoplasmic reticulum and the Golgi complex. *J Cell Sci* **129**, 1537-1545
135.   Gao, C., Cai, Y., Wang, Y., Kang, B. H., Aniento, F., Robinson, D. G., and Jiang, L. (2014) Retention mechanisms for ER and Golgi membrane proteins. *Trends Plant Sci* **19**, 508-515
136.   Stalder, D., and Gershlick, D. C. (2020) Direct trafficking pathways from the Golgi apparatus to the plasma membrane. *Semin Cell Dev Biol* **107**, 112-125
137.   Payne, G. S., and Schekman, R. (1985) A test of clathrin function in protein secretion and cell growth. *Science* **230**, 1009-1014
138.   Grant, B. D., and Donaldson, J. G. (2009) Pathways and mechanisms of endocytic recycling. *Nat Rev Mol Cell Biol* **10**, 597-608
139.   Steinman, R. M., Mellman, I. S., Muller, W. A., and Cohn, Z. A. (1983) Endocytosis and the recycling of plasma membrane. *J Cell Biol* **96**, 1-27
140.   Cullen, P. J., and Steinberg, F. (2018) To degrade or not to degrade: mechanisms and significance of endocytic recycling. *Nat Rev Mol Cell Biol* **19**, 679-696
141.   Nilsson, I. M., and von Heijne, G. (1993) Determination of the distance between the oligosaccharyltransferase active site and the endoplasmic reticulum membrane. *J Biol Chem* **268**, 5798-5801
142.   Whitley, P., Nilsson, I. M., and von Heijne, G. (1996) A nascent secretory protein may traverse the ribosome/endoplasmic reticulum translocase complex as an extended chain. *J Biol Chem* **271**, 6241-6244
143.   Shrimal, S., Cherepanova, N. A., and Gilmore, R. (2015) Cotranslational and posttranslocational N-glycosylation of proteins in the endoplasmic reticulum. *Semin Cell Dev Biol* **41**, 71-78
144.   Brodsky, J. L., and Skach, W. R. (2011) Protein folding and quality control in the endoplasmic reticulum: Recent lessons from yeast and mammalian cell systems. *Curr Opin Cell Biol* **23**, 464-475
145.   Pfeffer, S., Dudek, J., Gogala, M., Schorr, S., Linxweiler, J., Lang, S., Becker, T., Beckmann, R., Zimmermann, R., and Forster, F. (2014) Structure of the mammalian oligosaccharyl-transferase complex in the native ER protein translocon. *Nat Commun* **5**, 3072
146.   Mohorko, E., Owen, R. L., Malojcic, G., Brozzo, M. S., Aebi, M., and Glockshuber, R. (2014) Structural basis of substrate specificity of human oligosaccharyl transferase subunit N33/Tusc3 and its role in regulating protein N-glycosylation. *Structure* **22**, 590-601
147.   Cherepanova, N. A., Shrimal, S., and Gilmore, R. (2014) Oxidoreductase activity is necessary for N-glycosylation of cysteine-proximal acceptor sites in glycoproteins. *J Cell Biol* **206**, 525-539
148.   Deprez, P., Gautschi, M., and Helenius, A. (2005) More than one glycan is needed for ER glucosidase II to allow entry of glycoproteins into the calnexin/calreticulin cycle. *Mol Cell* **19**, 183-195
149.   Zapun, A., Petrescu, S. M., Rudd, P. M., Dwek, R. A., Thomas, D. Y., and Bergeron, J. J. M. (1997) Conformation-Independent Binding of Monoglucosylated Ribonuclease B to Calnexin. *Cell* **88**, 29-38
150.   Ou, W. J., Cameron, P. H., Thomas, D. Y., and Bergeron, J. J. (1993) Association of folding intermediates of glycoproteins with calnexin during protein maturation. *Nature* **364**, 771-776
151.   Kozlov, G., and Gehring, K. (2020) Calnexin cycle - structural features of the ER chaperone system. *FEBS J*
152.   Sousa, M., and Parodi, A. J. (1995) The molecular basis for the recognition of misfolded glycoproteins by the UDP-Glc:glycoprotein glucosyltransferase. *EMBO J* **14**, 4196-4203
153.   Trombetta, E. S., and Helenius, A. (2000) Conformational requirements for glycoprotein reglucosylation in the endoplasmic reticulum. *J Cell Biol* **148**, 1123-1129
154.   Frenkel, Z., Gregory, W., Kornfeld, S., and Lederkremer, G. Z. (2003) Endoplasmic reticulum-associated degradation of mammalian glycoproteins involves sugar chain trimming to Man6-5GlcNAc2. *J Biol Chem* **278**, 34119-34124
155.   Caramelo, J. J., and Parodi, A. J. (2015) A sweet code for glycoprotein folding. *FEBS Lett* **589**, 3379-3387
156.   Groisman, B., Shenkman, M., Ron, E., and Lederkremer, G. Z. (2011) Mannose trimming is required for delivery of a glycoprotein from EDEM1 to XTP3-B and to late endoplasmic reticulum-associated degradation steps. *J Biol Chem* **286**, 1292-1300
157.   Hosokawa, N., Kamiya, Y., Kamiya, D., Kato, K., and Nagata, K. (2009) Human OS-9, a lectin required for glycoprotein endoplasmic reticulum-associated degradation, recognizes mannose-trimmed N-glycans. *J Biol Chem* **284**, 17061-17068
158.   Leitman, J., Shenkman, M., Gofman, Y., Shtern, N. O., Ben-Tal, N., Hendershot, L. M., and Lederkremer, G. Z. (2014) Herp coordinates compartmentalization and recruitment of HRD1 and misfolded proteins for ERAD. *Mol Biol Cell* **25**, 1050-1060
159.   Sato, T., Sako, Y., Sho, M., Momohara, M., Suico, M. A., Shuto, T., Nishitoh, H., Okiyoneda, T., Kokame, K., Kaneko, M., Taura, M., Miyata, M., Chosa, K., Koga, T., Morino-Koga, S., Wada, I., and Kai, H. (2012) STT3B-dependent posttranslational N-glycosylation as a surveillance system for secretory protein. *Mol Cell* **47**, 99-110
160.   Amaral, M. D. (2004) CFTR and chaperones: processing and degradation. *J Mol Neurosci* **23**, 41-48
161.   Meacham, G. C., Lu, Z., King, S., Sorscher, E., Tousson, A., and Cyr, D. M. (1999) The Hdj-2/Hsc70 chaperone pair facilitates early steps in CFTR biogenesis. *EMBO J* **18**, 1492-1505
162.   Baaklini, I., Goncalves, C. C., Lukacs, G. L., and Young, J. C. (2020) Selective Binding of HSC70 and its Co-Chaperones to Structural Hotspots on CFTR. *Sci Rep* **10**, 4176
163.   Farinha, C. M., Nogueira, P., Mendes, F., Penque, D., and Amaral, M. D. (2002) The human DnaJ homologue (Hdj)-1/heat-shock protein (Hsp) 40 co-chaperone is required for the in vivo stabilization of the cystic fibrosis transmembrane conductance regulator by Hsp70. *Biochem J* **366**, 797-806
164.   Loo, M. A., Jensen, T. J., Cui, L., Hou, Y., Chang, X. B., and Riordan, J. R. (1998) Perturbation of Hsp90 interaction with nascent CFTR prevents its maturation and accelerates its degradation by the proteasome. *EMBO J* **17**, 6879-6887
165.   Haas, I. G., and Wabl, M. (1983) Immunoglobulin heavy chain binding protein. *Nature* **306**, 387-389
166.   Flynn, G. C., Pohl, J., Flocco, M. T., and Rothman, J. E. (1991) Peptide-binding specificity of the molecular chaperone BiP. *Nature* **353**, 726-730

167. Otero, J. H., Lizak, B., and Hendershot, L. M. (2010) Life and death of a BiP substrate. *Semin Cell Dev Biol* **21**, 472-478

168. Chung, K. T., Shen, Y., and Hendershot, L. M. (2002) BAP, a mammalian BiP-associated protein, is a nucleotide exchange factor that regulates the ATPase activity of BiP. *J Biol Chem* **277**, 47557-47563

169. Behnke, J., Feige, M. J., and Hendershot, L. M. (2015) BiP and its nucleotide exchange factors Grp170 and Sil1: mechanisms of action and biological functions. *Journal of molecular biology* **427**, 1589-1608

170. Williams, J. M., Inoue, T., Chen, G., and Tsai, B. (2015) The nucleotide exchange factors Grp170 and Sil1 induce cholera toxin release from BiP to enable retrotranslocation. *Mol Biol Cell* **26**, 2181-2189

171. Senderek, J., Krieger, M., Stendel, C., Bergmann, C., Moser, M., Breitbach-Faller, N., Rudnik-Schoneborn, S., Blaschek, A., Wolf, N. I., Harting, I., North, K., Smith, J., Muntoni, F., Brockington, M., Quijano-Roy, S., Renault, F., Herrmann, R., Hendershot, L. M., Schroder, J. M., Lochmuller, H., Topaloglu, H., Voit, T., Weis, J., Ebinger, F., and Zerres, K. (2005) Mutations in SIL1 cause Marinesco-Sjogren syndrome, a cerebellar ataxia with cataract and myopathy. *Nat Genet* **37**, 1312-1314

172. Kitao, Y., Ozawa, K., Miyazaki, M., Tamatani, M., Kobayashi, T., Yanagi, H., Okabe, M., Ikawa, M., Yamashima, T., Stern, D. M., Hori, O., and Ogawa, S. (2001) Expression of the endoplasmic reticulum molecular chaperone (ORP150) rescues hippocampal neurons from glutamate toxicity. *J Clin Invest* **108**, 1439-1450

173. Behnke, J., and Hendershot, L. M. (2014) The large Hsp70 Grp170 binds to unfolded protein substrates in vivo with a regulation distinct from conventional Hsp70s. *J Biol Chem* **289**, 2899-2907

174. Buck, T. M., Kolb, A. R., Boyd, C. R., Kleyman, T. R., and Brodsky, J. L. (2010) The endoplasmic reticulum-associated degradation of the epithelial sodium channel requires a unique complement of molecular chaperones. *Mol Biol Cell* **21**, 1047-1058

175. Buck, T. M., Plavchak, L., Roy, A., Donnelly, B. F., Kashlan, O. B., Kleyman, T. R., Subramanya, A. R., and Brodsky, J. L. (2013) The Lhs1/GRP170 chaperones facilitate the endoplasmic reticulum-associated degradation of the epithelial sodium channel. *J Biol Chem* **288**, 18366-18380

176. Inoue, T., and Tsai, B. (2016) The Grp170 nucleotide exchange factor executes a key role during ERAD of cellular misfolded clients. *Mol Biol Cell* **27**, 1650-1662

177. Misselwitz, B., Staeck, O., and Rapoport, T. A. (1998) J Proteins Catalytically Activate Hsp70 Molecules to Trap a Wide Range of Peptide Sequences. *Molecular Cell* **2**, 593-603

178. Tsai, J., and Douglas, M. G. (1996) A conserved HPD sequence of the J-domain is necessary for YDJ1 stimulation of Hsp70 ATPase activity at a site distinct from substrate binding. *J Biol Chem* **271**, 9347-9354

179. Jin, Y., Awad, W., Petrova, K., and Hendershot, L. M. (2008) Regulated release of ERdj3 from unfolded proteins by BiP. *EMBO J* **27**, 2873-2882

180. Pobre, K. F. R., Poet, G. J., and Hendershot, L. M. (2018) The endoplasmic reticulum (ER) chaperone BiP is a master regulator of ER functions: Getting by with a little help from ERdj friends. *J Biol Chem*

181. Behnke, J., Mann, M. J., Scruggs, F. L., Feige, M. J., and Hendershot, L. M. (2016) Members of the Hsp70 Family Recognize Distinct Types of Sequences to Execute ER Quality Control. *Mol Cell* **63**, 739-752

182. Maegawa, K. I., Watanabe, S., Noi, K., Okumura, M., Amagai, Y., Inoue, M., Ushioda, R., Nagata, K., Ogura, T., and Inaba, K. (2017) The Highly Dynamic Nature of ERdj5 Is Key to Efficient Elimination of Aberrant Protein Oligomers through ER-Associated Degradation. *Structure* **25**, 846-857 e844

183. Ohta, M., and Takaiwa, F. (2019) OsERdj7 is an ER-resident J-protein involved in ER quality control in rice endosperm. *J Plant Physiol* **245**, 153109

184. Glembotski, C. C., Thuerauf, D. J., Huang, C., Vekich, J. A., Gottlieb, R. A., and Doroudgar, S. (2012) Mesencephalic astrocyte-derived neurotrophic factor protects the heart from ischemic damage and is selectively secreted upon sarco/endoplasmic reticulum calcium depletion. *J Biol Chem* **287**, 25893-25904

185. Yan, Y., Rato, C., Rohland, L., Preissler, S., and Ron, D. (2019) MANF antagonizes nucleotide exchange by the endoplasmic reticulum chaperone BiP. *Nat Commun* **10**, 541

186. Hoter, A., El-Sabban, M. E., and Naim, H. Y. (2018) The HSP90 Family: Structure, Regulation, Function, and Implications in Health and Disease. *Int J Mol Sci* **19**

187. Frey, S., Leskovar, A., Reinstein, J., and Buchner, J. (2007) The ATPase cycle of the endoplasmic chaperone Grp94. *J Biol Chem* **282**, 35612-35620

188. Prodromou, C. (2016) Mechanisms of Hsp90 regulation. *Biochem J* **473**, 2439-2452

189. Dollins, D. E., Warren, J. J., Immormino, R. M., and Gewirth, D. T. (2007) Structures of GRP94-nucleotide complexes reveal mechanistic differences between the hsp90 chaperones. *Mol Cell* **28**, 41-56

190. Huck, J. D., Que, N. L., Hong, F., Li, Z., and Gewirth, D. T. (2017) Structural and Functional Analysis of GRP94 in the Closed State Reveals an Essential Role for the Pre-N Domain and a Potential Client-Binding Site. *Cell Rep* **20**, 2800-2809

191. Sun, M., Kotler, J. L. M., Liu, S., and Street, T. O. (2019) The endoplasmic reticulum (ER) chaperones BiP and Grp94 selectively associate when BiP is in the ADP conformation. *J Biol Chem* **294**, 6387-6396

192. Meacock, S. L., Lecomte, F. J., Crawshaw, S. G., and High, S. (2002) Different transmembrane domains associate with distinct endoplasmic reticulum components during membrane integration of a polytopic protein. *Mol Biol Cell* **13**, 4114-4129

193. Chitwood, P. J., and Hegde, R. S. (2020) An intramembrane chaperone complex facilitates membrane protein biogenesis. *Nature* **584**, 630-634

194. Appenzeller-Herzog, C., and Ellgaard, L. (2008) The human PDI family: versatility packed into a single fold. *Biochim Biophys Acta* **1783**, 535-548

195. Chen, Y., Zhang, Y., Yin, Y., Gao, G., Li, S., Jiang, Y., Gu, X., and Luo, J. (2005) SPD--a web-based secreted protein database. *Nucleic Acids Res* **33**, D169-173

196. Chen, W., Helenius, J., Braakman, I., and Helenius, A. (1995) Cotranslational folding and calnexin binding during glycoprotein synthesis. *Proc Natl Acad Sci U S A* **92**, 6229-6233

197. Givol, D., Goldberger, R. F., and Anfinsen, C. B. (1964) Oxidation and Disulfide Interchange in the Reactivation of Reduced Ribonuclease. *J Biol Chem* **239**, PC3114-3116

198. Pollard, M. G., Travers, K. J., and Weissman, J. S. (1998) Ero1p: a novel and ubiquitous protein with an essential role in oxidative protein folding in the endoplasmic reticulum. *Mol Cell* **1**, 171-182

199. Frand, A. R., and Kaiser, C. A. (1998) The ERO1 gene of yeast is required for oxidation of protein dithiols in the endoplasmic reticulum. *Mol Cell* **1**, 161-170

102

200. Benham, A. M., van Lith, M., Sitia, R., and Braakman, I. (2013) Ero1-PDI interactions, the response to redox flux and the implications for disulfide bond formation in the mammalian endoplasmic reticulum. *Philos Trans R Soc Lond B Biol Sci* **368**, 20110403

201. Galligan, J. J., and Petersen, D. R. (2012) The human protein disulfide isomerase gene family. *Hum Genomics* **6**, 6

202. Braakman, I., and Hebert, D. N. (2013) Protein folding in the endoplasmic reticulum. *Cold Spring Harb Perspect Biol* **5**, a013201

203. Fagioli, C., Mezghrani, A., and Sitia, R. (2001) Reduction of interchain disulfide bonds precedes the dislocation of Ig-mu chains from the endoplasmic reticulum to the cytosol for proteasomal degradation. *J Biol Chem* **276**, 40962-40967

204. Okuda-Shimizu, Y., and Hendershot, L. M. (2007) Characterization of an ERAD pathway for nonglycosylated BiP substrates, which require Herp. *Mol Cell* **28**, 544-554

205. He, K., Cunningham, C. N., Manickam, N., Liu, M., Arvan, P., and Tsai, B. (2015) PDI reductase acts on Akita mutant proinsulin to initiate retrotranslocation along the Hrd1/Sel1L-p97 axis. *Mol Biol Cell* **26**, 3413-3423

206. Ellgaard, L., Sevier, C. S., and Bulleid, N. J. (2017) How Are Proteins Reduced in the Endoplasmic Reticulum? *Trends Biochem Sci*

207. Chino, H., and Mizushima, N. (2020) ER-Phagy: Quality Control and Turnover of Endoplasmic Reticulum. *Trends Cell Biol* **30**, 384-398

208. Forrester, A., De Leonibus, C., Grumati, P., Fasana, E., Piemontese, M., Staiano, L., Fregno, I., Raimondi, A., Marazza, A., Bruno, G., Iavazzo, M., Intartaglia, D., Seczynska, M., van Anken, E., Conte, I., De Matteis, M. A., Dikic, I., Molinari, M., and Settembre, C. (2019) A selective ER-phagy exerts procollagen quality control via a Calnexin-FAM134B complex. *EMBO J* **38**

209. Carvalho, P., Goder, V., and Rapoport, T. A. (2006) Distinct ubiquitin-ligase complexes define convergent pathways for the degradation of ER proteins. *Cell* **126**, 361-373

210. Huyer, G., Piluek, W. F., Fansler, Z., Kreft, S. G., Hochstrasser, M., Brodsky, J. L., and Michaelis, S. (2004) Distinct machinery is required in Saccharomyces cerevisiae for the endoplasmic reticulum-associated degradation of a multispanning membrane protein and a soluble luminal protein. *J Biol Chem* **279**, 38369-38378

211. Nakatsukasa, K., Huyer, G., Michaelis, S., and Brodsky, J. L. (2008) Dissecting the ER-associated degradation of a misfolded polytopic membrane protein. *Cell* **132**, 101-112

212. Hassink, G., Kikkert, M., van Voorden, S., Lee, S. J., Spaapen, R., van Laar, T., Coleman, C. S., Bartee, E., Fruh, K., Chau, V., and Wiertz, E. (2005) TEB4 is a C4HC3 RING finger-containing ubiquitin ligase of the endoplasmic reticulum. *Biochem J* **388**, 647-655

213. Sun, Z., and Brodsky, J. L. (2019) Protein quality control in the secretory pathway. *J Cell Biol*

214. van der Goot, A. T., Pearce, M. M. P., Leto, D. E., Shaler, T. A., and Kopito, R. R. (2018) Redundant and Antagonistic Roles of XTP3B and OS9 in Decoding Glycan and Non-glycan Degrons in ER-Associated Degradation. *Mol Cell* **70**, 516-530 e516

215. Xie, W., Kanehara, K., Sayeed, A., and Ng, D. T. (2009) Intrinsic conformational determinants signal protein misfolding to the Hrd1/Htm1 endoplasmic reticulum-associated degradation system. *Mol Biol Cell* **20**, 3317-3329

216. Christianson, J. C., Shaler, T. A., Tyler, R. E., and Kopito, R. R. (2008) OS-9 and GRP94 deliver mutant alpha1-antitrypsin to the Hrd1-SEL1L ubiquitin ligase complex for ERAD. *Nat Cell Biol* **10**, 272-282

217. Lai, C. W., Otero, J. H., Hendershot, L. M., and Snapp, E. (2012) ERdj4 protein is a soluble endoplasmic reticulum (ER) DnaJ family protein that interacts with ER-associated degradation machinery. *J Biol Chem* **287**, 7969-7978

218. Oikonomou, C., and Hendershot, L. M. (2019) Disposing of misfolded ER proteins: A troubled substrate's way out of the ER. *Mol Cell Endocrinol*, 110630

219. Guna, A., and Hegde, R. S. (2018) Transmembrane Domain Recognition during Membrane Protein Biogenesis and Quality Control. *Curr Biol* **28**, R498-R511

220. Sato, B. K., Schulz, D., Do, P. H., and Hampton, R. Y. (2009) Misfolded membrane proteins are specifically recognized by the transmembrane domain of the Hrd1p ubiquitin ligase. *Mol Cell* **34**, 212-222

221. Fang, S., Ferrone, M., Yang, C., Jensen, J. P., Tiwari, S., and Weissman, A. M. (2001) The tumor autocrine motility factor receptor, gp78, is a ubiquitin protein ligase implicated in degradation from the endoplasmic reticulum. *Proc Natl Acad Sci U S A* **98**, 14422-14427

222. Bernasconi, R., Galli, C., Calanca, V., Nakajima, T., and Molinari, M. (2010) Stringent requirement for HRD1, SEL1L, and OS-9/XTP3-B for disposal of ERAD-LS substrates. *J Cell Biol* **188**, 223-235

223. Greenblatt, E. J., Olzmann, J. A., and Kopito, R. R. (2011) Derlin-1 is a rhomboid pseudoprotease required for the dislocation of mutant alpha-1 antitrypsin from the endoplasmic reticulum. *Nat Struct Mol Biol* **18**, 1147-1152

224. Sun, F., Zhang, R., Gong, X., Geng, X., Drain, P. F., and Frizzell, R. A. (2006) Derlin-1 promotes the efficient degradation of the cystic fibrosis transmembrane conductance regulator (CFTR) and CFTR folding mutants. *J Biol Chem* **281**, 36856-36863

225. Bernardi, K. M., Williams, J. M., Kikkert, M., van Voorden, S., Wiertz, E. J., Ye, Y., and Tsai, B. (2010) The E3 ubiquitin ligases Hrd1 and gp78 bind to and promote cholera toxin retro-translocation. *Mol Biol Cell* **21**, 140-151

226. Houck, S. A., and Cyr, D. M. (2012) Mechanisms for quality control of misfolded transmembrane proteins. *Biochim Biophys Acta* **1818**, 1108-1114

227. Fleig, L., Bergbold, N., Sahasrabudhe, P., Geiger, B., Kaltak, L., and Lemberg, M. K. (2012) Ubiquitin-dependent intramembrane rhomboid protease promotes ERAD of membrane proteins. *Mol Cell* **47**, 558-569

228. Knopf, J. D., Landscheidt, N., Pegg, C. L., Schulz, B. L., Kuhnle, N., Chao, C. W., Huck, S., and Lemberg, M. K. (2020) Intramembrane protease RHBDL4 cleaves oligosaccharyltransferase subunits to target them for ER-associated degradation. *J Cell Sci*

229. Chen, C. Y., Malchus, N. S., Hehn, B., Stelzer, W., Avci, D., Langosch, D., and Lemberg, M. K. (2014) Signal peptide peptidase functions in ERAD to cleave the unfolded protein response regulator XBP1u. *EMBO J* **33**, 2492-2506

230. Yucel, S. S., Stelzer, W., Lorenzoni, A., Wozny, M., Langosch, D., and Lemberg, M. K. (2019) The Metastable XBP1u Transmembrane Domain Defines Determinants for Intramembrane Proteolysis by Signal Peptide Peptidase. *Cell Rep* **26**, 3087-3099 e3011

231. Lambert, G., Becker, B., Schreiber, R., Boucherot, A., Reth, M., and Kunzelmann, K. (2001) Control of cystic fibrosis transmembrane conductance regulator expression by BAP31. *J Biol Chem* **276**, 20340-20345
232. Szczesna-Skorupa, E., and Kemper, B. (2006) BAP31 is involved in the retention of cytochrome P450 2C2 in the endoplasmic reticulum. *J Biol Chem* **281**, 4142-4148
233. Schamel, W. W., Kuppig, S., Becker, B., Gimborn, K., Hauri, H. P., and Reth, M. (2003) A high-molecular-weight complex of membrane proteins BAP29/BAP31 is involved in the retention of membrane-bound IgD in the endoplasmic reticulum. *Proc Natl Acad Sci U S A* **100**, 9861-9866
234. Sato, K., Sato, M., and Nakano, A. (2003) Rer1p, a retrieval receptor for ER membrane proteins, recognizes transmembrane domains in multiple modes. *Mol Biol Cell* **14**, 3605-3616
235. Briant, K., Johnson, N., and Swanton, E. (2017) Transmembrane domain quality control systems operate at the endoplasmic reticulum and Golgi apparatus. *PLoS One* **12**, e0173924
236. Spasic, D., Raemaekers, T., Dillen, K., Declerck, I., Baert, V., Serneels, L., Fullekrug, J., and Annaert, W. (2007) Rer1p competes with APH-1 for binding to nicastrin and regulates gamma-secretase complex assembly in the early secretory pathway. *J Cell Biol* **176**, 629-640
237. Kaether, C., Scheuermann, J., Fassler, M., Zilow, S., Shirotani, K., Valkova, C., Novak, B., Kacmar, S., Steiner, H., and Haass, C. (2007) Endoplasmic reticulum retention of the gamma-secretase complex component Pen2 by Rer1. *EMBO Rep* **8**, 743-748
238. Hara, T., Hashimoto, Y., Akuzawa, T., Hirai, R., Kobayashi, H., and Sato, K. (2014) Rer1 and calnexin regulate endoplasmic reticulum retention of a peripheral myelin protein 22 mutant that causes type 1A Charcot-Marie-Tooth disease. *Sci Rep* **4**, 6992
239. Ruggiano, A., Foresti, O., and Carvalho, P. (2014) Quality control: ER-associated degradation: protein quality control and beyond. *J Cell Biol* **204**, 869-879
240. Wiertz, E. J., Tortorella, D., Bogyo, M., Yu, J., Mothes, W., Jones, T. R., Rapoport, T. A., and Ploegh, H. L. (1996) Sec61-mediated transfer of a membrane protein from the endoplasmic reticulum to the proteasome for destruction. *Nature* **384**, 432-438
241. Romisch, K. (2017) A Case for Sec61 Channel Involvement in ERAD. *Trends Biochem Sci* **42**, 171-179
242. Elia, F., Yadhanapudi, L., Tretter, T., and Romisch, K. (2019) The N-terminus of Sec61p plays key roles in ER protein import and ERAD. *PLoS One* **14**, e0215950
243. Ye, Y., Shibata, Y., Yun, C., Ron, D., and Rapoport, T. A. (2004) A membrane protein complex mediates retro-translocation from the ER lumen into the cytosol. *Nature* **429**, 841-847
244. Lilley, B. N., and Ploegh, H. L. (2004) A membrane protein required for dislocation of misfolded proteins from the ER. *Nature* **429**, 834-840
245. Wahlman, J., DeMartino, G. N., Skach, W. R., Bulleid, N. J., Brodsky, J. L., and Johnson, A. E. (2007) Real-time fluorescence detection of ERAD substrate retrotranslocation in a mammalian in vitro system. *Cell* **129**, 943-955
246. Neal, S., Jaeger, P. A., Duttke, S. H., Benner, C. K., Glass, C., Ideker, T., and Hampton, R. (2018) The Dfm1 Derlin Is Required for ERAD Retrotranslocation of Integral Membrane Proteins. *Mol Cell* **69**, 306-320 e304
247. Carvalho, P., Stanley, A. M., and Rapoport, T. A. (2010) Retrotranslocation of a misfolded luminal ER protein by the ubiquitin-ligase Hrd1p. *Cell* **143**, 579-591
248. Baldridge, R. D., and Rapoport, T. A. (2016) Autoubiquitination of the Hrd1 Ligase Triggers Protein Retrotranslocation in ERAD. *Cell* **166**, 394-407
249. Peterson, B. G., Glaser, M. L., Rapoport, T. A., and Baldridge, R. D. (2019) Cycles of autoubiquitination and deubiquitination regulate the ERAD ubiquitin ligase Hrd1. *Elife* **8**
250. Vasic, V., Denkert, N., Schmidt, C. C., Riedel, D., Stein, A., and Meinecke, M. (2020) Hrd1 forms the retrotranslocation pore regulated by auto-ubiquitination and binding of misfolded proteins. *Nat Cell Biol*
251. Wu, X., Siggel, M., Ovchinnikov, S., Mi, W., Svetlov, V., Nudler, E., Liao, M., Hummer, G., and Rapoport, T. A. (2020) Structural basis of ER-associated protein degradation mediated by the Hrd1 ubiquitin ligase complex. *Science* **368**
252. Shi, J., Hu, X., Guo, Y., Wang, L., Ji, J., Li, J., and Zhang, Z. R. (2019) A technique for delineating the unfolding requirements for substrate entry into retrotranslocons during endoplasmic reticulum-associated degradation. *J Biol Chem*
253. McKenna, M. J., Sim, S. I., Ordureau, A., Wei, L., Harper, J. W., Shao, S., and Park, E. (2020) The endoplasmic reticulum P5A-ATPase is a transmembrane helix dislocase. *Science* **369**
254. Qin, Q., Zhao, T., Zou, W., Shen, K., and Wang, X. (2020) An Endoplasmic Reticulum ATPase Safeguards Endoplasmic Reticulum Identity by Removing Ectopically Localized Mitochondrial Proteins. *Cell Rep* **33**, 108363
255. Krumpe, K., Frumkin, I., Herzig, Y., Rimon, N., Ozbalci, C., Brugger, B., Rapaport, D., and Schuldiner, M. (2012) Ergosterol content specifies targeting of tail-anchored proteins to mitochondrial outer membranes. *Mol Biol Cell* **23**, 3927-3935
256. Dederer, V., Khmelinskii, A., Huhn, A. G., Okreglak, V., Knop, M., and Lemberg, M. K. (2019) Cooperation of mitochondrial and ER factors in quality control of tail-anchored proteins. *Elife* **8**
257. Lemus, L., and Goder, V. (2014) Regulation of Endoplasmic Reticulum-Associated Protein Degradation (ERAD) by Ubiquitin. *Cells* **3**, 824-847
258. Stewart, M. D., Ritterhoff, T., Klevit, R. E., and Brzovic, P. S. (2016) E2 enzymes: more than just middle men. *Cell Res* **26**, 423-440
259. Wang, X., Herr, R. A., Rabelink, M., Hoeben, R. C., Wiertz, E. J., and Hansen, T. H. (2009) Ube2j2 ubiquitinates hydroxylated amino acids on ER-associated degradation substrates. *J Cell Biol* **187**, 655-668
260. Oh, E., Akopian, D., and Rape, M. (2018) Principles of Ubiquitin-Dependent Signaling. *Annu Rev Cell Dev Biol* **34**, 137-162
261. Claessen, J. H., Kundrat, L., and Ploegh, H. L. (2012) Protein quality control in the ER: balancing the ubiquitin checkbook. *Trends Cell Biol* **22**, 22-32
262. Weber, A., Cohen, I., Popp, O., Dittmar, G., Reiss, Y., Sommer, T., Ravid, T., and Jarosch, E. (2016) Sequential Poly-ubiquitylation by Specialized Conjugating Enzymes Expands the Versatility of a Quality Control Ubiquitin Ligase. *Mol Cell* **63**, 827-839
263. Xu, P., Duong, D. M., Seyfried, N. T., Cheng, D., Xie, Y., Robert, J., Rush, J., Hochstrasser, M., Finley, D., and Peng, J. (2009) Quantitative proteomics reveals the function of unconventional ubiquitin chains in proteasomal degradation. *Cell* **137**, 133-145

264. Kostova, Z., Mariano, J., Scholz, S., Koenig, C., and Weissman, A. M. (2009) A Ubc7p-binding domain in Cue1p activates ER-associated protein degradation. *J Cell Sci* **122**, 1374-1381

265. Metzger, M. B., Liang, Y. H., Das, R., Mariano, J., Li, S., Li, J., Kostova, Z., Byrd, R. A., Ji, X., and Weissman, A. M. (2013) A structurally unique E2-binding domain activates ubiquitination by the ERAD E2, Ubc7p, through multiple mechanisms. *Mol Cell* **50**, 516-527

266. Fenech, E. J., Lari, F., Charles, P. D., Fischer, R., Laetitia-Thezenas, M., Bagola, K., Paton, A. W., Paton, J. C., Gyrd-Hansen, M., Kessler, B. M., and Christianson, J. C. (2020) Interaction mapping of endoplasmic reticulum ubiquitin ligases identifies modulators of innate immune signalling. *Elife* **9**

267. Leto, D. E., Morgens, D. W., Zhang, L., Walczak, C. P., Elias, J. E., Bassik, M. C., and Kopito, R. R. (2018) Genome-wide CRISPR Analysis Identifies Substrate-Specific Conjugation Modules in ER-Associated Degradation. *Mol Cell*

268. van de Weijer, M. L., Krshnan, L., Liberatori, S., Guerrero, E. N., Robson-Tull, J., Hahn, L., Lebbink, R. J., Wiertz, E., Fischer, R., Ebner, D., and Carvalho, P. (2020) Quality Control of ER Membrane Proteins by the RNF185/Membralin Ubiquitin Ligase Complex. *Mol Cell*

269. Stefanovic-Barrett, S., Dickson, A. S., Burr, S. P., Williamson, J. C., Lobb, I. T., van den Boomen, D. J., Lehner, P. J., and Nathan, J. A. (2018) MARCH6 and TRC8 facilitate the quality control of cytosolic and tail-anchored proteins. *EMBO Rep* **19**

270. Morito, D., Hirao, K., Oda, Y., Hosokawa, N., Tokunaga, F., Cyr, D. M., Tanaka, K., Iwai, K., and Nagata, K. (2008) Gp78 cooperates with RMA1 in endoplasmic reticulum-associated degradation of CFTRDeltaF508. *Mol Biol Cell* **19**, 1328-1336

271. Song, X., Liu, S., Wang, W., Ma, Z., Cao, X., and Jiang, M. (2020) E3 ubiquitin ligase RNF170 inhibits innate immune responses by targeting and degrading TLR3 in murine cells. *Cell Mol Immunol* **17**, 865-874

272. Kostova, Z., Tsai, Y. C., and Weissman, A. M. (2007) Ubiquitin ligases, critical mediators of endoplasmic reticulum-associated degradation. *Semin Cell Dev Biol* **18**, 770-779

273. Li, W., Tu, D., Brunger, A. T., and Ye, Y. (2007) A ubiquitin ligase transfers preformed polyubiquitin chains from a conjugating enzyme to a substrate. *Nature* **446**, 333-337

274. Klemm, E. J., Spooner, E., and Ploegh, H. L. (2011) Dual role of ancient ubiquitous protein 1 (AUP1) in lipid droplet accumulation and endoplasmic reticulum (ER) protein quality control. *J Biol Chem* **286**, 37602-37614

275. Chen, B., Mariano, J., Tsai, Y. C., Chan, A. H., Cohen, M., and Weissman, A. M. (2006) The activity of a human endoplasmic reticulum-associated degradation E3, gp78, requires its Cue domain, RING finger, and an E2-binding site. *Proc Natl Acad Sci U S A* **103**, 341-346

276. Meyer, H. J., and Rape, M. (2014) Enhanced protein degradation by branched ubiquitin chains. *Cell* **157**, 910-921

277. Olzmann, J. A., Kopito, R. R., and Christianson, J. C. (2013) The mammalian endoplasmic reticulum-associated degradation system. *Cold Spring Harb Perspect Biol* **5**

278. Ye, Y., Meyer, H. H., and Rapoport, T. A. (2001) The AAA ATPase Cdc48/p97 and its partners transport proteins from the ER into the cytosol. *Nature* **414**, 652-656

279. Meyer, H. H., Wang, Y., and Warren, G. (2002) Direct binding of ubiquitin conjugates by the mammalian p97 adaptor complexes, p47 and Ufd1-Npl4. *EMBO J* **21**, 5645-5652

280. Zhong, X., Shen, Y., Ballar, P., Apostolou, A., Agami, R., and Fang, S. (2004) AAA ATPase p97/valosin-containing protein interacts with gp78, a ubiquitin ligase for endoplasmic reticulum-associated degradation. *J Biol Chem* **279**, 45676-45684

281. Morreale, G., Conforti, L., Coadwell, J., Wilbrey, A. L., and Coleman, M. P. (2009) Evolutionary divergence of valosin-containing protein/cell division cycle protein 48 binding interactions among endoplasmic reticulum-associated degradation proteins. *FEBS J* **276**, 1208-1220

282. Bodnar, N., and Rapoport, T. (2017) Toward an understanding of the Cdc48/p97 ATPase. *F1000Res* **6**, 1318

283. Blythe, E. E., Olson, K. C., Chau, V., and Deshaies, R. J. (2017) Ubiquitin- and ATP-dependent unfoldase activity of P97/VCP*NPLOC4*UFD1L is enhanced by a mutation that causes multisystem proteinopathy. *Proc Natl Acad Sci U S A* **114**, E4380-E4388

284. Olszewski, M. M., Williams, C., Dong, K. C., and Martin, A. (2019) The Cdc48 unfoldase prepares well-folded protein substrates for degradation by the 26S proteasome. *Commun Biol* **2**, 29

285. Li, G., Zhao, G., Zhou, X., Schindelin, H., and Lennarz, W. J. (2006) The AAA ATPase p97 links peptide N-glycanase to the endoplasmic reticulum-associated E3 ligase autocrine motility factor receptor. *Proc Natl Acad Sci U S A* **103**, 8348-8353

286. Ernst, R., Mueller, B., Ploegh, H. L., and Schlieker, C. (2009) The otubain YOD1 is a deubiquitinating enzyme that associates with p97 to facilitate protein dislocation from the ER. *Mol Cell* **36**, 28-38

287. Richly, H., Rape, M., Braun, S., Rumpf, S., Hoege, C., and Jentsch, S. (2005) A series of ubiquitin binding factors connects CDC48/p97 to substrate multiubiquitylation and proteasomal targeting. *Cell* **120**, 73-84

288. Wang, Q., Liu, Y., Soetandyo, N., Baek, K., Hegde, R., and Ye, Y. (2011) A ubiquitin ligase-associated chaperone holdase maintains polypeptides in soluble states for proteasome degradation. *Mol Cell* **42**, 758-770

289. Hu, X., Wang, L., Wang, Y., Ji, J., Li, J., Wang, Z., Li, C., Zhang, Y., and Zhang, Z. R. (2020) RNF126-Mediated Reubiquitination Is Required for Proteasomal Degradation of p97-Extracted Membrane Proteins. *Mol Cell*

290. Medicherla, B., Kostova, Z., Schaefer, A., and Wolf, D. H. (2004) A genomic screen identifies Dsk2p and Rad23p as essential components of ER-associated degradation. *EMBO Rep* **5**, 692-697

291. Elsasser, S., Chandler-Militello, D., Muller, B., Hanna, J., and Finley, D. (2004) Rad23 and Rpn10 serve as alternative ubiquitin receptors for the proteasome. *J Biol Chem* **279**, 26817-26822

292. Bard, J. A. M., Bashore, C., Dong, K. C., and Martin, A. (2019) The 26S Proteasome Utilizes a Kinetic Gateway to Prioritize Substrate Degradation. *Cell* **177**, 286-298 e215

293. Greene, E. R., Dong, K. C., and Martin, A. (2020) Understanding the 26S proteasome molecular machine from a structural and conformational dynamics perspective. *Curr Opin Struct Biol* **61**, 33-41

294. Preissler, S., and Ron, D. (2018) Early Events in the Endoplasmic Reticulum Unfolded Protein Response. *Cold Spring Harb Perspect Biol*

295. Kozutsumi, Y., Segal, M., Normington, K., Gething, M. J., and Sambrook, J. (1988) The presence of malfolded proteins in the endoplasmic reticulum signals the induction of glucose-regulated proteins. *Nature* **332**, 462-464

296. Ron, D., and Walter, P. (2007) Signal integration in the endoplasmic reticulum unfolded protein response. *Nat Rev Mol Cell Biol* **8**, 519-529

297. Karagoz, G. E., Acosta-Alvear, D., and Walter, P. (2019) The Unfolded Protein Response: Detecting and Responding to Fluctuations in the Protein-Folding Capacity of the Endoplasmic Reticulum. *Cold Spring Harb Perspect Biol*

298. Okamura, K., Kimata, Y., Higashio, H., Tsuru, A., and Kohno, K. (2000) Dissociation of Kar2p/BiP from an ER sensory molecule, Ire1p, triggers the unfolded protein response in yeast. *Biochem Biophys Res Commun* **279**, 445-450

299. Amin-Wetzel, N., Saunders, R. A., Kamphuis, M. J., Rato, C., Preissler, S., Harding, H. P., and Ron, D. (2017) A J-Protein Co-chaperone Recruits BiP to Monomerize IRE1 and Repress the Unfolded Protein Response. *Cell*

300. Cox, J. S., Shamu, C. E., and Walter, P. (1993) Transcriptional induction of genes encoding endoplasmic reticulum resident proteins requires a transmembrane protein kinase. *Cell* **73**, 1197-1206

301. Korennykh, A. V., Egea, P. F., Korostelev, A. A., Finer-Moore, J., Zhang, C., Shokat, K. M., Stroud, R. M., and Walter, P. (2009) The unfolded protein response signals through high-order assembly of Ire1. *Nature* **457**, 687-693

302. Yoshida, H., Matsui, T., Yamamoto, A., Okada, T., and Mori, K. (2001) XBP1 mRNA is induced by ATF6 and spliced by IRE1 in response to ER stress to produce a highly active transcription factor. *Cell* **107**, 881-891

303. Hollien, J., and Weissman, J. S. (2006) Decay of endoplasmic reticulum-localized mRNAs during the unfolded protein response. *Science* **313**, 104-107

304. Shen, J., Chen, X., Hendershot, L., and Prywes, R. (2002) ER stress regulation of ATF6 localization by dissociation of BiP/GRP78 binding and unmasking of Golgi localization signals. *Dev Cell* **3**, 99-111

305. Oka, O. B., van Lith, M., Rudolf, J., Tungkum, W., Pringle, M. A., and Bulleid, N. J. (2019) ERp18 regulates activation of ATF6alpha during unfolded protein response. *EMBO J* **38**, e100990

306. Haze, K., Yoshida, H., Yanagi, H., Yura, T., and Mori, K. (1999) Mammalian transcription factor ATF6 is synthesized as a transmembrane protein and activated by proteolysis in response to endoplasmic reticulum stress. *Mol Biol Cell* **10**, 3787-3799

307. Yoshida, H., Haze, K., Yanagi, H., Yura, T., and Mori, K. (1998) Identification of the cis-acting endoplasmic reticulum stress response element responsible for transcriptional induction of mammalian glucose-regulated proteins. Involvement of basic leucine zipper transcription factors. *J Biol Chem* **273**, 33741-33749

308. Harding, H. P., Zhang, Y., and Ron, D. (1999) Protein translation and folding are coupled by an endoplasmic-reticulum-resident kinase. *Nature* **397**, 271-274

309. Harding, H. P., Novoa, I., Zhang, Y., Zeng, H., Wek, R., Schapira, M., and Ron, D. (2000) Regulated translation initiation controls stress-induced gene expression in mammalian cells. *Mol Cell* **6**, 1099-1108

310. Estaquier, J., Vallette, F., Vayssiere, J. L., and Mignotte, B. (2012) The mitochondrial pathways of apoptosis. *Adv Exp Med Biol* **942**, 157-183

311. Hu, H., Tian, M., Ding, C., and Yu, S. (2018) The C/EBP Homologous Protein (CHOP) Transcription Factor Functions in Endoplasmic Reticulum Stress-Induced Apoptosis and Microbial Infection. *Front Immunol* **9**, 3083

312. Rao, J., Zhang, C., Wang, P., Lu, L., Qian, X., Qin, J., Pan, X., Li, G., Wang, X., and Zhang, F. (2015) C/EBP homologous protein (CHOP) contributes to hepatocyte death via the promotion of ERO1alpha signalling in acute liver failure. *Biochem J* **466**, 369-378

313. Preissler, S., Rato, C., Chen, R., Antrobus, R., Ding, S., Fearnley, I. M., and Ron, D. (2015) AMPylation matches BiP activity to client protein load in the endoplasmic reticulum. *Elife* **4**, e12621

314. Preissler, S., Chambers, J. E., Crespillo-Casado, A., Avezov, E., Miranda, E., Perez, J., Hendershot, L. M., Harding, H. P., and Ron, D. (2015) Physiological modulation of BiP activity by trans-protomer engagement of the interdomain linker. *Elife* **4**, e08961

315. Sanyal, A., Chen, A. J., Nakayasu, E. S., Lazar, C. S., Zbornik, E. A., Worby, C. A., Koller, A., and Mattoo, S. (2015) A novel link between Fic (filamentation induced by cAMP)-mediated adenylylation/AMPylation and the unfolded protein response. *J Biol Chem* **290**, 8482-8499

316. Preissler, S., Rohland, L., Yan, Y., Chen, R., Read, R. J., and Ron, D. (2017) AMPylation targets the rate-limiting step of BiP's ATPase cycle for its functional inactivation. *Elife* **6**

317. Yu, J., Li, T., Liu, Y., Wang, X., Zhang, J., Wang, X., Shi, G., Lou, J., Wang, L., Wang, C. C., and Wang, L. (2020) Phosphorylation switches protein disulfide isomerase activity to maintain proteostasis and attenuate ER stress. *EMBO J* **39**, e103841

318. Sohl, G., and Willecke, K. (2003) An update on connexin genes and their nomenclature in mouse and man. *Cell Commun Adhes* **10**, 173-180

319. Srinivas, M., Verselis, V. K., and White, T. W. (2018) Human diseases associated with connexin mutations. *Biochim Biophys Acta Biomembr* **1860**, 192-201

320. Das Sarma, J., Wang, F., and Koval, M. (2002) Targeted gap junction protein constructs reveal connexin-specific differences in oligomerization. *J Biol Chem* **277**, 20911-20918

321. Vanslyke, J. K., Naus, C. C., and Musil, L. S. (2009) Conformational maturation and post-ER multisubunit assembly of gap junction proteins. *Mol Biol Cell* **20**, 2451-2463

322. Gilula, N. B. (1978). in *Intercellular Junctions and Synapses* (Feldman, J., Gilula, N. B., and Pitts, J. D. eds.), Chapman & Hill London. pp 1-22

323. Valiunas, V., Cohen, I. S., and Brink, P. R. (2018) Defining the factors that affect solute permeation of gap junction channels. *Biochim Biophys Acta Biomembr* **1860**, 96-101

324. Tyanova, S., Temu, T., Sinitcyn, P., Carlson, A., Hein, M. Y., Geiger, T., Mann, M., and Cox, J. (2016) The Perseus computational platform for comprehensive analysis of (prote)omics data. *Nat Methods* **13**, 731-740

325. White, T. W., and Paul, D. L. (1999) Genetic diseases and gene knockouts reveal diverse connexin functions. *Annu Rev Physiol* **61**, 283-310

326. Alexander, D. B., and Goldberg, G. S. (2003) Transfer of biologically important molecules between cells through gap junction channels. *Curr Med Chem* **10**, 2045-2058

327. Vinken, M., Vanhaecke, T., Papeleu, P., Snykers, S., Henkens, T., and Rogiers, V. (2006) Connexins and their channels in cell growth and cell death. *Cell Signal* **18**, 592-600

328. Falk, M. M., Buehler, L. K., Kumar, N. M., and Gilula, N. B. (1997) Cell-free synthesis and assembly of connexins into functional gap junction membrane channels. *EMBO J* **16**, 2703-2716

329. Falk, M. M. (2000) Connexin-specific distribution within gap junctions revealed in living cells. *J Cell Sci* **113 (Pt 22)**, 4109-4120

330. Gaietta, G., Deerinck, T. J., Adams, S. R., Bouwer, J., Tour, O., Laird, D. W., Sosinsky, G. E., Tsien, R. Y., and Ellisman, M. H. (2002) Multicolor and electron microscopic imaging of connexin trafficking. *Science* **296**, 503-507

331. Lauf, U., Giepmans, B. N., Lopez, P., Braconnot, S., Chen, S. C., and Falk, M. M. (2002) Dynamic trafficking and delivery of connexons to the plasma membrane and accretion to gap junctions in living cells. *Proc Natl Acad Sci U S A* **99**, 10446-10451

332. Falk, M. M., Bell, C. L., Kells Andrews, R. M., and Murray, S. A. (2016) Molecular mechanisms regulating formation, trafficking and processing of annular gap junctions. *BMC Cell Biol* **17 Suppl 1**, 22

333. Kjenseth, A., Fykerud, T., Rivedal, E., and Leithe, E. (2010) Regulation of gap junction intercellular communication by the ubiquitin system. *Cell Signal* **22**, 1267-1273

334. Nielsen, M. S., Axelsen, L. N., Sorgen, P. L., Verma, V., Delmar, M., and Holstein-Rathlou, N. H. (2012) Gap junctions. *Compr Physiol* **2**, 1981-2035

335. Totland, M. Z., Bergsland, C. H., Fykerud, T. A., Knudsen, L. M., Rasmussen, N. L., Eide, P. W., Yohannes, Z., Sorensen, V., Brech, A., Lothe, R. A., and Leithe, E. (2017) The E3 ubiquitin ligase NEDD4 induces endocytosis and lysosomal sorting of connexin 43 to promote loss of gap junctions. *J Cell Sci* **130**, 2867-2882

336. Zimmer, D. B., Green, C. R., Evans, W. H., and Gilula, N. B. (1987) Topological analysis of the major protein in isolated intact rat liver gap junctions and gap junction-derived single membrane structures. *J Biol Chem* **262**, 7751-7763

337. Milks, L. C., Kumar, N. M., Houghten, R., Unwin, N., and Gilula, N. B. (1988) Topology of the 32-kd liver gap junction protein determined by site-directed antibody localizations. *EMBO J* **7**, 2967-2975

338. Laird, D. W. (2006) Life cycle of connexins in health and disease. *Biochem J* **394**, 527-543

339. Abascal, F., and Zardoya, R. (2013) Evolutionary analyses of gap junction protein families. *Biochim Biophys Acta* **1828**, 4-14

340. Verselis, V. K., Ginter, C. S., and Bargiello, T. A. (1994) Opposite voltage gating polarities of two closely related connexins. *Nature* **368**, 348-351

341. Purnick, P. E., Oh, S., Abrams, C. K., Verselis, V. K., and Bargiello, T. A. (2000) Reversal of the gating polarity of gap junctions by negative charge substitutions in the N-terminus of connexin 32. *Biophys J* **79**, 2403-2415

342. Purnick, P. E., Benjamin, D. C., Verselis, V. K., Bargiello, T. A., and Dowd, T. L. (2000) Structure of the amino terminus of a gap junction protein. *Arch Biochem Biophys* **381**, 181-190

343. Kalmatsky, B. D., Bhagan, S., Tang, Q., Bargiello, T. A., and Dowd, T. L. (2009) Structural studies of the N-terminus of Connexin 32 using 1H NMR spectroscopy. *Arch Biochem Biophys* **490**, 9-16

344. Oshima, A., Tani, K., Hiroaki, Y., Fujiyoshi, Y., and Sosinsky, G. E. (2008) Projection structure of a N-terminal deletion mutant of connexin 26 channel with decreased central pore density. *Cell Commun Adhes* **15**, 85-93

345. Maeda, S., Nakagawa, S., Suga, M., Yamashita, E., Oshima, A., Fujiyoshi, Y., and Tsukihara, T. (2009) Structure of the connexin 26 gap junction channel at 3.5 A resolution. *Nature* **458**, 597-602

346. Myers, J. B., Haddad, B. G., O'Neill, S. E., Chorev, D. S., Yoshioka, C. C., Robinson, C. V., Zuckerman, D. M., and Reichow, S. L. (2018) Structure of native lens connexin 46/50 intercellular channels by cryo-EM. *Nature* **564**, 372-377

347. Lee, H. J., Jeong, H., Hyun, J., Ryu, B., Park, K., Lim, H. H., Yoo, J., and Woo, J. S. (2020) Cryo-EM structure of human Cx31.3/GJC3 connexin hemichannel. *Sci Adv* **6**, eaba4996

348. Zhou, X. W., Pfahnl, A., Werner, R., Hudder, A., Llanes, A., Luebke, A., and Dahl, G. (1997) Identification of a pore lining segment in gap junction hemichannels. *Biophys J* **72**, 1946-1953

349. Kronengold, J., Trexler, E. B., Bukauskas, F. F., Bargiello, T. A., and Verselis, V. K. (2003) Single-channel SCAM identifies pore-lining residues in the first extracellular loop and first transmembrane domains of Cx46 hemichannels. *J Gen Physiol* **122**, 389-405

350. Kwon, T., Harris, A. L., Rossi, A., and Bargiello, T. A. (2011) Molecular dynamics simulations of the Cx26 hemichannel: evaluation of structural models with Brownian dynamics. *J Gen Physiol* **138**, 475-493

351. Zonta, F., Polles, G., Sanasi, M. F., Bortolozzi, M., and Mammano, F. (2013) The 3.5 angstrom X-ray structure of the human connexin26 gap junction channel is unlikely that of a fully open channel. *Cell Commun Signal* **11**, 15

352. Trexler, E. B., Bukauskas, F. F., Kronengold, J., Bargiello, T. A., and Verselis, V. K. (2000) The First Extracellular Loop Domain Is a Major Determinant of Charge Selectivity in Connexin46 Channels. *Biophysical Journal* **79**, 3036-3051

353. Hu, X., Ma, M., and Dahl, G. (2006) Conductance of connexin hemichannels segregates with the first transmembrane segment. *Biophys J* **90**, 140-150

354. Nakagawa, S., Maeda, S., and Tsukihara, T. (2010) Structural and functional studies of gap junction channels. *Curr Opin Struct Biol* **20**, 423-430

355. Suchyna, T. M., Xu, L. X., Gao, F., Fourtner, C. R., and Nicholson, B. J. (1993) Identification of a proline residue as a transduction element involved in voltage gating of gap junctions. *Nature* **365**, 847-849

356. Kuntzer, T., Dunand, M., Schorderet, D. F., Vallat, J.-M., Hahn, A. F., and Bogousslavsky, J. (2003) Phenotypic expression of a Pro 87 to Leu mutation in the connexin 32 gene in a large Swiss family with Charcot–Marie–Tooth neuropathy. *Journal of the Neurological Sciences* **207**, 77-86

357. Unwin, N. (1989) The structure of ion channels in membranes of excitable cells. *Neuron* **3**, 665-676

358. Bennett, M. V., Barrio, L. C., Bargiello, T. A., Spray, D. C., Hertzberg, E., and Saez, J. C. (1991) Gap junctions: new tools, new answers, new questions. *Neuron* **6**, 305-320

359. Skerrett, I. M., Aronowitz, J., Shin, J. H., Cymes, G., Kasperek, E., Cao, F. L., and Nicholson, B. J. (2002) Identification of amino acid residues lining the pore of a gap junction channel. *J Cell Biol* **159**, 349-360

360. Fleishman, S. J., Unger, V. M., Yeager, M., and Ben-Tal, N. (2004) A Calpha model for the transmembrane alpha helices of gap junction intercellular channels. *Mol Cell* **15**, 879-888

361. Ahmad, S., Martin, P. E., and Evans, W. H. (2001) Assembly of gap junction channels: mechanism, effects of calmodulin antagonists and identification of connexin oligomerization determinants. *Eur J Biochem* **268**, 4544-4552

362. Martinez, A. D., Maripillan, J., Acuna, R., Minogue, P. J., Berthoud, V. M., and Beyer, E. C. (2011) Different domains are critical for oligomerization compatibility of different connexins. *Biochem J* **436**, 35-43

363. Garcia, I. E., Prado, P., Pupo, A., Jara, O., Rojas-Gomez, D., Mujica, P., Flores-Munoz, C., Gonzalez-Casanova, J., Soto-Riveros, C., Pinto, B. I., Retamal, M. A., Gonzalez, C., and Martinez, A. D. (2016) Connexinopathies: a structural and functional glimpse. *BMC Cell Biol* **17 Suppl 1**, 17

364. Rahman, S., and Evans, W. H. (1991) Topography of connexin32 in rat liver gap junctions. Evidence for an intramolecular disulphide linkage connecting the two extracellular peptide loops. *J Cell Sci* **100 (Pt 3)**, 567-578

365. Foote, C. I., Zhou, L., Zhu, X., and Nicholson, B. J. (1998) The pattern of disulfide linkages in the extracellular loop regions of connexin 32 suggests a model for the docking interface of gap junctions. *J Cell Biol* **140**, 1187-1197

366. Nakagawa, S., Gong, X. Q., Maeda, S., Dong, Y., Misumi, Y., Tsukihara, T., and Bai, D. (2011) Asparagine 175 of connexin32 is a critical residue for docking and forming functional heterotypic gap junction channels with connexin26. *J Biol Chem* **286**, 19672-19681

367. Spagnol, G., Al-Mugotir, M., Kopanic, J. L., Zach, S., Li, H., Trease, A. J., Stauch, K. L., Grosely, R., Cervantes, M., and Sorgen, P. L. (2016) Secondary structural analysis of the carboxyl-terminal domain from different connexin isoforms. *Biopolymers* **105**, 143-162

368. Traub, O., Look, J., Dermietzel, R., Brummer, F., Hulser, D., and Willecke, K. (1989) Comparative characterization of the 21-kD and 26-kD gap junction proteins in murine liver and cultured hepatocytes. *J Cell Biol* **108**, 1039-1051

369. Grosely, R., Kopanic, J. L., Nabors, S., Kieken, F., Spagnol, G., Al-Mugotir, M., Zach, S., and Sorgen, P. L. (2013) Effects of phosphorylation on the structure and backbone dynamics of the intrinsically disordered connexin43 C-terminal domain. *J Biol Chem* **288**, 24857-24870

370. D'Hondt, C., Iyyathurai, J., Vinken, M., Rogiers, V., Leybaert, L., Himpens, B., and Bultynck, G. (2013) Regulation of connexin- and pannexin-based channels by post-translational modifications. *Biol Cell* **105**, 373-398

371. Leithe, E., Mesnil, M., and Aasen, T. (2018) The connexin 43 C-terminus: A tail of many tales. *Biochim Biophys Acta Biomembr* **1860**, 48-64

372. Alaei, S. R., Abrams, C. K., Bulinski, J. C., Hertzberg, E. L., and Freidin, M. M. (2018) Acetylation of C-terminal lysines modulates protein turnover and stability of Connexin-32. *BMC Cell Biol* **19**, 22

373. Ripps, H., Qian, H., and Zakevicius, J. (2004) Properties of connexin26 hemichannels expressed in Xenopus oocytes. *Cell Mol Neurobiol* **24**, 647-665

374. Saez, J. C., Retamal, M. A., Basilio, D., Bukauskas, F. F., and Bennett, M. V. (2005) Connexin-based gap junction hemichannels: gating mechanisms. *Biochim Biophys Acta* **1711**, 215-224

375. Harris, A. L. (2002) Voltage-sensing and substate rectification: moving parts of connexin channels. *J Gen Physiol* **119**, 165-169

376. Oh, S., Abrams, C. K., Verselis, V. K., and Bargiello, T. A. (2000) Stoichiometry of transjunctional voltage-gating polarity reversal by a negative charge substitution in the amino terminus of a connexin32 chimera. *J Gen Physiol* **116**, 13-31

377. Bargiello, T. A., Oh, S., Tang, Q., Bargiello, N. K., Dowd, T. L., and Kwon, T. (2018) Gating of Connexin Channels by transjunctional-voltage: Conformations and models of open and closed states. *Biochim Biophys Acta Biomembr* **1860**, 22-39

378. Muller, D. J., Hand, G. M., Engel, A., and Sosinsky, G. E. (2002) Conformational changes in surface structures of isolated connexin 26 gap junctions. *EMBO J* **21**, 3598-3607

379. Tang, Q., Dowd, T. L., Verselis, V. K., and Bargiello, T. A. (2009) Conformational changes in a pore-forming region underlie voltage-dependent "loop gating" of an unapposed connexin hemichannel. *J Gen Physiol* **133**, 555-570

380. Verselis, V. K., Trelles, M. P., Rubinos, C., Bargiello, T. A., and Srinivas, M. (2009) Loop gating of connexin hemichannels involves movement of pore-lining residues in the first extracellular loop domain. *J Biol Chem* **284**, 4484-4493

381. Kwon, T., Roux, B., Jo, S., Klauda, J. B., Harris, A. L., and Bargiello, T. A. (2012) Molecular dynamics simulations of the Cx26 hemichannel: insights into voltage-dependent loop-gating. *Biophys J* **102**, 1341-1351

382. Oshima, A. (2014) Structure and closure of connexin gap junction channels. *FEBS Lett* **588**, 1230-1237

383. Unwin, P. N., and Zampighi, G. (1980) Structure of the junction between communicating cells. *Nature* **283**, 545-549

384. Unwin, P. N., and Ennis, P. D. (1984) Two configurations of a channel-forming membrane protein. *Nature* **307**, 609-613

385. Paul, D. L., Ebihara, L., Takemoto, L. J., Swenson, K. I., and Goodenough, D. A. (1991) Connexin46, a novel lens gap junction protein, induces voltage-gated currents in nonjunctional plasma membrane of Xenopus oocytes. *J Cell Biol* **115**, 1077-1089

386. Bennett, B. C., Purdy, M. D., Baker, K. A., Acharya, C., McIntire, W. E., Stevens, R. C., Zhang, Q., Harris, A. L., Abagyan, R., and Yeager, M. (2016) An electrostatic mechanism for Ca(2+)-mediated regulation of gap junction channels. *Nat Commun* **7**, 8770

387. Lopez, W., Ramachandran, J., Alsamarah, A., Luo, Y., Harris, A. L., and Contreras, J. E. (2016) Mechanism of gating by calcium in connexin hemichannels. *Proc Natl Acad Sci U S A* **113**, E7986-E7995

388. Turin, L., and Warner, A. (1977) Carbon dioxide reversibly abolishes ionic communication between cells of early amphibian embryo. *Nature* **270**, 56-57

389. Spray, D. C., Harris, A. L., and Bennett, M. V. (1981) Gap junctional conductance is a simple and sensitive function of intracellular pH. *Science* **211**, 712-715

390. Wang, X., Li, L., Peracchia, L. L., and Peracchia, C. (1996) Chimeric evidence for a role of the connexin cytoplasmic loop in gap junction channel gating. *Pflugers Arch* **431**, 844-852

391. Peracchia, C. (2004) Chemical gating of gap junction channels; roles of calcium, pH and calmodulin. *Biochim Biophys Acta* **1662**, 61-80

392. Wang, X. G., and Peracchia, C. (1997) Positive charges of the initial C-terminus domain of Cx32 inhibit gap junction gating sensitivity to CO2. *Biophys J* **73**, 798-806

393. Delmar, M., Coombs, W., Sorgen, P., Duffy, H. S., and Taffet, S. M. (2004) Structural bases for the chemical regulation of Connexin43 channels. *Cardiovasc Res* **62**, 268-275

108

394.	Bergoffen, J., Scherer, S. S., Wang, S., Scott, M. O., Bone, L. J., Paul, D. L., Chen, K., Lensch, M. W., Chance, P. F., and Fischbeck, K. H. (1993) Connexin mutations in X-linked Charcot-Marie-Tooth disease. *Science* **262**, 2039-2042
395.	Paul, D. L. (1986) Molecular cloning of cDNA for rat liver gap junction protein. *J Cell Biol* **103**, 123-134
396.	Scherer, S. S., Deschenes, S. M., Xu, Y. T., Grinspan, J. B., Fischbeck, K. H., and Paul, D. L. (1995) Connexin32 is a myelin-related protein in the PNS and CNS. *J Neurosci* **15**, 8281-8294
397.	Cisterna, B. A., Arroyo, P., and Puebla, C. (2019) Role of Connexin-Based Gap Junction Channels in Communication of Myelin Sheath in Schwann Cells. *Front Cell Neurosci* **13**, 69
398.	Meier, C., Dermietzel, R., Davidson, K. G., Yasumura, T., and Rash, J. E. (2004) Connexin32-containing gap junctions in Schwann cells at the internodal zone of partial myelin compaction and in Schmidt-Lanterman incisures. *J Neurosci* **24**, 3186-3198
399.	Balice-Gordon, R. J., Bone, L. J., and Scherer, S. S. (1998) Functional gap junctions in the schwann cell myelin sheath. *J Cell Biol* **142**, 1095-1104
400.	Bortolozzi, M. (2018) What's the Function of Connexin 32 in the Peripheral Nervous System? *Front Mol Neurosci* **11**, 227
401.	Abrams, C. K. (1998) GJB1 Disorders: Charcot Marie Tooth Neuropathy (CMT1X) and Central Nervous System Phenotypes., Seattle (WA), University of Washington, Seattle
402.	Abrams, C. K., and Freidin, M. (2015) GJB1-associated X-linked Charcot-Marie-Tooth disease, a disorder affecting the central and peripheral nervous systems. *Cell Tissue Res* **360**, 659-673
403.	Scherer, S. S., and Kleopa, K. A. (2012) X-linked Charcot-Marie-Tooth disease. *J Peripher Nerv Syst* **17 Suppl 3**, 9-13
404.	Vavlitou, N., Sargiannidou, I., Markoullis, K., Kyriacou, K., Scherer, S. S., and Kleopa, K. A. (2010) Axonal pathology precedes demyelination in a mouse model of X-linked demyelinating/type I Charcot-Marie Tooth neuropathy. *J Neuropathol Exp Neurol* **69**, 945-958
405.	Scherer, S. S., Xu, Y. T., Nelles, E., Fischbeck, K., Willecke, K., and Bone, L. J. (1998) Connexin32-null mice develop demyelinating peripheral neuropathy. *Glia* **24**, 8-20
406.	Anzini, P., Neuberg, D. H., Schachner, M., Nelles, E., Willecke, K., Zielasek, J., Toyka, K. V., Suter, U., and Martini, R. (1997) Structural abnormalities and deficient maintenance of peripheral nerve myelin in mice lacking the gap junction protein connexin 32. *J Neurosci* **17**, 4545-4551
407.	Partridge, A. W., Therien, A. G., and Deber, C. M. (2004) Missense mutations in transmembrane domains of proteins: phenotypic propensity of polar residues for human disease. *Proteins* **54**, 648-656
408.	Hendershot, L. M., Wei, J. Y., Gaut, J. R., Lawson, B., Freiden, P. J., and Murti, K. G. (1995) In vivo expression of mammalian BiP ATPase mutants causes disruption of the endoplasmic reticulum. *Mol Biol Cell* **6**, 283-296
409.	Keilhauer, E. C., Hein, M. Y., and Mann, M. (2015) Accurate protein complex retrieval by affinity enrichment mass spectrometry (AE-MS) rather than affinity purification mass spectrometry (AP-MS). *Mol Cell Proteomics* **14**, 120-135
410.	Cox, J., and Mann, M. (2008) MaxQuant enables high peptide identification rates, individualized p.p.b.-range mass accuracies and proteome-wide protein quantification. *Nat Biotechnol* **26**, 1367-1372
411.	Richter, K. N., Revelo, N. H., Seitz, K. J., Helm, M. S., Sarkar, D., Saleeb, R. S., D'Este, E., Eberle, J., Wagner, E., Vogl, C., Lazaro, D. F., Richter, F., Coy-Vergara, J., Coceano, G., Boyden, E. S., Duncan, R. R., Hell, S. W., Lauterbach, M. A., Lehnart, S. E., Moser, T., Outeiro, T. F., Rehling, P., Schwappach, B., Testa, I., Zapiec, B., and Rizzoli, S. O. (2018) Glyoxal as an alternative fixative to formaldehyde in immunostaining and super-resolution microscopy. *EMBO J* **37**, 139-159
412.	Yang, J., Yan, R., Roy, A., Xu, D., Poisson, J., and Zhang, Y. (2015) The I-TASSER Suite: protein structure and function prediction. *Nat Methods* **12**, 7-8
413.	Land, H., and Humble, M. S. (2018) YASARA: A Tool to Obtain Structural Guidance in Biocatalytic Investigations. *Methods Mol Biol* **1685**, 43-67
414.	Pettersen, E. F., Goddard, T. D., Huang, C. C., Couch, G. S., Greenblatt, D. M., Meng, E. C., and Ferrin, T. E. (2004) UCSF Chimera--a visualization system for exploratory research and analysis. *J Comput Chem* **25**, 1605-1612
415.	Waterhouse, A. M., Procter, J. B., Martin, D. M., Clamp, M., and Barton, G. J. (2009) Jalview Version 2--a multiple sequence alignment editor and analysis workbench. *Bioinformatics* **25**, 1189-1191
416.	Tsirigos, K. D., Peters, C., Shu, N., Kall, L., and Elofsson, A. (2015) The TOPCONS web server for consensus prediction of membrane protein topology and signal peptides. *Nucleic Acids Res* **43**, W401-407
417.	Bendtsen, J. D., Nielsen, H., von Heijne, G., and Brunak, S. (2004) Improved prediction of signal peptides: SignalP 3.0. *J Mol Biol* **340**, 783-795
418.	Petersen, T. N., Brunak, S., von Heijne, G., and Nielsen, H. (2011) SignalP 4.0: discriminating signal peptides from transmembrane regions. *Nat Methods* **8**, 785-786
419.	Illergard, K., Kauko, A., and Elofsson, A. (2011) Why are polar residues within the membrane core evolutionary conserved? *Proteins* **79**, 79-91
420.	Wong, W. C., Maurer-Stroh, S., and Eisenhaber, F. (2011) Not all transmembrane helices are born equal: Towards the extension of the sequence homology concept to membrane proteins. *Biol Direct* **6**, 57
421.	Kauko, A., Hedin, L. E., Thebaud, E., Cristobal, S., Elofsson, A., and von Heijne, G. (2010) Repositioning of transmembrane alpha-helices during membrane protein folding. *Journal of molecular biology* **397**, 190-201
422.	Abrams, C. K., Goman, M., Wong, S., Scherer, S. S., Kleopa, K. A., Peinado, A., and Freidin, M. M. (2017) Loss of Coupling Distinguishes GJB1 Mutations Associated with CNS Manifestations of CMT1X from Those Without CNS Manifestations. *Sci Rep* **7**, 40166
423.	Chitwood, P. J., and Hegde, R. S. (2019) The Role of EMC during Membrane Protein Biogenesis. *Trends Cell Biol* **29**, 371-384
424.	Shmueli, A., Tsai, Y. C., Yang, M., Braun, M. A., and Weissman, A. M. (2009) Targeting of gp78 for ubiquitin-mediated proteasomal degradation by Hrd1: cross-talk between E3s in the endoplasmic reticulum. *Biochem Biophys Res Commun* **390**, 758-762
425.	Nadav, E., Shmueli, A., Barr, H., Gonen, H., Ciechanover, A., and Reiss, Y. (2003) A novel mammalian endoplasmic reticulum ubiquitin ligase homologous to the yeast Hrd1. *Biochem Biophys Res Commun* **303**, 91-97

426. Beyer, E. C., and Berthoud, V. M. (2018) Gap junction gene and protein families: Connexins, innexins, and pannexins. *Biochim Biophys Acta Biomembr* **1860**, 5-8

427. Paetzel, M., Karla, A., Strynadka, N. C., and Dalbey, R. E. (2002) Signal peptidases. *Chem Rev* **102**, 4549-4580

428. Snapp, E. L., McCaul, N., Quandte, M., Cabartova, Z., Bontjer, I., Kallgren, C., Nilsson, I., Land, A., von Heijne, G., Sanders, R. W., and Braakman, I. (2017) Structure and topology around the cleavage site regulate post-translational cleavage of the HIV-1 gp160 signal peptide. *Elife* **6**

429. Gardner, R. G., Swarbrick, G. M., Bays, N. W., Cronin, S. R., Wilhovsky, S., Seelig, L., Kim, C., and Hampton, R. Y. (2000) Endoplasmic reticulum degradation requires lumen to cytosol signaling. Transmembrane control of Hrd1p by Hrd3p. *J Cell Biol* **151**, 69-82

430. Dahl, G., Werner, R., Levine, E., and Rabadan-Diehl, C. (1992) Mutational analysis of gap junction formation. *Biophys J* **62**, 172-180; discussion 180-172

431. Oslowski, C. M., and Urano, F. (2011) Measuring ER stress and the unfolded protein response using mammalian tissue culture system. *Methods Enzymol* **490**, 71-92

432. Aasen, T., Johnstone, S., Vidal-Brime, L., Lynn, K. S., and Koval, M. (2018) Connexins: Synthesis, Post-Translational Modifications, and Trafficking in Health and Disease. *Int J Mol Sci* **19**

433. Dunlop, J., Jones, P. C., and Finbow, M. E. (1995) Membrane insertion and assembly of ductin: a polytopic channel with dual orientations. *EMBO J* **14**, 3609-3616

434. Ota, K., Sakaguchi, M., von Heijne, G., Hamasaki, N., and Mihara, K. (1998) Forced transmembrane orientation of hydrophilic polypeptide segments in multispanning membrane proteins. *Mol Cell* **2**, 495-503

435. Gafvelin, G., and von Heijne, G. (1994) Topological "frustration" in multispanning E. coli inner membrane proteins. *Cell* **77**, 401-412

436. Swanton, E., High, S., and Woodman, P. (2003) Role of calnexin in the glycan-independent quality control of proteolipid protein. *EMBO J* **22**, 2948-2958

437. Brockmeier, A., and Williams, D. B. (2006) Potent lectin-independent chaperone function of calnexin under conditions prevalent within the lumen of the endoplasmic reticulum. *Biochemistry* **45**, 12906-12916

438. Satoh, T., Ohba, A., Liu, Z., Inagaki, T., and Satoh, A. K. (2015) dPob/EMC is essential for biosynthesis of rhodopsin and other multi-pass membrane proteins in Drosophila photoreceptors. *Elife* **4**

439. Blond-Elguindi, S., Cwirla, S. E., Dower, W. J., Lipshutz, R. J., Sprang, S. R., Sambrook, J. F., and Gething, M. J. (1993) Affinity panning of a library of peptides displayed on bacteriophages reveals the binding specificity of BiP. *Cell* **75**, 717-728

440. Otero, J. H., Lizak, B., Feige, M. J., and Hendershot, L. M. (2014) Dissection of structural and functional requirements that underlie the interaction of ERdj3 protein with substrates in the endoplasmic reticulum. *J Biol Chem* **289**, 27504-27512

441. Joshi, V., Upadhyay, A., Kumar, A., and Mishra, A. (2017) Gp78 E3 Ubiquitin Ligase: Essential Functions and Contributions in Proteostasis. *Front Cell Neurosci* **11**, 259

442. Hwang, J., Walczak, C. P., Shaler, T. A., Olzmann, J. A., Zhang, L., Elias, J. E., and Kopito, R. R. (2017) Characterization of protein complexes of the endoplasmic reticulum associated degradation E3 ubiquitin ligase Hrd1. *J Biol Chem*

443. Rane, N. S., Chakrabarti, O., Feigenbaum, L., and Hegde, R. S. (2010) Signal sequence insufficiency contributes to neurodegeneration caused by transmembrane prion protein. *J Cell Biol* **188**, 515-526

444. Sakaguchi, M., Tomiyoshi, R., Kuroiwa, T., Mihara, K., and Omura, T. (1992) Functions of signal and signal-anchor sequences are determined by the balance between the hydrophobic segment and the N-terminal charge. *Proc Natl Acad Sci U S A* **89**, 16-19

445. Berndt, U., Oellerer, S., Zhang, Y., Johnson, A. E., and Rospert, S. (2009) A signal-anchor sequence stimulates signal recognition particle binding to ribosomes from inside the exit tunnel. *Proc Natl Acad Sci U S A* **106**, 1398-1403

446. Schrul, B., Kapp, K., Sinning, I., and Dobberstein, B. (2010) Signal peptide peptidase (SPP) assembles with substrates and misfolded membrane proteins into distinct oligomeric complexes. *Biochem J* **427**, 523-534

447. Schmidt, O., Weyer, Y., Baumann, V., Widerin, M. A., Eising, S., Angelova, M., Schleiffer, A., Kremser, L., Lindner, H., Peter, M., Frohlich, F., and Teis, D. (2019) Endosome and Golgi-associated degradation (EGAD) of membrane proteins regulates sphingolipid metabolism. *EMBO J* **38**, e101433

448. Okiyoneda, T., Barriere, H., Bagdany, M., Rabeh, W. M., Du, K., Hohfeld, J., Young, J. C., and Lukacs, G. L. (2010) Peripheral protein quality control removes unfolded CFTR from the plasma membrane. *Science* **329**, 805-810

449. Okiyoneda, T., Veit, G., Sakai, R., Aki, M., Fujihara, T., Higashi, M., Susuki-Miyata, S., Miyata, M., Fukuda, N., Yoshida, A., Xu, H., Apaja, P. M., and Lukacs, G. L. (2018) Chaperone-Independent Peripheral Quality Control of CFTR by RFFL E3 Ligase. *Dev Cell*